

Copyright  
by  
Ryan Scott Gray  
2009

**The Dissertation Committee for Ryan Scott Gray Certifies that this is the approved  
version of the following dissertation:**

**Insights Into Intracellular Events of the Planar Cell Polarity Pathway:  
A New Paradigm For the Mechanisms of Dishevelleds and Dishevelled  
Dependent Effector Proteins.**

**Committee:**

---

John B. Wallingford, Supervisor

---

Jeff M. Gross

---

Edward M. Marcotte

---

John C. Sisson

---

Scott W. Stevens

---



**Insights Into Intracellular Events of the Planar Cell Polarity Pathway:  
A New Paradigm For the Mechanisms of Dishevelleds and Dishevelled  
Dependent Effector Proteins.**

**by**

**Ryan Scott Gray, B.S.**

**Dissertation**

Presented to the Faculty of the Graduate School of

The University of Texas at Austin

in Partial Fulfillment

of the Requirements

for the Degree of

**Doctor of Philosophy**

**The University of Texas at Austin**

**May 2009**

## **Dedication**

This work is dedicated to my mother Mary Helen Gray who instilled in me the importance of reading and going to the library.

## Acknowledgements

I must first give thanks to my mentor John B. Wallingford for being at times both encouraging and hesitant for many of my ‘hair-brained schemes’ I have had throughout my tenure in his lab. The score is easily in his favor. Additionally, I need to thank the multiple collaborations and/or helpful advice from a number of wonderful people: Richard H. Finnell for the collaboration of the Fuz mouse with my work; Bogdan J. Wlodarczyk for his work on the Fuz mouse; Karen J. Liu and Heather L. Szabo-Rodgers for the wonderful anti-body stained sections of the Fuz mouse cranium; Greg Weiss and Insuk Lee for aid with Fuz bioinformatics; Edward M. Marcotte for bioinformatics inspiration and the ‘magic hat’; Otis Blanchard and Tae Joo Park for aid with biochemistry; Phillip B. Abitua for his electron microscopy work and serendipity; Roy D. Bayly and Seema Agarwala for chick *in situs*; Stephen A. Green and Christopher J. Lowe for helpful advice on phylogenetic questions and the hemichordate *in situs*; Paul Paukstelis for helpful advice on protein modeling; Kate Monzo and Ian Quigley for always talking science; and the members of the Wallingford lab both past and present.

**Insights Into Intracellular Events of the Planar Cell Polarity Pathway:  
A New Paradigm For the Mechanisms of Dishevelleds and Dishevelled  
Dependent Effector Proteins.**

Publication No. \_\_\_\_\_

Ryan Scott Gray Ph.D.

The University of Texas at Austin, 2009

Supervisor: John B. Wallingford

Dishevelled (Dvl) proteins are key transducers of Wnt signaling and are encoded by members of a multi-gene family in vertebrates. We report here divergent, tissue-specific expression patterns for all three Dvl genes in *Xenopus* embryos, which contrast dramatically with their expression in the mouse. Moreover, we find that the expression patterns of Dvl genes in the chick diverge significantly from those of *Xenopus*. In addition, in hemichordates, one of the outgroups to chordates, we find that the one Dvl gene is dynamically expressed in a tissue-specific manner. Using knockdowns, we find that Dvl1 and Dvl2 are required for early neural crest specification and for somite segmentation. Most strikingly, we report a novel role for Dvl3 in the maintenance of differentiated muscle and the development of the *Xenopus* sclerotome. Together, these data demonstrate that the expression patterns and developmental functions of specific Dvl genes have diverged significantly during chordate evolution.

The planar cell polarity (PCP) signaling pathway is essential for embryonic development because it governs diverse cellular behaviors, and the “core PCP” proteins, such as Dishevelled and Frizzled, have been extensively characterized. By contrast, the “PCP effector” proteins, such as Intu and Fuz, remain largely unstudied. These proteins

are essential for PCP signaling, but they have never been investigated in a mammal and their cell biological activities remain entirely unknown. We report here that Fuz mutant mice display neural tube defects, polydactyly, and skeletal dysmorphologies that stem from defective ciliogenesis. Using bioinformatics and imaging of an *in vivo* mucociliary epithelium, we establish a central role for Fuz in membrane trafficking, showing that Fuz is essential for apical trafficking of ciliogenesis factors in ciliated cells and also for exocytosis in secretory cells. We identify a novel, Rab-related small GTPase as an interaction partner for Fuz, and this GTPase also is essential for ciliogenesis and secretion. These results are significant because they provide novel insights into the mechanisms by which developmental regulatory systems like PCP signaling interface with fundamental cellular systems such as the vesicle trafficking machinery.

## Table of Contents

List of Tables .....	xiii
List of Figures .....	xiv
1 Chapter 1: Functions of Dishevelled (Dvl) Family Genes During Embryonic Development.....	1
1.1.Introduction.....	1
1.2. Cell biology and embryology of Wnt signaling events.....	3
1.2.1. Bifurcation of the Wnt signaling pathway.....	3
1.2.2. Cell biology and embryology of Wnt signaling events.....	7
1.2.2.1.Canonical signals during development.....	7
1.2.2.2. Non-canonical signals of development.....	8
1.3. General introduction to <i>Xenopus</i> embryology.....	10
1.3.1. The morphogenesis of neural tube closure.....	11
1.3.2. Neural crest induction.....	11
1.3.3. Somitogenesis.....	13
1.4. Molecular biology of Dishevelled during embryonic development.....	15
1.4.1. Molecular signaling downstream of Dishevelled proteins.....	15
1.4.1.1.Canonical Wnt/b catenin signals.....	15
1.4.1.2.Non-canonical planar cell polarity (PCP) signals.....	16
1.4.1.3.Genetic studies of Dishevelled.....	18
1.5. Conclusion.....	20

2	Chapter 2: Diversification of the Expression Patterns and Developmental Functions of the Dishevelled (Dvl) Gene Family During Chordate Evolution.....	21
2.1.	Introduction.....	21
2.2.	Divergence of Dvl genes during chordate evolution.....	23
2.2.1.	The patterns of Dvl1, Dvl2, and Dvl3 expression differ between mouse and <i>Xenopus</i> .....	24
2.2.2.	Dvl expression patterns in the chick differ substantially from those in <i>Xenopus</i> .....	32
2.2.3.	Dvl transcription is tightly regulated in the embryos of the basal deuterostome, <i>Saccoglossus kowalevskii</i> .....	33
2.3.	Dishevelled family gene function during neural crest induction.....	36
2.3.1.	Knockdown of Dvl1 and Dvl2, but not Dvl3, disrupts early neural crest specification in <i>Xenopus</i> .....	36
2.4.	Dishevelled family gene function during somitogenesis.....	40
2.4.1.	A conserved role for Dvl1 and Dvl2 in somite segmentation.....	40
2.4.2.	A novel role for Dvl3 in the maintenance of muscle cell identity in <i>Xenopus</i> .....	41
2.4.3.	A novel role for Dvl3 in sclerotome development in <i>Xenopus</i> .....	44
2.5.	Discussion.....	47
3	Chapter 3: Planar Cell Polarity Effector Gene Family.....	49
3.1.	Introduction.....	49
3.2.	Cell biology and embryology of PCP effector genes.....	49

3.2.1.	PCP effector proteins and the cytoskeleton.....	50
3.2.2.	PCP complex subcellular localization.....	51
3.3.	Molecular biology of PCP effectors.....	53
3.3.1.	Sequence homologies of PCP effector genes.....	53
3.3.2.	Molecular interactions of PCP effector proteins.....	54
3.4.	The primary cilia: A crossroads of multiple developmental signaling events.....	54
3.4.1.	To move or not to move.....	55
3.4.2.	The cilia and human disease.....	55
3.4.3.	Cilia are signaling organelles.....	57
3.4.4.	Transit mechanisms of the cilia.....	59
3.5.	Conclusion.....	61
4	Chapter 4: The Planar Cell Polarity Effector Fuzzy is Essential for Targeted Membrane Trafficking, Ciliogenesis, and Mouse Embryonic Development.....	62
4.1.	Introduction.....	62
4.2.	Mice lacking a functional Fuzzy gene display multiple developmental defects..	62
4.3.	Homology modeling and network predictions suggest fuzzy involvement with vesicle trafficking.....	69
4.4.	A novel fuzzy binding partner, RSG1.....	75
4.4.1.	A dominant negative RSG1 <sup>T65N</sup> displays GTPase specific disruption of ciliogenesis, exocytosis, and CLAMP localization.....	75
4.5.	<i>Xenopus</i> , loss of function fuzzy (morphant) experiments display multiple developmental defects.....	83



4.5.1. Fuzzy morphants exhibit general defects in ciliogenesis and of cytoplasmic ciliary components.....	83
4.5.2. Fuzzy morphant embryos display secretory defects of <i>Xenopus</i> epidermis.....	84
4.6. Discussion.....	88
5 Chapter 5: Future Directions.....	89
5.1. Introduction.....	89
5.1.1. Wnt signaling: To PCP or not to PCP.....	89
5.1.2. Dishevelled is a multi-potential protein downstream of Wnt signaling...	90
5.2. Integrating trafficking defects with fuzzy function during development.....	92
5.2.1. The C-terminal domain of Fuz: A longin-like fold domain is a dominant-negative molecule during <i>Xenopus</i> development.....	97
5.3. Are PCP family proteins inherently vesicle trafficking proteins?.....	102
6 Chapter 6: Methods and Materials.....	105
6.1. Embryo Manipulations.....	105
6.2. Biochemistry.....	107
6.3. Cloning-PCR.....	109
6.4. In situ Hybridizations and Histology.....	112
6.5. Immunohistochemistry.....	116
6.6. Bioinformatics, Image analysis and Modeling.....	116

References .....	119
Vita .....	137

## List of Tables

Table 1:	Table 1: Dvl morpholino binding mismatches compared to all <i>Xenopus laevis</i> Dvl genes .....38
Table 2:	MouseFUNC predicts a vesicle trafficking function for Fuz.....71

## List of Figures

Figure 1:	Phylogeny of Dishevelled family genes.....	25
Figure 2:	Divergent expression patterns of Dvl1, Dvl 2, and Dvl3 in <i>Xenopus</i> embryos.....	27
Figure 3:	Dvl1 <i>in situ</i> hybridization.....	28
Figure 4:	Dvl1 expression in cranial placodes .....	29
Figure 5:	Dvl2 <i>in situ</i> hybridization.....	30
Figure 6:	Dvl3 <i>in situ</i> hybridization .....	31
Figure 7:	Divergent expression patterns of <i>Dvl1</i> and <i>Dvl3</i> in the chick.....	34
Figure 8:	Wholemount <i>in situ</i> hybridization of <i>S. kowalevskii</i> <i>Dvl</i> .....	35
Figure 9:	Neural crest induction in <i>Xenopus</i> requires Dvl1 and Dvl2, but not Dvl3.....	39
Figure 10:	Divergent, gene-specific somite defects in Dvl morphants .....	42
Figure 11:	Knockdown of distinct Dishevelled genes generates distinct somite phenotypes .....	43
Figure 12:	Knockdown of Dvl3 in presomitic mesodermal tissues disrupts normal expression of both paraxis and Pax-1 genes .....	46
Figure 13:	<i>Xenopus laevis</i> Fuz antibody labels cell membranes and ciliary rootlet.....	52
Figure 14:	Mice lacking a functional Fuz gene display multiple developmental defects .....	64
Figure 15:	PCR genotyping of Fuz mutant mice.....	65
Figure 16:	Variable penetrance neural tube closure defects and organogenesis defects in mice lacking a functional Fuz gene.....	66

Figure 17:	Individual measurements of acetylated tubulin signal of Meckels cartilage mesenchyme.....	68
Figure 18:	Structure modeling of the Fuz protein.....	72
Figure 19:	Network diagram of functional interactions between other structurally related Fuz like longin-domain containing proteins.....	73
Figure 20:	Homology modeling and network predictions suggest a vesicle trafficking function for Fuz.....	74
Figure 21:	Human chromosome 1 open-reading frame 89 encodes a novel Rab-Similar GTPase (RSG) that is a Fuz interacting protein.....	77
Figure 22:	Dorsally targeted RSG1 MO displays anterior neural tube closure defects that is rescued by co-injection of a GFP-RSG mRNA.....	78
Figure 23:	Loss of Nkx2.2 in Xenopus RSGmorphants.....	79
Figure 24:	Fuzzy and RSG1 function in multiple vesicle trafficking events in the Xenopus epidermis.....	80
Figure 25:	Localization and function of RSG1 in formaldehyde fixed multi-ciliated epidermal cells.....	81
Figure 26:	Fuzzy and RSG1 control mechanisms of ciliogenesis and mucous secretion.....	82
Figure 27:	Knockdown of Fuz disrupts exocytosis in mucus-secreting cells.....	86
Figure 28:	Additional TEM analysis of mucus secreting cells in Fuz morphants...	87
Figure 29:	SNAP-25 localizes to the distal tips of epithelial cilia.....	95
Figure 30:	SNAP-25 localization to the distal tip of cilia is disrupted in Fuz mosaic ciliated cells .....	96

Figure 31: C-Fuz acts as a dominant-negative for anterior neural tube closure	98
Figure 32: C-Fuz generates dose dependent defects of craino-facial development	99
Figure 33: The predicted longin-like fold of Fuz binds GFP-RSG1	101
Figure 34: Modeling of PCP-effector protein domains	104

# Chapter 1: Functions of Dishevelled (Dvl) Family Genes During Embryonic Development

## 1.1. Introduction

Since the discovery that the *wingless* mutant (Nusslein-Volhard and Wieschaus, 1980) a segment polarity gene of the *Drosophila melanogaster* and the INT gene in vertebrates were homologous (Rijsewijk et al., 1987), conventional nomenclature has integrated both gene names into the ‘wnt’ or ‘Wnt’ signaling pathway. As of this publication, some 8000 articles can be found in a PubMed using the search term “wnt”. Clearly much research has been devoted to elucidation of the Wnt dependent signaling pathways. As well, the mechanism of the cytoplasmic “messengers” of wnt signaling, namely the core planar cell polarity (PCP) genes, Vangl/strabismus, Prickle, Starry Night (Flamingo), and Dishevelled (Dvl) are the focus of multiple publications. Surprisingly, a paucity of data exists regarding the mechanisms of transcriptional regulation and cell biology of the core PCP genes, particularly towards Dvl and the Dvl effector genes Fuzzy, Fritz, and Inturned during vertebrate development.

One result of Wnt signaling are the ‘canonical’  $\beta$ -catenin dependent processes of gene transcription downstream of Wnt/ligand and Frizzled (Fz)/receptor interactions (Moon et al., 2002; Kimelman and Xu, 2006). Additionally, Wnt/Fz interactions are known to generate cytoskeletal changes and cytoplasmic signaling events, independent of  $\beta$ -catenin based gene regulation, commonly called the ‘non-canonical’ or PCP pathway (Kato, 2005). It is also true that some evidence points to a third pathway classified by calcium signaling events (Sheldahl et al., 2003; Wallingford and Habas, 2005).

This dissertation will be biased in scope towards the elucidation of mechanisms of PCP signaling events during vertebrate development. Additionally, this work will explore roles of specific Dvl family genes in the orchestration of regulated Wnt and PCP signaling events during embryonic development. Chapter 2 will summarize efforts to better understand the role of restricted Dvl transcription during the development of three

diverse organisms, the *Xenopus* frog, the chick, and the hemichordate acorn worm. As well, antisense morpholino oligonucleotides (MO) loss-of-function experiments in the frog suggest divergent roles for individual development processes of the three Dvl genes.

The PCP pathway was first established by a fly-based model of planar cell polarity, the *Drosophila* wing hair (or trichome) epithelium (Adler and Lee, 2001; Adler, 2002). More plainly, PCP references how cells orient themselves not in an apical-basal polarity, rather how cells are polarized within the plane of a tissue. ‘Fly-pushing’ by Paul Adler and colleagues gave us many of the genes important for the cytoplasmic effects of PCP signaling events (Adler et al., 2004; Collier et al., 2005). Many key insights of these PCP effector genes have been made in both fly and more recently in vertebrates (Park et al., 2006). Chapter 4 will summarize our contributions to better understand one PCP gene, Fuzzy, during vertebrate development of both the mouse and the frog (Chapter 4 this work). Chapter 5 will explore future directions towards a better elucidation of the mechanisms of the PCP effector genes.

In closing, this work further suggests that regulation of Dvl genes may provide some regulation of Wnt signaling events during embryonic development. Moreover, that by investigation of Dvl family gene expression, *in situ*, we might better understand the role that Wnt signaling plays in shaping the diversity of embryonic development. In closing, by integrating knowledge from the fly we move closer to a better understanding of the etiology of vertebrate development; To the contrary of recent political rhetoric.

*...Where does a lot of that earmark money end up anyway? [...] You've heard about some of these pet projects they really don't make a whole lot of sense and sometimes these dollars go to projects that have little or nothing to do with the public good. Things like fruit fly research in Paris, France. I kid you not...*

***Sarah Palin***

***Pittsburgh, Penn. 10/4/08***

*([http://scienceblogs.com/pharyngula/2008/10/sarah\\_palin\\_ignorant\\_and\\_antis.php](http://scienceblogs.com/pharyngula/2008/10/sarah_palin_ignorant_and_antis.php)).*



## **1.2. Cell biology and embryology of Wnt signaling events**

### **1.2.1 Bifurcation of the Wnt signaling pathway**

The binding of a Wnt molecule to a Frizzled (Fz) receptor and a co-receptor Arrow/Lrp5/6 delineates the basic extracellular arm of the Wnt pathway understood at this time. However, less well understood is how this pathway diverges towards, for instance, a 'canonical' or 'non-canonical' pathway in the cytoplasm after these ligand-receptor interactions occur. It appears that some instructive cues are given by the actual Wnt/ligand gene products themselves; Silberblick (Wnt11) and Pipetail (Wnt5) are reported PCP pathway determinants in vertebrate development (Myers et al., 2002; Westfall et al., 2003); Whereas, Wnt-1 and Wnt-8 are thought to determine a  $\beta$ -catenin dependent secondary axis in *Xenopus* embryos (Sokol et al., 1991). Interestingly, a Wnt instructive for PCP signaling has yet to be uncovered in the fly. This could be a divergent mechanism of the fly, alternately it might highlight the hierarchy of cytoplasmic determinants to effect Wnt pathway flux towards the canonical versus non-canonical pathway.

One could also expect that pathway bifurcation or pathway flux may diverge at the level of regulation of expression of various Frizzled receptors. In vertebrates, multiple Fz genes (for example Fz2, Fz3, Fz4, and Fz6) predominately activate the PCP pathway, whereas, Fz1 and Fz7 activate the canonical pathway (Sheldahl et al., 1999; Kuhl et al., 2000). More recently, the importance of the co-receptors LRP5/6 in the context of canonical Wnt/ $\beta$ -catenin signaling (Tamai et al., 2000; Wehrli et al., 2000) and Ryk in the context of the non-canonical PCP signaling pathway (Kim et al., 2008a) have added to the complexity of Wnt signaling events during embryonic development.

Additional regulatory receptors for Wnt signaling include: Ror2 and Kypnek. Ror2 belongs to the Ror family of receptor tyrosine kinases and possess extracellular cysteine-rich domains (CRD) which resembles the Wnt-binding sites of the Frizzled (Fz) proteins and associate directly with Fz2 receptor. Additionally, both Ror2<sup>-/-</sup> and Wnt5a<sup>-/-</sup> mice exhibit apparently identical developmental defects (Oishi et al., 2003). The interaction of Wnt5a and Ror2 activates a downstream effector of the PCP pathway, JNK.

However, overexpression of Ror2 in *Xenopus* convergent-extension (C/E) assays inhibited elongation of Vg1 induced animal caps. These results suggest a cell context dependence for the Ror2 receptor or that JNK activation is not a *bone fide* effector of PCP signals.

Knypek encodes a member of the glypican family of heparan sulfate proteoglycans (Topczewski et al., 2001). Mutations in knypek result in C/E defects in the zebrafish. Furthermore, Wnt11 and knypek exhibit genetic interactions of heterozygous alleles. This again implicates a non-canonical Wnt co-receptor in flux towards the non-canonical Wnt pathway.

However, it is likely that all decisions between the canonical and non-canonical pathways are context dependent. For instance, Wnt5a, associated with non-canonical signaling, is insufficient to cause a secondary axis in *Xenopus* (Torres et al., 1996). Conversely, given the right complement of receptor (Fz4) and coreceptor (Lrp5) one can assay significant canonical signaling flux (Mikels and Nusse, 2006). Furthermore, Wnt11 is thought to be a PCP specific Wnt ligand; additionally exhibits canonical pathway activation during early stages of development (Tao et al., 2005).

A number of studies point to contributions of  $\beta$ -arrestins ( $\beta$ -arr), part of the endocytosis machinery, in pathway selection. The role of  $\beta$ -arr in the termination and transduction of G-protein-coupled receptor (GPCR) signals has been the subject of intensive study (reviewed by (Luttrell and Lefkowitz, 2002)). In short, binding of  $\beta$ -arr with a cognate GPCR disrupts the interaction of the receptor with its associated trimeric G ( $\alpha, \beta, \gamma$ ) protein complex. Similarly,  $\beta$ -arr aids in the bifurcation of Wnt signals in the cytoplasm (Chen et al., 2003; Bryja et al., 2007a) and reviewed by (Gagliardi et al., 2008). This concept serves to highlight the need to explore the mechanism of the cytoplasmic effectors of Wnt signals, rather than focusing efforts on the extracellular molecules.

Both Fzs and GPCRs share similarities in that they exhibit structurally related seven transmembrane-spanning (7TMS) protein domains. It seems plausible that  $\beta$ -arr dependent regulations of Fz receptor may exist. In fact, this inference is indeed supported by work in cell culture. Wherein, Wnt5A conditioned media in the presence of 1  $\mu$ M

phorbol myristoyl acetate (PMA) -which activates protein kinase C (PKC)- initiated the internalization of a Fz4-GFP fusion protein from the cell surface to intracellular vesicles (Chen et al., 2003). Moreover, it was found that endogenous  $\beta$ -arrestin 2 ( $\beta$ arr2) was associated with Fz4 at the membrane in a Dvl2 dependent manner, but that internalization of a Fz4/Dvl2/ $\beta$ arr2 protein complex required Wnt5A stimulation. The recruitment of  $\beta$ arr2-GFP to the cellular membrane in cells expressing Fz4/Dvl2 requires activation of PKC, while a PKC inhibitor did not affect the membrane localization of Fz4/Dvl2. This implicates PKC activation in the initiation of  $\beta$ arr2 dependent internalization of a Wnt/Fz/Dvl protein complex.

Importantly, activation of PKC by PMA in cell culture generates a phosphorylated Dvl2 protein. PKC was further shown to directly phosphorylate Dvl2 using reconstituted proteins *in vitro*. Whether this mechanism in cell culture is reflective of canonical or non-canonical signaling was not adequately examined.

Another study addressed this caveat by using both cell culture and the *Xenopus* Keller explant (Wilson et al., 1989). The Keller explant is the dorsal marginal zone (DMZ) removed from an early *Xenopus* gastrula embryo and cultured *sole vitro* to prevent curling of the explant tissue; effectively assaying convergent-extension (C/E) movements of the neural tissue and the mesoderm of which each can be individually scored for length to width ratios. These morphogenic movements are known to be dependent on non-canonical or PCP signaling and independent of canonical signals (Wallingford et al., 2000). These *in vivo* studies showed that casein kinase 1 and 2 (CK1/2) act as a ‘switch’, via phosphorylation of Dvl protein, to push the Wnt signaling flux towards the non-canonical branch (Bryja et al., 2008). Moreover, a  $\beta$ arr morpholino knockdown based approach rescued the explant elongation defect as the result of the overexpression of Wnt11 (a presumed PCP Wnt in the frog). As over activation of PCP signals are known to generate C/E defects (Wallingford et al., 2000); these results suggest that  $\beta$ -arr indeed has a role in the amplification of the non-canonical PCP pathway.

Additional studies seem to implicate the  $\beta$ -arr dependent internalization of the Wnt/Fz/Dvl complex as the branch that facilitates the recruitment of Axin and the subsequent accumulation of  $\beta$ -catenin resulting in canonical PCP signaling (Bryja et al.,

2007b). *In vivo* experiments in the *Xenopus* animal cap, a naive epithelium, suggest that Wnt11/Fz7 interactions are not sufficient in to induce internalization. However, the additional expression of Ryk -a Wnt coreceptor- allowed Wnt11/Fz7 to become endocytosed in a Dvl/Rab5/ $\beta$ arr2 dependent manner (Kim et al., 2008a). Furthermore, Ryk was implicated in the internalization of Fz; leading to signaling flux towards the non-canonical pathway.

In contrast, a caveolin dependent internalization of Wnt/Fz ligand-receptor have been described (Yamamoto et al., 2006). Wherein, the researchers utilize Wnt3A/Fz5 interactions along with the LRP6 co-receptor of Fz. In the presence of LRP6, Fz5 was internalized via interactions with caveolin; conversely, in the absence of LRP6, Fz5 was endocytosed via clathrin dependent processes. The researchers further conclude that the caveolin dependent endocytosis of Fz5 results in increased Wnt/ $\beta$ -catenin signals whereas the clathrin dependent internalization leads to the non-canonical PCP signaling.

This hypothesis seems to be supported well *in vivo*, as inhibition of LRP6 function appears to have no effect on gastrulation movements in *Xenopus*, a non-canonical PCP process (Semenov et al., 2001). This is interesting, given that Wnt3A has been shown to be multi-functional in promoting both ‘canonical’ and ‘non-canonical’ Wnt signals (Habas et al., 2003) and (Kishida et al., 2004). Again these data seem to establish that the individual Fz receptors or Wnt ligands are not sufficient to specify canonical versus non-canonical signals; Rather, it is the contextual variables of an individual cell type which ultimately determines pathway bifurcation.

Certainly, extracellular molecules can aid in this bifurcation of the Wnt pathway. For instance, a report by Yamamoto and colleagues shows that Dkk1, an antagonist of Wnt signaling pathway that is known to bind LRP5/6 receptors, may provide an extracellular ‘switch’ to facilitate or promote pathway choice. What is clear, from the overview of these experiments *in toto*, is that Frizzled/Wnt interactions are internalized by endocytic machineries; this internalization is accomplished by at least two distinct mechanisms of endocytosis; a caveolin dependent method and an AP2/ $\beta$ -arr/clathrin dependent method; and these divergent mechanisms of receptor internalization seemingly aid in pathway choices during development. While this is true for cells in culture; all three caveolin

homologous were singly knocked out in mouse with no gross developmental defects early, however a reduction in life span was noted. In addition, multiple double knockouts exhibited few additional and mild physiological defects (Cohen et al., 2004). Thus, a role for caveolin *in vivo* is at least redundant of other mechanisms of endocytosis in the progress of multiple Wnt/ $\beta$ -cat dependent developmental signaling events.

By exploring the cytoplasmic determinates of canonical versus non-canonical signaling we will add greatly to the mechanisms of Wnt dependent events during the development of all organisms.

### **1.2.2. Cell biology and embryology of Wnt signaling events**

#### **1.2.2.1. Canonical signals during development**

The Wnt/ $\beta$ -cat signaling pathway comprises numerous development decisions in vertebrate and invertebrates. In fact, every major organ system uses Wnt in some development event. In addition, Wnt/ $\beta$ -catenin signaling is crucial for cell fate decisions, cell proliferation, cell migration, stem cell maintenance, tumor suppression, and oncogenesis (Chien et al., 2009). The basic pathway prescribes that Wnt/Fz interactions lead to phosphorylation of Dvl protein. This phosphorylated Dvl protein inhibits the activity of Glycogen synthase kinase 3 (GSK3). This inhibition of GSK3 relieves the GSK3 dependent destruction of  $\beta$ -cat protein. Accumulation of  $\beta$ -cat protein allows translocation to the nucleus in order to upregulate gene transcription in collaboration with various co-transcription factors, for example the LEF-1/TCF-1 molecules. The mechanism of Dvl dependent relief of  $\beta$ -catenin might be achieved by binding of Axin molecules; thought to provide a scaffold for the  $\beta$ -catenin destruction complex. These concepts are more completely covered elsewhere (as reviewed by (Kimelman and Xu, 2006)).

Various, knockout alleles of the Wnts have been reported. Most phenotypes are readily explained as loss of canonical signaling; however, it is important to consider a loss-of-function of non-canonical signaling in the phenomenology of Wnt or Frizzled mutant embryos. The best alternative might be a loss-of-function  $\beta$ -cat; however, as  $\beta$ -cat protein provides a structural component for epithelial cells this analysis would be problematic *in vivo*. Interestingly, a double mutant mouse of the  $\beta$ -catenin co-

transcription factor LEF-1 and TCF-1 generates phenotypes akin to a *wnt3a* null mouse (Galceran et al., 1999). Defects in limb patterning/formation and axial mesodermal markers of myotomes and sclerotome development were most apparent. However, this cannot represent a complete loss-of-function of canonical signals, as the formation of the dorsal axis is apparent. This is likely reflective of additional transcriptional genes that are semi-redundant for canonical transcriptional events. This redundancy is likely necessary for any such robust development-signaling pathway.

A key function of  $\beta$ -cat signaling is the development of the dorsal-ventral axis. In that, Dvl dependent accumulation of dorsal  $\beta$ -catenin generates the dorsal axis (Rothbacher et al., 1995). As well, accumulation of Dvl protein along the dorsal axis in early frog embryos generates dorsalizing signals (Rothbacher et al., 1995). Ectopic injections of INT-1 (Wnt-1) or Dvl capped mRNAs into a vegetal blastomere -fated to become ventral tissues- of the 4-cell frog embryo generates a complete axis duplication (McMahon and Moon, 1989; Sokol et al., 1991). Moreover, multiple genes important for formation of the dorsal organizer have been directly shown to contain LEF-1/TCF-1 regulatory regions (e.g. *Xnr3*) (McKendry et al., 1997).

In conclusion, Wnt/ $\beta$ -catenin signaling is crucial for developmental signaling pathways in addition to exhibiting effects throughout the lifecycle of most organisms. Defects in  $\beta$ -cat signaling are pleiotrophic and comprehensive of most tissue and organ systems. In addition, multiple cancers and progressive disease are dependent on this pathway.

#### **1.2.2.2. Non-canonical signals of development**

PCP signaling is essential for a variety of vertebrate developmental events, including morphogenesis of the neural tube, heart, kidney, and ear (Simons and Mlodzik, 2008). A unifying mechanism for the range of phenotype associated with PCP is troubled by the inability in most cases to generate loss-of-function PCP defects without compromising canonical signaling defects. In addition, it is not clear how a loss of cell polarity generates the pleiotrophic defects seen in PCP mutant experiments. In addition, the polarized deposition of the 'core' PCP proteins, seen in fly is not observed to be as robust

in vertebrate models. Regardless, there are very good examples of PCP defects which generate developmental dysmorphogenesis.

One of the first clear indications that PCP functioned in vertebrate polarity dependent tissue morphogenesis was given by work of the *Xenopus laevis*. In this, disruption of Dvl function generated cells that defective in the persistence and polarity of actin-rich lamellapodia. These lamellapodia function to provide directed cell motility and the dependence of Dvl functioning was shown to affect both neural tube closure and gastrulation by abolishing the morphogenic process of C/E (Wallingford et al., 2000; Keller, 2002; Wallingford and Harland, 2002). The development of the neural tube and the organ of Corti are disrupted in mutant mouse alleles of a variety of PCP genes. As, Vang2/Ltap (Montcouquiol et al., 2008), Fz3/Fz6 (Guo et al., 2004; Wang et al., 2006b) and the Celsr (Flamingo) mouse exhibits defects in stereocilia polarity and neural tube defects (Curtin et al., 2003). Limited reports have implicated PCP on the polarization of cell division. This is covered more completely elsewhere (as reviewed by (Wallingford and Habas, 2005)).

The formation of the neuromuscular synapse has recently been shown to be dependent on Dvl (Luo et al., 2002). In this report a specificity of canonical versus non-canonical signaling was not examined, however there are clearly input towards the activation of small GTPases, RAC and CDC42, and the JNK pathways in the process of Agrin/MuSK accumulation. The formation of the neuromuscular pre-synaptic terminal is associated with F-actin accumulation. The exact mechanism remains unclear, it is possible this regulation is through Dvl dependent PCP signaling. These results are again tempered by the results of the Dvl1 mouse that displays specific neurological defects ((Lijam et al., 1997) and this work Chapter 1.1.4.3).

This work describes the first insights into the mechanism of a loss-of-function PCP in a vertebrate, by targeted knockout of a PCP effector gene fuzzy (Chapter 4 this work). Multiple defects clearly overlap with loss-of-function PCP previously reported; however, subtle differences are apparent. Interestingly, these defects are best explained by defects in the formation of the primary cilia. This will be extensively reviewed in Chapter 3 and reported in Chapter 4 of this work.

### 1.3. General introduction to *Xenopus* embryology

One clear aspect of the developing *Xenopus* embryo is the robust nature of neural tube development. This has been extensively studied using basic ‘cut and paste’ transplantations and surgical techniques that are highly tractable in the frog embryo in order to study the large-scale contributions of cells and tissues to the morphogenesis of the neural tube. Multiple cell and tissue rearrangements comprise the development of the neural tube such as: convergent-extension; apical constriction; and epiboly (extensively reviewed by (Keller et al., 2003) and (Solnica-Krezel, 2005)). These processes are highly tractable in the frog. Many cells are on the order of 30 $\mu$ M during many of these morphogenic events, allowing for great resolution during image collection.

In addition, the developing multi-ciliated epidermis of the tadpole stage frog embryo has recently been exploited to study basic cilia biogenesis (ciliogenesis) (Park et al., 2006; Hayes et al., 2007; Mitchell et al., 2007; Park, 2008). As well, the multi-ciliated frog epidermis has been historically characterized using electron microscopy as well as novel molecular investigations into gene products responsible for normal epithelial functions of the frog (Steinman, 1968; Nagata et al., 2003; Stubbs et al., 2006). Importantly, biological events regarding the secretion of large mucous granules, akin to the secretion of pancreatic zymogen granules, might be studied using the frog epidermis. Lastly, the presence of a poorly studied ionocyte population may provide insights into ion channel dependent regulations (Ian Quigley, personal communication).

Many molecular techniques are easily employed in the frog. High concentrations [ $\sim$ 1ng] of *in vitro* transcribed capped-mRNA can be injected into embryos. It also follows that dominant negative constructs or constitutively active mRNA constructs have been extensively employed to test protein function in *Xenopus*. In addition, both splice-blocking and translation-blocking anti-sense morpholino oligonucleotides (morpholinos (MOs)) have been utilized in numerous publications.



### **1.3.1. Morphogenesis of neural tube closure**

Defects in neural tube closure are among the most common human birth defects, effecting 1 to 2 per 1000 births (Kibar et al., 2007a). Neural tube closure is a complex orchestration of multiple modes of cell motility and shape changes. Two major processes contributing to neural tube closure are convergent-extension and apical constriction. Convergent-extension (C/E) describes how cells intercalate towards the midline to generate forces necessary to extend the head from tail (Keller et al., 1985; Keller et al., 2000; Keller, 2002). Apical constriction is the process by which cells decrease the apical surface area of the cell. For example, the cells lining the neural tube will decrease the lumen facing sides, generating wedge shaped cells, in order to facilitate the bending of the neural folds (Hildebrand, 2005; Lee and Harland, 2007).

Research in neural tube closure of mammalian models is hampered by the intractable availability of the developing embryo at times at which the neural tube is closing. However, the amphibian *Xenopus laevis* embryo provides a wonderful model organism with which to study the mechanisms of neural tube closure. It will be of great interest to begin processing information gained in the frog and confirmed in the mouse, for clinical investigations.

To date, no other genes except the gene encoding 5,10-methylenetetrahydrofolate reductase have been specifically implicated in predisposition to NTDs (Coskun et al., 2009). Importantly, the mouse PCP genes, Scribble and Vangl2 in double heterozygosity have been shown to cause defects seen in homozygous mutant alleles of each gene individually (Phillips et al., 2007). However, two studies investigated Vangl1, Vangl2 and Dvl3 in human NTD patients; surprisingly, found no significant associations with the disease phenotypes (Boyles et al., 2005; Doudney et al., 2005). Regardless, all *bone fide* PCP genes as well as the PCP effector gene should be considered as candidates for a role in the etiology of human NTDs ((Kibar et al., 2007a) and the Chapter 4 this work).

### **1.3.2. Neural crest induction**

The neural crest (NC) was first described in 1868 by His, as ‘zwischenstrang’ or ‘in-between strip’ (as reviewed (Gammill and Bronner-Fraser, 2003)). The development of

NC tissue is an orchestration of three major signaling pathways: BMPs; Wnts; and FGFs (Gammill and Bronner-Fraser, 2003). These signals converge on a specific region, emanating from the developing apical neuroectoderm and the basal developing somitic mesoderm. The neural crest cells (NCC) develop between the overlying non-neural ectoderm and the underlying neural plate. How these signals integrate is becoming clearer; however, importantly many model organisms use divergent mechanisms of induction.

The importance of Wnt signaling on NC induction is clear in multiple organisms. Whereas, Wnts are both necessary and sufficient to induce NC marker expression in avian neuroepithelium (Garcia-Castro et al., 2002). The Wnt1/Wnt3a double knock out mouse displays pleiotrophic defects associated with loss of neural crest including: reduction of melanocytes; skeletal dysmorphogenesis; and loss of sensory neurons (Ikeya et al., 1997). Additionally, overexpression of Wnt1 and Wnt3a, in frog embryos, results in an expansion of the normal NC markers (Saint-Jeannet et al., 1997). This review will focus on the mechanisms of Wnt dependent NCC induction in the *Xenopus laevis*.

Induction of NCCs are commonly assayed by activation of a class of zinc-finger transcriptional repressor proteins: Slug and Snail (del Barrio and Nieto, 2002; Aybar et al., 2003). Interestingly, Slug expression in the frog is directly regulated by canonical Wnt/ $\beta$ -catenin LEF/TCF dependent signaling and is thought to be one of the earliest markers of NCCs (LaBonne and Bronner-Fraser, 1999; Vallin et al., 2001). Indeed, proper expression of Slug in frog is crucial for both induction and migration of NCCs *in vivo* (Nieto et al., 1992; Carl et al., 1999; LaBonne and Bronner-Fraser, 2000; Aybar et al., 2003). The zinc-finger transcription factor, Twist, is considered a marker of late stage NC induction (Hopwood et al., 1989a). The expression of Twist is repressed by knockdown of Slug by injection of anti-sense mRNA targeted to the 3'-UTR of Slug (Carl et al., 1999). It is not known whether Wnts directly regulate Twist expression, however Slug appears to directly effect the expression of Twist. Thus, Wnt signaling events directly initiate and maintain both early and late induction of transcription factors necessary for NCC induction and migration.

This idea is further supported by investigations into human birth defects that may result from defects of NCCs in addition to Wnt signaling (e.g. DiGeorge syndrome) (Minier et al., 2005; Walker and Trainor, 2006). DiGeorge syndrome (DGS) is characterized in part by genetic lesions of the human chromosomal region 22q11. The syndrome is correlated with multiple craniofacial malformations and cardiac anomalies (Farlie et al., 2004). DGS is observed as multiple phenotypes including: facial dysmorphology, cleft palate, conotruncal defects, and hypoplasia of thyroid and parathyroid glands, all derivatives of the migratory NCC lineages (Farlie et al., 2004). Interestingly, a Dishevelled homologue, named DVL1L1 or DVL4, is deleted in some human DGS patients (Pizzuti et al., 1996).

The mechanism of NCC migration depend on events downstream of Dvl signaling (De Calisto et al., 2005). As well defects in NCC migration are very likely to underlie many craniofacial disease in human and vertebrate animal models (Tobin et al., 2008). Inputs of Wnt signaling, function for both the induction and migration of NCCs. Interestingly, Dvl proteins have been shown to control both polarized cell migrations as well as basal body docking of the cilia (Walston et al., 2006; Park et al., 2008). As well, recent observations show that NCCs contain signaling cilia (Tobin et al., 2008). In addition, some PCP and ciliogenesis defective mutants exhibit developmental defects prescribed to defects of NCCs. This allows speculation that the subtle craniofacial phenotypes of BBS patients (e.g. poor frontonasal and maxillary outgrowths) are reflective of defective ciliogenesis in NCCs. It will be interesting to explore possible integrations of ciliogenesis defects with NC defects.

### **1.3.3. Somitogenesis**

The development of vertebrate musculature proceeds through an iterative process of compartmentalization of mesoderm or pre-somitic mesoderm (PSM) into somites. Somitogenesis happens in a wave from the anterior to posterior, in that the eldest somites are anteriorly localized, while the segmentation of a new somite happens at the posterior growth zone (Martin and Kimelman, 2009). This posterior growth zone has been described molecularly to generate the variable ranges of vertebrate somite number

(e.g. ~35 in zebrafish compared to ~300 in the corn snake)(Gomez et al., 2008). The molecular and cell biological mechanisms of somitogenesis between divergent vertebrate species are highly variable. In fact, the pipid *Xenopus laevis* frog exhibits a highly derived somite rotation mechanism not yet observed in other amphibian species (Afonin et al., 2006; Handrigan and Wassersug, 2007). Thus, an attempt to give a general overview of how somitogenesis proceeds in the *Xenopus* must distill from knowledge of the chick and mouse.

Compartmentalization of the somites give rise to different musculatures (e.g. myotomes: epaxial muscles and hypaxial muscles and the primordial skeleton or sclerotome. The main signaling inputs during somitogenesis are the Wnt and Hedgehog (Hh) signaling pathways. The sources of Wnt molecules are the surface ectoderm and the dorsal neural tube, where the notochord and the ventral neural tube secrete Hh (Brent and Tabin, 2002; Christ et al., 2004). The paradigm is as follows: Sonic Hedgehog (SHH), a ventral originating molecule, serves to ventralize the somite tissue; while, Wnts, dorsally derived molecules aid in the induction of dorsal somite markers; and finally at some medial level the dorsal and ventral signals are opposed thus generating the variable ranges of the cell types seen during somitogenesis. In fact, ectopic expression of Wnt-1, -3a, and -4 is sufficient to induce Pax3, a dorsal myotome marker (Wagner et al., 2000). While ectopic Wnt1 expression suppresses the ventral, sclerotome associated markers, Pax1 and Pax9 (Capdevila et al., 1998). Conversely, SHH is necessary to induce expression of Pax1 in PSM explant tissues, albeit in the presence of endogenous Wnt5b (Linker et al., 2003). However, experiments suggest that many of these inductive events in fact require the combined inputs of both Wnt and Hh signaling to activate myogenic programs (Lassar and Munsterberg, 1996).

Mechanisms of compartmentalization of the sclerotome are highly divergent throughout vertebrate organisms. Both the chick and the mouse exhibit well-defined regions of sclerotome; easily seen with light-microscopy in cross section; and molecularly defined by *in situ* hybridization of the sclerotomal markers, Pax1 or Pax9 (Christ et al., 2004). Conversely, anurans and urodeles, such as the zebrafish and the *Xenopus laevis* have very small sclerotomes; observed as a few mesenchymal cells surrounding the

notochord (Youn et al., 1980; Keller, 2000; Handrigan and Wassersug, 2007). A wonderful proposal has been presented by Handrigan and Wassersug. Wherein, the early aquatic lifestyle gives the flexible unossified tail of the tadpole a selective advantage for prey avoidance. As well the mechanism of tail re-adsorption of the maturing froglet is facilitated by the minimal bone/cartilage formation in the developing tadpole (Handrigan et al., 2007).

The synergy of Wnt and Hh signaling is most likely directed by activation of Gli effector proteins. Indeed, Wnts regulates Gli expression in PSM (Borycki et al., 2000). In light of the wealth of data suggesting that cilia are necessary for Hh signaling and Wnt signaling events it will be interesting to see if the primary cilia are involved in this synergy of Wnt and Hh during somitogenesis upstream of the Gli proteins (See Chapter 3.4 this work).

## **1.4. Molecular biology of Dishevelled during embryonic development**

### **1.4.1. Molecular signaling downstream of Dishevelled proteins**

As described in section 1.2 of this work we are not yet clear on the complexity of molecular decisions downstream of Wnt signals in the cell. There are however molecular determinates and assays of canonical versus non-canonical Wnt signaling events. What is clear is that Dvl proteins play major roles in both the canonical and non-canonical pathways downstream of Wnt/Fz interactions. A multitude of protein interactions have been described for Dvl (Wharton, 2003; Wallingford and Habas, 2005). Clearly, many of these protein effectors of Dvl generate specificity of pathway flux by subtle changes in the localization, phosphorylation state, or other molecular collaborations of Dvl proteins with the cytoplasmic milieu. Chapter 4 will describe our work towards understanding Fuz -an effector protein downstream of Dvl that aids in PCP signaling- during embryonic development of the mouse and the frog.

#### **1.4.1.1. Canonical Wnt/ $\beta$ -catenin signals**

One of the more eloquent assays of canonical Wnt/ $\beta$ -catenin signaling is seen using the *Xenopus* embryo. One can take a molecule of interest, inject it into the ventral blastomere

of a 4-cell frog embryo and assay the presence of a secondary dorsal axis (Harland, 2008). In which, the formation of the dorsal axis is dependent of the canonical Wnt signaling molecular cascade. The formation of secondary axis, first described by Hilde Mangold and Hans Spemann in 1924, as the results of transplanting ‘organizer’ tissue derived from the involution dorsal marginal zone into the ventral region of another embryo (reviewed by (Harland, 2008)). This results in the formation of a ‘secondary axis’ containing both axial mesoderm and neural tissues (e.g. notochord, neural tissues, and somites), arising from the donor embryonic tissues and induced by the donor organizer tissues. The formation of ‘secondary axis’ powerfully illustrates the complexity of a developing organism however might generate false positives or negatives depending on the context of the gene products present in the embryo.

Other assays involve the TOPFLASH system of the reporting the presence of increase canonical signals by a TCF/LEF promoter driving the expression of, for instance a luciferase reporter construct (Darken and Wilson, 2001; Filali et al., 2002). The TCF/LEF promoter is known to be important for  $\beta$ -catenin dependent gene transcription in a variety of model organisms; a double *lef/tcf* mutant mouse recapitulates in many respects the *wnt3a* mutant mouse (Galceran et al., 1999). However, many aspects of development are unaffected such as dorsal axis specification, thus LEF1/TCF1 cannot be crucial many basic Wnt/ $\beta$ -cat signaling events.

#### **1.4.1.2. Non-canonical planar cell polarity (PCP) signals**

Assays for non-canonical signaling have mainly focused on the activation of small GTPases RHO, RAC, and JNK (Habas et al., 2001; Yamanaka et al., 2002; Habas et al., 2003; Habas and Dawid, 2005; Rosso et al., 2005). The small GTPases RAC and RHO are certainly important for neural tube development. Dorsal targeted dominant negative and constitutively active forms of RHO and RAC cause C/E defects in the frog (Tahinci and Symes, 2003). Dishevelled activation of RHO has been shown to be dependent on DAAM1 (Dishevelled associated activator of morphogenesis 1), a formin-like actin nucleator (Habas et al., 2001). The importance of RAC activation during C/E is further illustrated by observations that a single point mutant of DvlKM, the vertebrate

homologue of the fly *dsh*<sup>l</sup> allele, does not activate RAC in the a similar assay in which activation of RHO was observed (Park et al., 2005). The DvlKM mutation was thought to disrupt membrane association of Dvl. While evidence for this exists, a structural model implicates this lysine residue in an area well removed from a polybasic region electrochemically likely to interact with the cell membrane (Wang et al., 2006a; Simons et al., 2009). One hypothesis is that a protein-protein interaction is disrupted in the DvlKM protein that is responsible for the activation of Rac protein. As well, the residue might additionally provide an increased fidelity of membrane association through a more indirect protein-protein interaction (Simons et al., 2009).

Additionally, it may be important to focus on effects of the cytoskeleton, both actin and microtubules, as well the polarization of the Golgi stacks. These ideas are supported by work that shows the polarization of dynamic microtubule arrays via the microtubule capping protein EB3 (Shindo et al., 2008). Interestingly, the polarity of dynamic microtubules proceeds the formation of the lamellapodia; actin-rich structures shown to be disrupted in persistence and polarity in loss-of-function PCP assays of the neural plate cells (Wallingford et al., 2000). In addition, the polarity of the microtubule network proceeds any changes of the length to width ratio observed in cells undergoing C/E processes.

As well, the polarization of a cadre of subcellular organelles and protein complexes or W-RAMP was recently described (Witze et al., 2008). The W-RAMP structure after, Wnt-mediated Receptor-Actin-Mysin Polarity, was shown in cell culture to be dependent on Dvl2, Fz3 receptor, and PKC. This suggests that the W-RAMP structure may provide an accurate intracellular assay of PCP signaling. Interestingly, expression of dominant negative dynamin and Rab4 molecules disrupted the formation and polarity of the W-RAMP structures. This suggests that indeed PCP signaling is dependent on the endocytosis of the Fz receptor in the former and that PCP signaling might involve the activity of the recycling endosome in the latter.

By looking at the polarization of these major organelles and cytoplasmic macrostructures, we will be more able to unify the plethora of defects seen in PCP mutants models. As well, by understanding the basic cell biological processes of cell

polarity we will be better suited to initiate candidate gene approaches for hypothesis driven research. At least, we may better utilize the wealth of bioinformatics data that already exists concerning these processes.

#### **1.4.1.3. Genetic studies of Dishevelled**

In mouse, all three Dvl genes are reported to be broadly expressed during embryonic development and in adult tissues (Sussman et al., 1994; Klingensmith et al., 1996; Tsang et al., 1996). Recently, all three Dishevelled genes have been singly knocked out in the mouse; as well as, various combinations of double knockouts (Lijam et al., 1997; Hamblet et al., 2002; Etheridge et al., 2008).

Interestingly, loss of Dvl1 does not generate gross embryonic defects, rather the “normal” looking mice have defects in sensorimotor gating as well as defects in social behaviors such as grooming (Lijam et al., 1997).

Loss of function Dvl2 has higher degree of pleiotrophic developmental defects, such as malformations in the cardiac outflow tracts, an ~50% penetrance of other conotruncal defects, vertebral and rib malformations, defects somite segmentation as well a low penetrance of thoracic spina bifida (Hamblet et al., 2002). In the case of the cardiac defects, it was found that the expression of two cardiac neural crest markers, *Pitx2* and *Plexin A2* were diminished in the migrating crest as well as the outflow tracts of the developing heart. The defects of somite segmentation were assayed by looking at well-established markers of somite segmentation. *Myogenin*, a myotome marker was expressed normally however subtle expansion of expression that crossed the somite boundaries were observed. In addition, this was observed with *Uncx4.1*, a segment marker, taken together these results suggest a mild defect in somite segmentation.

In the case of the Dvl3 null mouse, conotruncal abnormalities, organ of Corti defects, a xiphoid bifurcation defects are observed (a process commonly seen in wild type litter mates) (Etheridge et al., 2008). The conotruncal defects include double outlet right ventricle (DORV), TGA transposition of the great arteries (TGA), and persistent truncus arteriosus (PTA). DORV is classified as a misconnection of the aorta to the right ventricle. Normally, only the pulmonary artery that carries blood to the lungs for oxygen arises



from the right ventricle. The aorta, which carries oxygenated blood from the heart to the body, normally arises from the left ventricle. TGA is observed in that the aorta and pulmonary artery are reversed. The aorta receives the oxygen-poor blood from the right ventricle, but it's carried back to the body without receiving more oxygen. Likewise, the pulmonary artery receives the oxygen-rich blood from the left ventricle but carries it back to the lungs. PTA is classified by occurs when the primitive truncus vessel does not divide into the pulmonary artery and aorta, resulting in a single large artery that overlies a ventricular septal defect. Consequently, a mixture of oxygenated and deoxygenated blood enters systemic, pulmonary, and coronary circulations.

In order to test for the redundancy of the function of the three Dvls, multiple combinations of homozygous Dvl mutants were examined (Etheridge et al., 2008). The incidence of a more severe form of neural tube closure defect craniorachishisis or a complete open neural tube from head to tail; as well, the defects in the axial skeleton and somite segmentation were greatly increased in Dvl1/2 double null mice. However, the double null Dvl1/2 null mice did not display an increase in the cardiac outflow tract defects, indication that Dvl1 is not redundant in function at least in this regard. In addition, the Dvl1/2 null mice displayed defects in the organ of Corti. The Dvl 1/3 homozygous null mice exhibit lethality between E13.5 and E 15.5. The Dvl3 null mice with one copy of Dvl2 exhibit lethality at E9.5, crainorachishisis, severe heart defects, and a posterior truncation.

In an attempt to further investigate the functional redundancy of individual Dvls the researchers used Bacterial Artificial Chromosome (BAC) clones to drive expression of different Dvls in the loss of function Dvl mouse backgrounds (Etheridge et al., 2008). In summary, Dvl1 or Dvl3 was able to rescue the conotruncal defects associated with the Dvl3-/- mice. However, Dvl1 was unable to rescue the heart defects in the Dvl2-/- mouse. There are considerable caveats associated with these experiment, such as expression levels of the individual Dvls from a BAC clone. True knock-in constructs under the control of endogenous promoters must be examined in order to truly understand if individual Dvls can function in the guise of another isoform.

### **1.5. Conclusion**

The Wnt dependent pathways of  $\beta$ -cat signaling and PCP are involved in most major development processes. In addition, multiple functions in the continued physiology of organismal life are dependent on these pathways. Much work has been devoted to the elucidation of the Wnts and Fz mechanism and transcriptional regulations. These experiments have largely been ignored for Dvl and the PCP effector genes. As these molecules have been shown to affect such a diverse list of development processes; the importance of understanding transcriptional regulation of these molecules on human health is apparent; In addition, the elucidation of the mechanisms of PCP signaling will likely generate interesting cell biology insights. In closing, the diverse forms of organismal life are largely defined by how they are shaped. A better understanding of the mechanisms and controls of the Dvls and the Dvl effector molecules will aid models of the mechanisms of the diversity of morphogenesis on this planet.

## **Chapter 2: Diversification of the Expression Patterns and Developmental Functions of the Dishevelled (Dvl) Gene Family during Chordate Evolution**

### **2.1. Introduction**

Dishevelled (Dvl) is a multi-functional adaptor protein that transduces both canonical Wnt/ $\beta$ -catenin and planar cell polarity (PCP) signaling pathways, and recent studies also suggest roles for Dvl in vesicle trafficking and microtubule organization (Wallingford and Habas, 2005). As a component of the canonical Wnt pathway, Dvl functions downstream of Frizzled to govern the activity of Axin and GSK3, thereby impacting  $\beta$ -catenin ( $\beta$ -cat) stability and nuclear localization (Baltzinger et al., 1999; Smalley et al., 1999; Amit et al., 2002; Bilic et al., 2007). Dvl has been implicated in a plethora of Wnt-mediated cell-fate specification events in multi-cellular animals including cnidarians, ecdysozoans, and deuterostomes (Noordermeer et al., 1994; Sokol et al., 1995; Weitzel et al., 2004; Lee et al., 2007b). Dvl-dependent PCP signaling controls a variety of polarized cell behaviors, including wing hair outgrowth in *Drosophila* (Theisen et al., 1994; Krasnow et al., 1995), and convergent extension cell movements, neural tube closure, and ciliogenesis in vertebrates (Sokol, 1996; Wallingford et al., 2000; Wallingford and Harland, 2002; Oishi et al., 2006; Wang et al., 2006a; Park et al., 2008).

Wnt ligands and their Frizzled receptors are encoded by multi-gene families, and the precise expression patterns of the many Wnt and Frizzled genes have been well documented in animals ranging from vertebrates to cnidarians (Hotta et al., 2003; Kusserow et al., 2005; Garriock and Krieg, 2007). Indeed, the developmental and evolutionary significance of the individual Wnt genes has been the subject of intensive studies (e.g. (van Amerongen and Berns, 2006)). Like the Wnts and Frizzleds, vertebrate Dvls are also encoded by a multi-gene family, and the recent explosion of genome data has revealed that the number of Dvl genes varies among deuterostomes from one in ascidians and sea urchins to three discrete Dvl genes in most vertebrates genomes (Hotta et al., 2003). Based on current models of vertebrate genome evolution, the presence of three vertebrate paralogs is most likely the result of two rounds of genome duplication

followed by gene loss of one of the paralogs (Sidow, 1996; Sidow et al., 1999; Wolfe, 2001; Dehal and Boore, 2005). Unlike the situation with Wnt and Frizzled genes however, the precise expression patterns and the developmental significance of the various Dvl genes has remained largely unexplored outside of the mouse.

Null mutants for Dvl1 in the mouse exhibit deficits in social interaction and sensorimotor gating (Lijam et al., 1997), and these mice display defects in synaptogenesis and in dendritic arborization (Rosso et al., 2005; Ahmad-Annuar et al., 2006). On the other hand, mouse Dvl2 is essential for normal cardiac morphogenesis, somite segmentation, and neural tube closure in the mouse (Hamblet et al., 2002). Mouse Dvl1 and Dvl2 are functionally redundant at least in part; the Dvl1/2 double null mutants display more severe phenotypes than the Dvl2 null mouse alone (Hamblet et al., 2002).

Our knowledge of the distinct developmental roles played by discrete Dvl genes in other vertebrates is almost completely lacking. Specific knockdown of *Xenopus* Dvl2 (previously called Xdsh, see below) has been shown to cause defects in the positioning of retinal progenitors (Lee et al., 2006), but the vast majority of experiments concerning Dvl function in other vertebrates have been carried out using dominant-negative constructs that are thought to disrupt the function of all three Dvls. As such, the specific roles of the different genes and the degree of redundancy among these genes, has not been investigated in vertebrate animals other than the mouse.

Dvl gene expression patterns have been reported for the mouse, where they are very broadly expressed (Sussman et al., 1994; Klingensmith et al., 1996; Steitz et al., 1996; Tissir and Goffinet, 2006). The broad expression patterns reported for Dvl genes in the mouse have been paraphrased as being ubiquitous, and so the transcriptional control of Dvl genes has been entirely ignored. Here, we show that the three Dvl genes have divergent and specific expression patterns in early embryogenesis in *Xenopus* and that these patterns differ significantly from those in the mouse. Moreover, we show that expression patterns of Dvl genes in the chick differ substantially from those in *Xenopus* and mouse. For a broader evolutionary perspective we investigated the expression of the single copy of Dvl during the development of hemichordates, an outgroup to chordates, and show it is also developmentally dynamic and tissue-specific.

To better understand the developmental control of Wnt signaling mechanisms, we will need to correlate specific Wnt-mediated developmental events with the various Dvl genes in a variety of vertebrate animals. We therefore report on the embryonic phenotypes that result from knockdown of specific Dvl genes in *Xenopus*. As described for mice, we find key roles for Dvl1 and Dvl2 in somite segmentation, while in contrast to the mouse, we observed specific roles for Dvl1 and Dvl2 in early neural crest specification. Finally, we identify a novel role for Dvl3 as a regulator of myotome and sclerotome cell fates in *Xenopus*. These *Xenopus*-specific functions for Dvl3 may reflect the evolutionarily derived mechanisms of muscle and sclerotome development in amphibia (Keller, 2000; Scaal and Wiegrefe, 2006; Handrigan and Wassersug, 2007).

Together, these data reveal a surprising divergence in the expression, and therefore, the function of specific Dvl genes in the vertebrates. Moreover, the data suggest that transcriptional control of Dvl gene expression may be an important regulator of Wnt-dependent developmental events in vertebrates, and when considered in combination with the spatially and temporally regulated expression of Dvl in hemichordates, this likely represents a common regulatory mechanism within the deuterostomes.

## **2.2. Divergence of Dvl genes during chordate evolution**

Examination of the *Xenopus tropicalis* genome and EST collections for both *tropicalis* and *laevis* reveal that *Xenopus* has three Dvl genes, as in mammals. We assigned *Xenopus* Dvl gene names based upon comparison of *Xenopus* sequence to known human and mouse orthologues. The original Xdsh clone has thus been re-assigned as *Xenopus* Dvl2 (U31552)(Sokol et al., 1995). We obtained full-length EST clones for Dvl1 and Dvl3 (CD362859 and BJ636385, respectively).

Phylogenetic analyses comparing *Xenopus*, human and mouse Dvl protein sequences clearly placed the three *Xenopus* Dvl genes into three different clades with orthologous mouse and human Dvls, strongly supporting orthology of each gene (Fig. 1). The genomes of deuterostomes vary in their number of Dvl genes, from one in hemichordates, urchins, and ascidians, to three in most vertebrates. We therefore

examined sequence information to begin to understand the divergence of Dvl genes in the deuterostomes. Hemichordates and sea urchins are basal deuterostomes, and like the non-deuterostome *Drosophila*, each has only one Dvl gene (Fig. 1). This is consistent with a model in which the common ancestor of deuterostomes had only one Dvl gene. The other deuterostomes, the chordates, are divided into three groups: the urochordates (including ascidians), cephalochordates (including *Amphioxus*) and vertebrates. Ascidians have only one Dvl gene, but interestingly, searches of EST data identify two Dvl genes in the genome assembly of the cephalochordate amphioxus (*Branchiostoma fl.* (Putnam et al., 2008)). Phylogenetic analyses place these two genes within their own clade, separate from the vertebrate Dvls (Fig. 1), indicating these genes are a product of a duplication within the cephalochordate lineage, independent of gene duplications in the vertebrate lineage. Together, these data suggest there was one Dvl gene in the common ancestor of chordates.

Of the three Dvl genes in most vertebrates, phylogenetic analysis suggests Dvl2 and Dvl3 form a clade distinct from Dvl1 (Fig. 1). This suggests that within the vertebrate lineage, the ancestral Dvl duplicated once to produce two lineages represented by Dvl1 and Dvl2/3, and a secondary duplication in the latter gene lineage produced Dvl2 and Dvl3. If these duplications are a result of the two whole-genome duplications early within the vertebrate lineage, then another paralogue within the Dvl1 subfamily (Dvl4) was subsequently lost. While, a Dishevelled homologue named DVL1L1 or DVL4; localized to the human chromosome 22q11; this gene does not reflect a full length Dvl protein (Pizzuti et al., 1996).

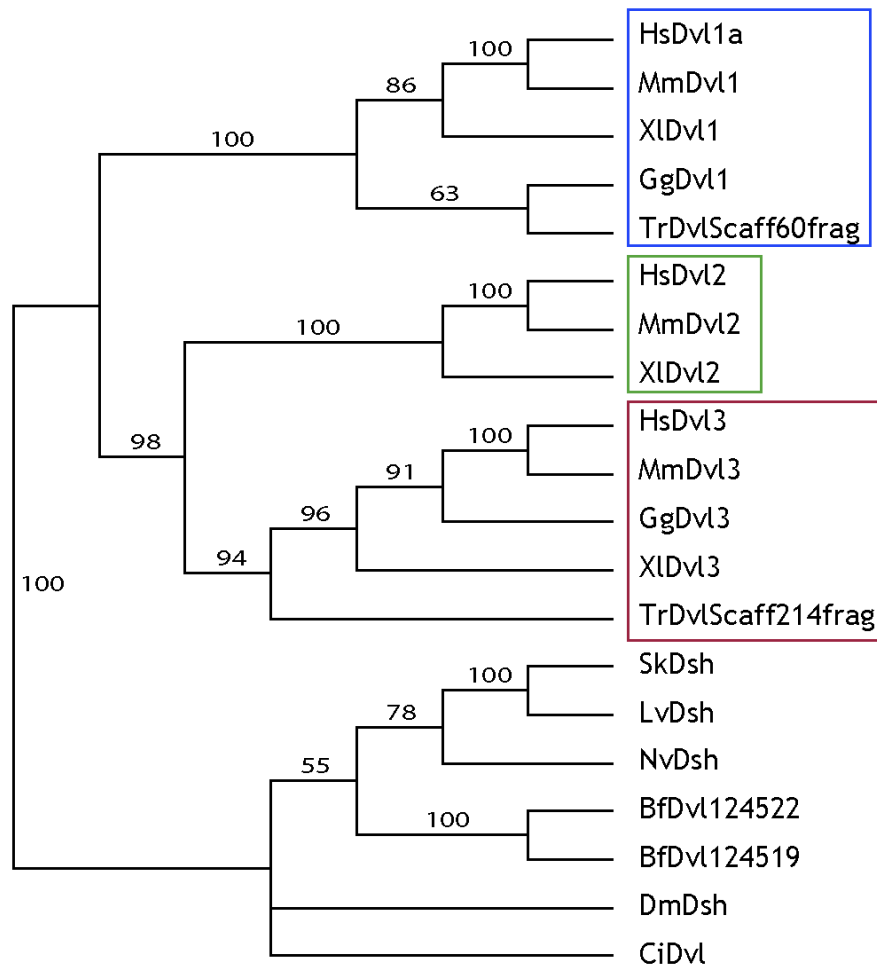


**Figure 1: Phylogenetic analysis of Dishevelled (Dvl) family genes.** Blue box outlines Dvl1 family genes. Green box outlines Dvl2 family genes. Red box outlines Dvl3 family genes. Hs- *Homo sapiens*; Mm- *Mus musculus*; Xl- *Xenopus laevis*; Gg- *Gallus gallus*; Tr- *Takifugu rubripes*; Sk- *Saccoglossus kowalevskii*; Lv- *Lytechinus variegates*; Nv- *Nematostella vetensis*; Bf- *Branchiostoma floridae*; Dm- *Drosophila melanogaster*; Ci- *Ciona intestinalis*. This figure was produced in collaboration with Stephen A. Green and Christopher J. Lowe.

### **2.2.1. The patterns of Dvl1, Dvl2, and Dvl3 expression differ substantially between mouse and *Xenopus***

To understand the roles played by Dvl1, Dvl2 and Dvl3 during *Xenopus* development, we first examined their expression patterns by *in situ* hybridization. The pattern of Dvl1 expression in *Xenopus* shares some similarity with the expression of Dvl1 in the mouse, in particular the robust expression in the neural tube and somites (Fig. 2-4) (Sussman et al., 1994). Moreover, later strong expression of Dvl1 in the cranial placodes of *Xenopus* (Fig. 4) may reflect expression of mouse Dvl1 in cranial ganglia (Sussman et al., 1994; Tissir and Goffinet, 2006).

To our surprise however, there were several important points of divergence between the expression patterns of Dvl1 in *Xenopus* and mouse. For example, while Dvl1 is not expressed in the mouse node (Sussman et al., 1994), Dvl1 was robustly expressed during gastrulation in involuting dorsal tissues, with pan-dorsal expression during neurulation (Fig. 2A-C; Fig. 3). The most significant difference was the strong and specific expression of Dvl1 in the developing neural crest and in the otic placodes (Fig. 2A, B; Fig. 4).



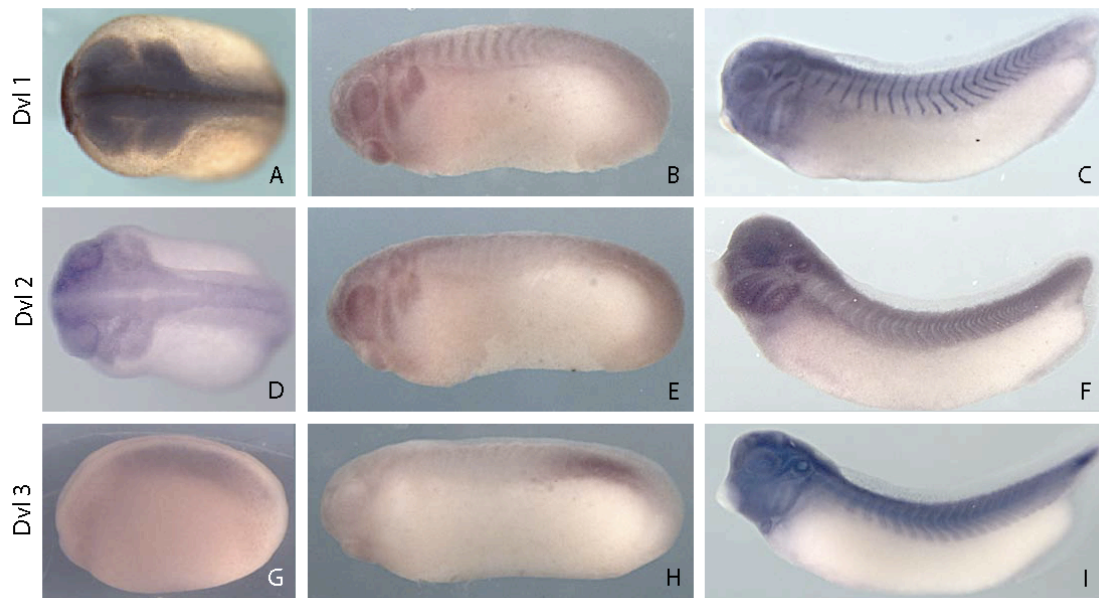


**Figure 2: Divergent expression patterns of Dvl1, Dvl2, and Dvl3 in *Xenopus* embryos.** (A): Dorsal view of a stage 20 embryo exhibits Dvl1 expression in neural crest, optic placodes, and neural folds. (B): Lateral view of a stage 23 embryo shows continued Dvl1 expression in the streaming cranial neural crest and the developing eye, as well as the otic placodes and the segmenting somites. (C): Lateral view of a stage 29/30 embryo expressing Dvl1 in the somites and in multiple cranial placodes (see Supp Fig. 2). (D): Dorsal view of a stage 22 embryo exhibiting Dvl2 expression in the streaming cranial neural crest, developing eyes, and neural folds. (E): Lateral view of a stage 23 embryo expressing Dvl2 in the otic placodes, neural crest and eyes. (F): Lateral view of a stage 29/30 embryo exhibits Dvl2 staining in the somites, developing eye, and branchial arches. (G): Lateral view of a stage 18 embryo expressing Dvl3 in paraxial mesoderm. (H): Lateral view of a stage 23 embryo exhibits Dvl3 expression in the presomitic mesoderm and developing somitomeres. (I): Lateral view of a stage 35/36 embryo expressing Dvl3 in mature somites, multiple head placodes, and the developing heart.

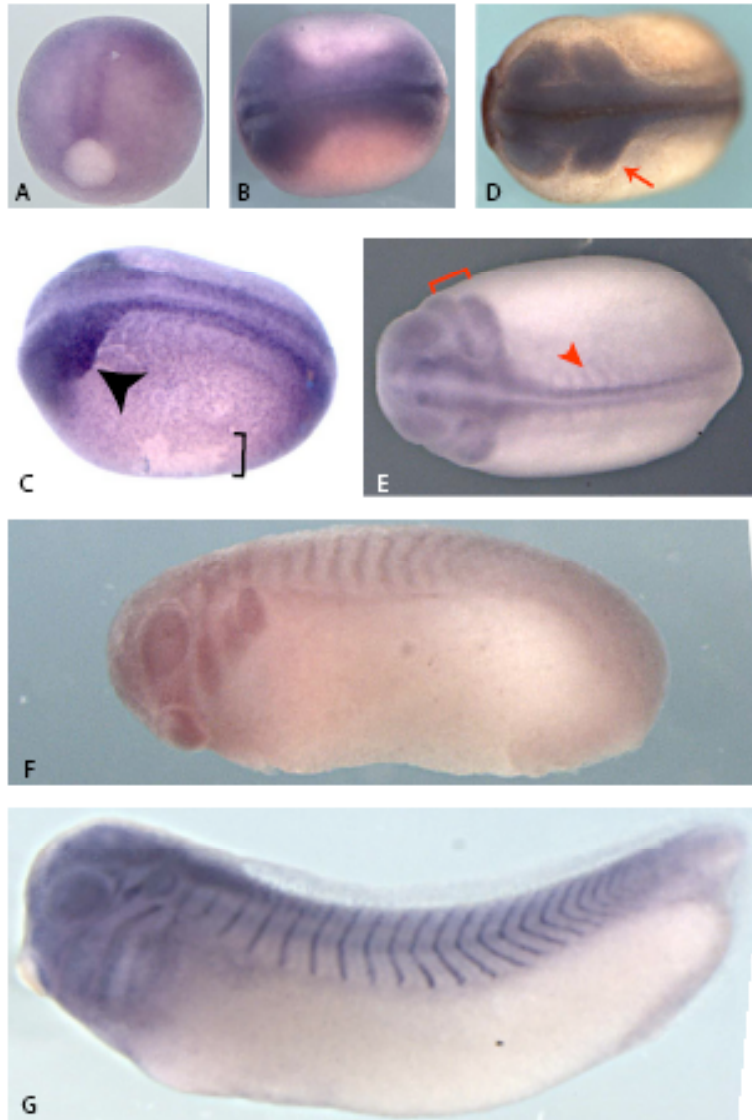


**Figure 3: Dvl1 *in situ* hybridization.**

(A): stage 12 embryo exhibiting staining in the involuting dorsal marginal zone. (B): stage 13/14 embryo displaying ubiquitous staining of the dorsal tissues. (C): stage 16/17 embryo shows an attenuation of staining to the neural folds. The neural crest exhibit increased *in situ* staining (black arrowhead). This over stained embryo exhibits the presence of spotted ectodermal staining. The black bracket outlines peeling of the epithelium. (D): Stage 20 dorsal view unbleached embryo exhibits staining in the developing forebrain, eye cups, and the streaming neural crest (red arrow). (E): Stage 21 embryo dorsal view exhibits staining in the streaming neural crest (red bracket), eyecups, and the developing forebrain. The anterior somites (red arrowhead) are beginning to express Dvl1 mRNA. (F): Stage 23 embryo exhibits continued staining in the streaming neural crest as well as the otic vesicle and the segmenting somites. (G): Stage 29/30 embryo shows continued nuclear somite expression as well as epidermal placodes.

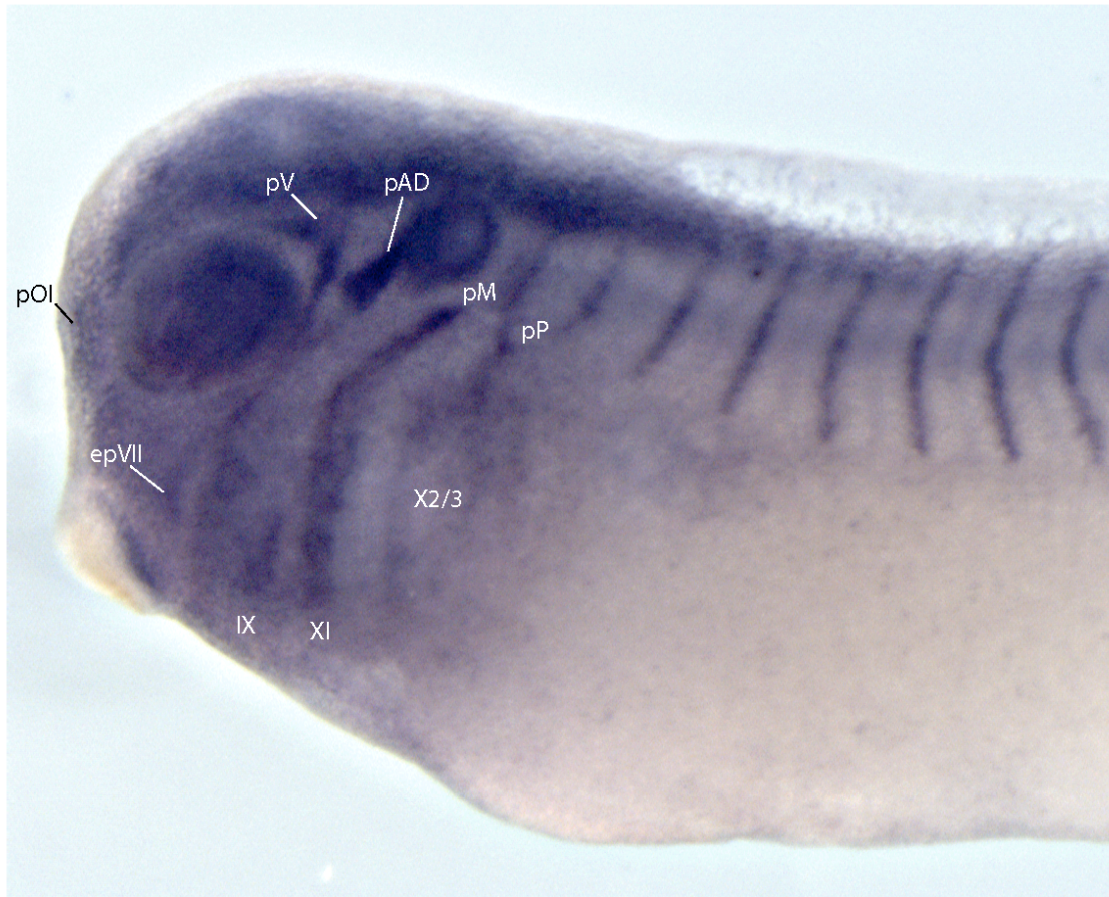


**Figure 4: Dvl1 expression in cranial placodes.**

Close up image of a 29/30 embryo *in situ* hybridized for Dvl1: olfactory placode (pOI), trigeminal placode (pV), anterodorsal lateral line placode (pAD), middle lateral line placode (pM), posteriorlateral line placode (pP), facial epibranchial placodes (epVII), glossopharyngeal placodes (epIX), first vagal epibranchial placode (epXI), and the fused second and third vagal epibranchial placodes (epX2/3).



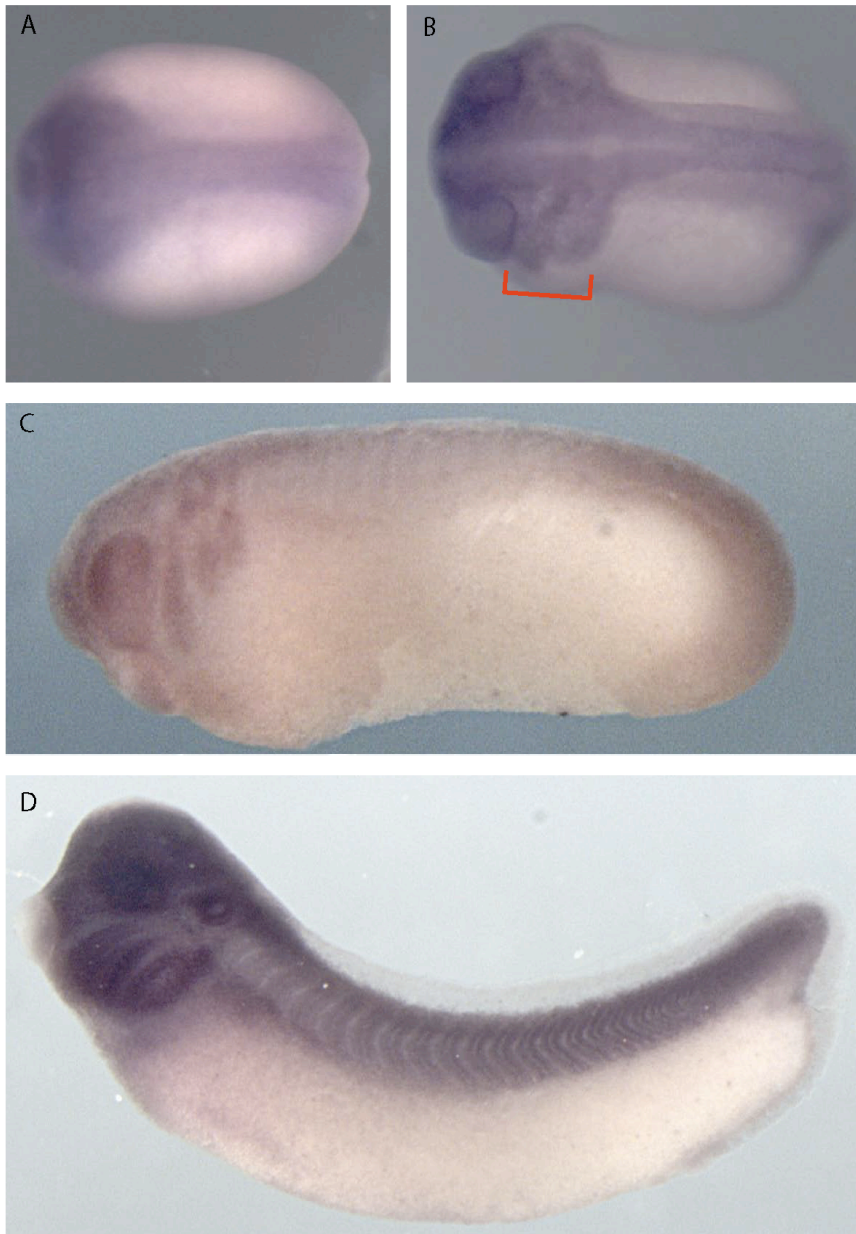


**Figure 5: Dvl2 *in situ* hybridization.**

(A): Stage 13/14 embryo exhibits general expression in dorsal tissue akin to Dvl1 expression. (B): Stage 21 dorsal view exhibits staining in the streaming neural crest (red bracket) as well as the developing forebrain and eye cups. (C): Stage 23 embryo exhibits staining in the otic vesicle, streaming cranial neural crest, and eye cups. (D): Stage 29/30 embryo exhibits staining in the somites, developing eyes, and branchial arches.

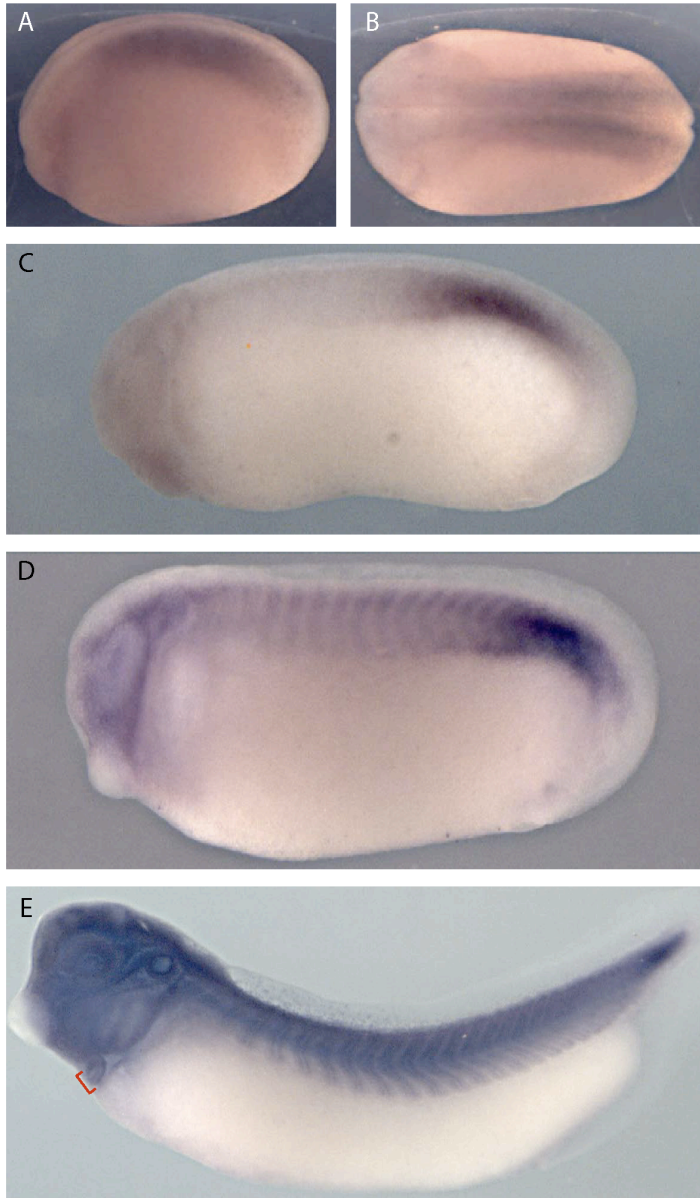


**Figure 6: Dvl3 *in situ* hybridization.**

(A): Lateral view stage 18 embryo exhibits staining in the presomitic mesoderm. (B): Dorsal view of a stage 18 embryo exhibits staining of the presomitic mesoderm. (C): Stage 23 embryo exhibits staining in the presomitic mesoderm and the developing somitomeres. (D): Stage 26/27 embryo exhibits staining in the otic vesicle and the somites as well as continued expression in the pre-somitic mesoderm. (E): Stage 35/36 embryos exhibit continued expression in somites, the developing head region, and the developing heart (red bracket).

Divergence in expression patterns between mouse and *Xenopus* was even more pronounced for Dvl2. In the mouse, embryonic Dvl2 expression has been reported to be essentially ubiquitous (Klingensmith et al., 1996; Tissir and Goffinet, 2006). By contrast, Dvl2 expression was highly upregulated in dorsal tissues during *Xenopus* neurulation, and strong expression of Dvl2 was observed in the migrating neural crest at early tailbud stages. At later tailbud stages, Dvl2 is very strongly expressed in the branchial arches, otic placodes and also in the somites (Fig. 2F; Fig. 5).

Most surprising was the divergence of the *Xenopus* Dvl3 expression patterns from those of other Dvl family members in *Xenopus* and also the divergence between Dvl3 expression patterns in *Xenopus* and mouse. In the mouse, early expression of Dvl3 is ubiquitous, but Dvl3 transcription is subsequently upregulated in neural tissue and somites, before again becoming ubiquitous (Tsang et al., 1996; Tissir and Goffinet, 2006). Dvl3 expression in *Xenopus* is entirely different. During neurulation, we consistently observed restriction of Dvl3 gene expression to the paraxial mesoderm and then later to presomitic mesoderm (Fig. 2G, H; Fig. 6). This pattern is maintained well into the late tailbud stages, at which time Dvl3 is also expressed in the developed somites. At these stages, we also observed strong Dvl3 expression in the heart and in a subset of cranial placodes (Fig. 2I; Fig. 6).

### **2.2.2. Dvl expression patterns in the chick differ substantially from those in *Xenopus***

Given that Dvl gene expression in the mouse has been thought to be somewhat ubiquitous, we found the divergent, tissue-specific expression patterns for Dvl genes in *Xenopus* to be striking. To ask whether or not such tissue-specific expression of Dvl genes was a general feature of vertebrate animals, we examined Dvl gene expression in the chick. In contrast to *Xenopus* and mouse, we identified only two Dvl homologues in the chick genome, consistent with previous reports (Sweetman et al., 2008). Based upon primary sequence, the two chick Dvls corresponded to Dvl1 and Dvl3 (Fig. 1).

The expression patterns of these two Dvl genes differed dramatically from those observed in *Xenopus*. Dvl1 was not detected by *in situ* hybridization in embryonic day 2 (E2) chick embryos (not shown), consistent with previous reports that it does not mediate

the PCP-dependent cell movements during chick gastrulation (Hardy et al., 2008; Sweetman et al., 2008). By E3, Dvl1 is very highly expressed, but its expression is largely restricted to the optic stalk and ventral forebrain (Fig. 7A). Upon longer exposure, Dvl1 was also detected throughout the ventral spinal cord and the notochord (Fig. 7a', a''). (We also observed staining in the midbrain and forebrain, but these are most likely artifacts of trapping of the chromogenic substrate in the lumen of the brain). We observed no expression of Dvl1 in the somites or neural crest in the chick.

In stark contrast to the very localized expression of Dvl3 in *Xenopus*, Chick Dvl3 was quite broadly expressed. At E2, Dvl3 was observed in the brain, spinal cord and in the somites (Fig. 7B). Examination in cross-section revealed an elevated level of *Dvl3* expression in the ventricular layer of cells in the spinal cord in addition to its localization in the presomitic mesoderm and the notochord (Fig. 7E). By E3, *Dvl3* expression remained within the neural tube, notochord, and the somites but also was observed in the eye and the fore- and hind-limb buds (Fig. 7C, D). Interestingly, *Dvl3* expression in the developing somites was restricted to the sclerotome as well as part of the dermomyotome (Fig. 7F, f').

### **2.2.3. Dvl transcription is tightly regulated in the embryos of the basal deuterostome, *Saccoglossus kowalevskii***

Because mouse, frog and chick homologs of Dvl have such divergent expression domains, we decided to examine the Dvl gene family in a non-chordate deuterostome phylum. The hemichordate *Saccoglossus kowalevskii* is a good outgroup for examinations of chordate Dvl genes (Lowe, 2008). We found one Dvl ortholog by searching the hemichordate EST library and genome trace archives. Sequence analysis shows that it is a homolog to vertebrate Dvl genes (Fig. 1). *In situ* hybridization of this Dvl gene shows expression is limited to specific tissues during early development (Fig. 8).

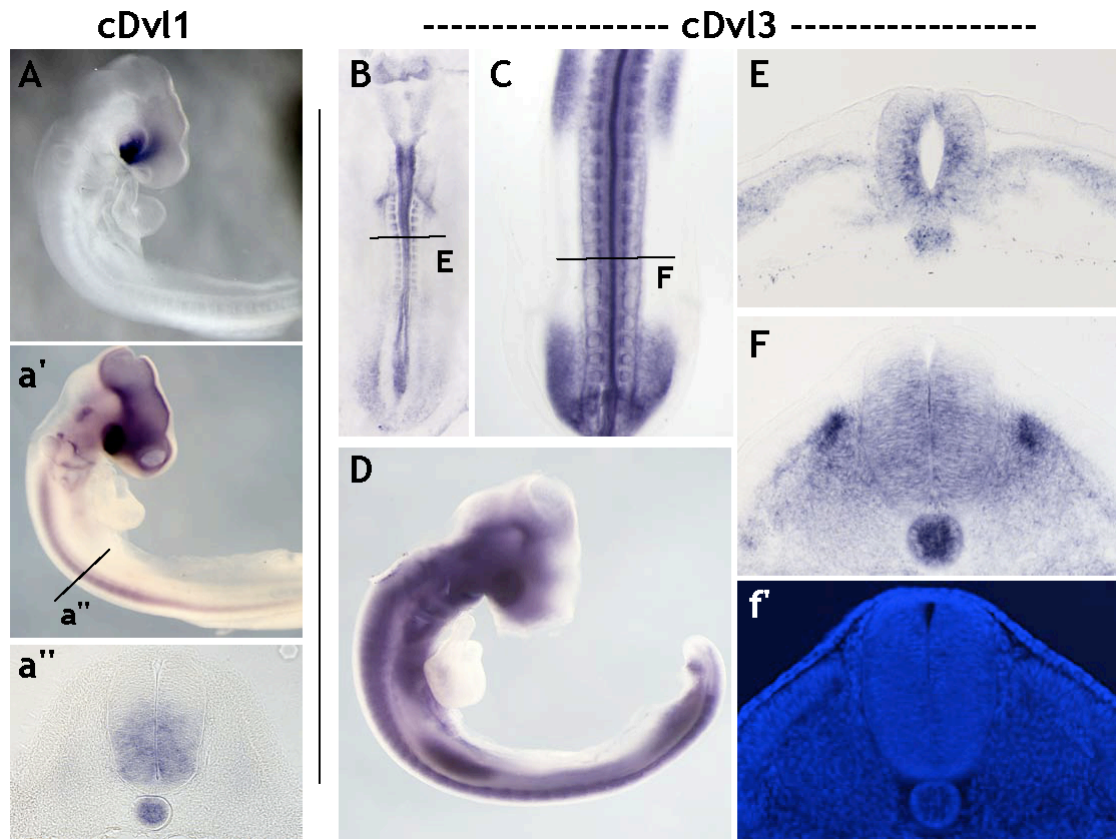


**Figure 7: Divergent expression patterns of *Dvl1* and *Dvl3* in the chick.** (A): Lateral view of *Dvl1* expression in an E3 chicken embryo. *Dvl1* transcripts are strongly localized to the optic stalk and the ventral forebrain. (a'): Extending the length of the color development reveals *Dvl1* expression throughout the midbrain, forebrain, eye, spinal cord and notochord. (a''): A cross-section through the spinal cord at the level indicated in (a'). *Dvl1* expression is restricted to the notochord and the ventral spinal cord. (B): Dorsal view of *Dvl3* expression in an E2 chicken embryo. *Dvl3* is expressed in the somites, the tail bud, and throughout the neural tube. (C): Dorsal view of *Dvl3* expression in the posterior half of an E3 chicken embryo. *Dvl3* expression remains within the neural tube and somites, but is also present in the fore- and hind-limb buds. (D): Lateral view of *Dvl3* expression in an E3 embryo. (E): A cross-section through an E2 embryo as indicated in (B). *Dvl3* is expressed in the neural tube, the notochord and presomitic mesoderm. Note the elevated level of *Dvl3* expression within the cells of the ventricular layer. (F): A cross-section through an E3 embryo as indicated in (C). *Dvl3* transcripts are observed in the notochord and the entire spinal cord except for the dorsal-most region. *Dvl3* expression in the developing somites is restricted to the ventral dermomyotome, the dorsal sclerotome and the myotome itself. Note the increased level of *Dvl3* expression in the medial dermomyotome. (f'): DAPI staining of the section shown in (F) clearly reveals the organization of the somite and the cells within. This figure was produced in collaboration with Roy D. Bayly and Seema Agarwala.



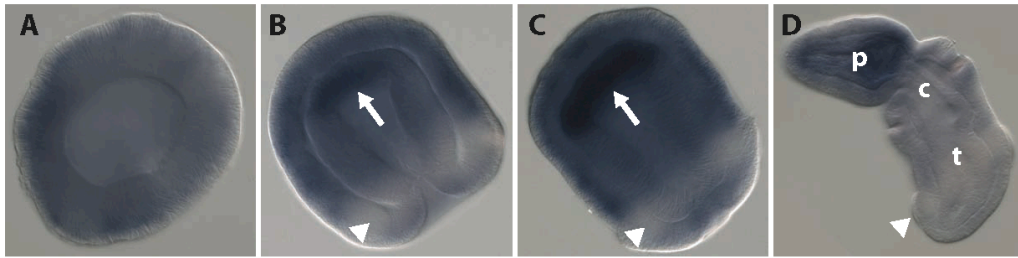


**Figure 8: Wholemount *in situ* hybridization of *S. kowalevskii* *Dvl*** at the following stages: a) blastula, b) gastrula, c) elongating gastrula, and d) prehatching juvenile. All embryos are shown with anterior to the upper left, and the juvenile embryo has dorsal positioned to the upper right. White arrows indicate *Dvl* up regulation in the anterior mesoderm, and the white arrowheads note the location of the ectodermal ciliated band. p: proboscis, c: collar, t: trunk. This figure was produced solely by Stephen A. Green and Christopher J. Lowe.

In blastulae, Dvl is expressed ubiquitously, but by gastrulation Dvl is downregulated in the posterior ectoderm surrounding the ciliated band (Fig. 8A, B). During late gastrulation, Dvl is heavily upregulated in anterior mesoderm, but downregulated in endoderm and posterior mesoderm. In juveniles, Dvl is expressed heavily in the anterior, including the ectoderm and mesoderm, but in posterior tissues is either expressed at lower levels or is completely absent (Fig. 8C, D).

Thus, expression patterns of *S. kowalevskii* Dvl are highly regulated and tissue-specific, including expression within the ectoderm and mesoderm. Since both a non-chordate and vertebrates show extensive regulation of Dvl genes at the level of transcription, it is highly likely that ancestral chordate Dvl gene was subject to temporal and spatial transcriptional regulation during early development.

### **2.3. Dishevelled Family gene functions during neural crest induction**

#### **2.3.1. Knockdown of Dvl1 and Dvl2, but not Dvl3, disrupts early neural crest specification in *Xenopus***

Because the Dvl genes have divergent expression patterns in *Xenopus* embryos as compared to mouse embryos, we next sought to uncover the developmental functions of the three Dvls in *Xenopus* and to ask if the assignment of specific Dvl genes to specific developmental events varied between *Xenopus* and mice. We have generated translation-blocking morpholinos (MOs) that specifically target each Dvl gene in *Xenopus* (Table 1). The specificity of these MOs for particular *Xenopus* Dvls has been demonstrated previously using *in vitro* translated proteins and western blotting of embryo lysates with anti-Dvl antibodies (Park et al., 2008).

Dorsally-targeted triple knockdown of all *Xenopus* Dvls resulted in defects consistent with previous reports using dominant-negative to disrupt Dishevelled function (Sokol et al., 1995; Sokol, 1996). We observed failure of convergent extension and defects in the anterior-posterior pattern of the central nervous system (not shown). The aim of this study, however, is to understand gene-specific Dvl functions and how they differ between vertebrates. One key difference in Dvl gene expression between mouse

and *Xenopus* is the strong and specific expression of Dvl1 and Dvl2 in the *Xenopus* neural crest. Dominant-negative studies have implicated Dvl in mediating PCP signals that govern neural crest migration in *Xenopus* (De Calisto et al., 2005), but the role of Dvl in early neural crest specification has not been directly examined. Canonical Wnt signaling is known to be crucial to *Xenopus* neural crest induction (LaBonne and Bronner-Fraser, 1998b; Monsoro-Burq et al., 2005), though this mechanism may not be conserved in amniotes (Schmidt et al., 2007).

To probe the significance of the strong expression of Dvl in *Xenopus* neural crest, we injected Dvl1 MO to one dorsal-lateral blastomere at the 16-cell stage of development in order to unilaterally affect the presumptive neural crest (Moody and Kline, 1990). MOs were co-injected with a fluorescent dextran lineage tracer, and only properly targeted embryos (Fig. 9A', B') were processed for *in situ* hybridization for Slug as a marker of early neural crest and Twist as a marker of later neural crest (Aybar et al., 2003). Injection of the Dvl1 MO at a high dose disrupted the expression of Slug in over 80% of embryos (Fig. 9A, C). At later stages, the Dvl1 morphants showed similar disruptions of Twist expression (Fig. 9B, D).

To demonstrate the specificity of this neural crest phenotype, we designed a 5-bp mismatch MO to Dvl1 (Dvl1MMMO). Injection of this Dvl1MMMO at a high dose had no effect on Slug or Twist expression (Fig. 9C', D'). Moreover, the effects of Dvl1MO were dose-dependent; co-injection of one-half doses of Dvl1MO and the Dvl1MMMO resulted in a dramatic reduction in the number of embryos with disrupted Slug or Twist expression as compared to injection of a high dose of Dvl1MO alone (Fig. 9C, D).

Dvl2 is co-expressed in the *Xenopus* neural crest with Dvl1, so we next tested the role of Dvl2 in neural crest specification. Like Dvl1 morphants, Dvl2 morphants also failed to express Slug or Twist (Fig. 9C, D). Consistent with functional redundancy between Dvl1 and Dvl2, we observed that injection of a combined half-dose of Dvl1MO and Dvl2MO resulted in neural crest defects equivalent to injection of a full dose of either MO alone. In contrast, injection of a half doses of the Dvl2MO and Dvl1MMMO(s) resulted in far fewer disruptions of slug or twist expression (Fig. 9C',

D'). These data indicate that the MO phenotypes are specific and that Dvl1 and Dvl2 share some functional redundancy in mediating neural crest induction in *Xenopus*.

Gene →	Dvl1	Dvl2	Dvl3
Morpholinos:			
Dvl1	0	5	4
Dvl1 MM	5	7	9
Dvl2	9	0	9
Dvl3	4	5	0
Dvl3B	12	11	0
Dvl3 MM	9	7	5

**Table 1: Dvl morpholino binding mismatches compared to all *Xenopus laevis* Dvl genes.** MM= 5 base pair mismatch; B= alternate MO targeting a non-overlapping sequence in the 5'-UTR.

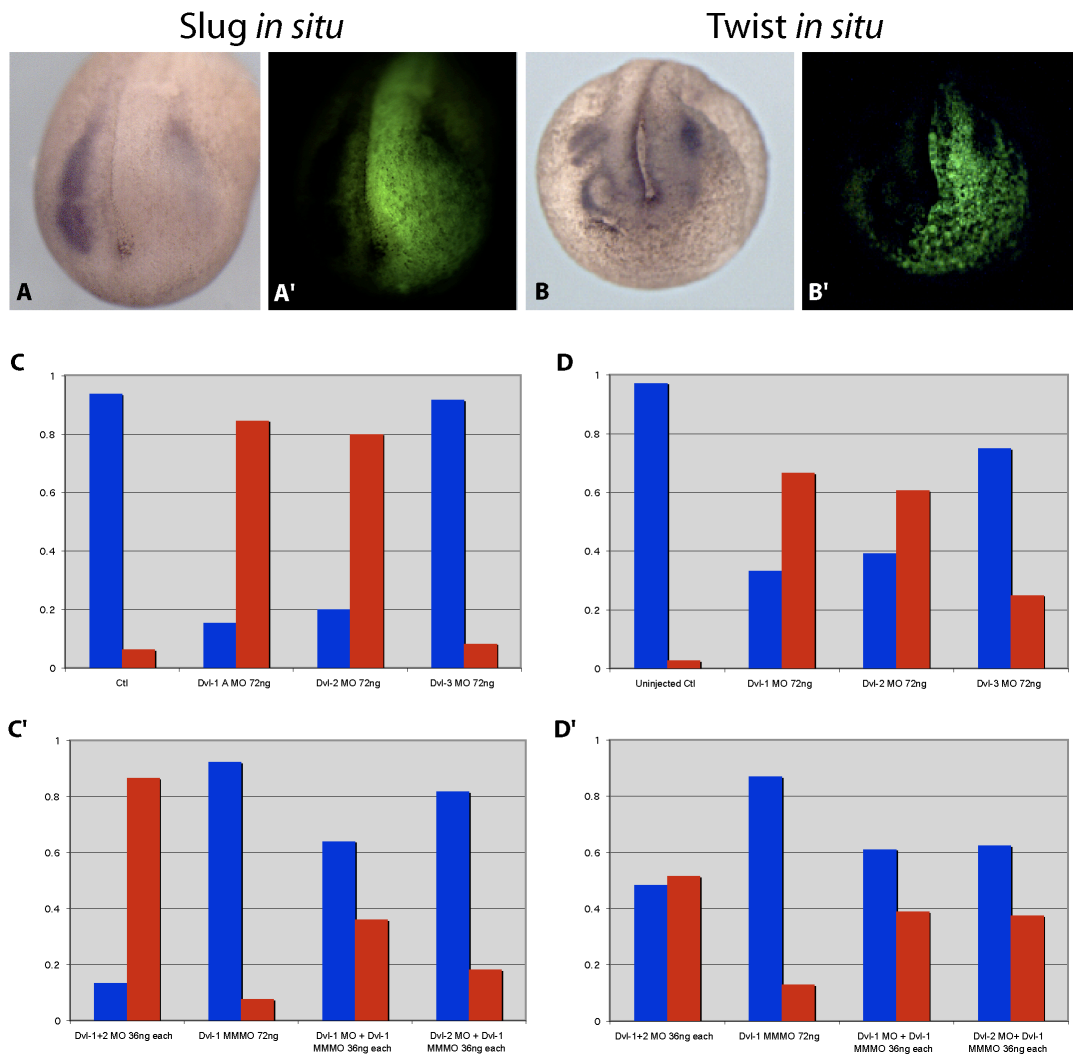


**Figure 9: Neural crest induction in *Xenopus* requires Dvl1 and Dvl2, but not Dvl3.** (A-A''): Unilateral injection of MOs + GFP mRNA targeted to one dorsal lateral blastomere of a 16 cell embryo. Slug expression is lost on the injected side due to Dvl1 and Dvl2 morpholinos. (B-B''): Dvl1 and Dvl2 MOs eliminate expression of Twist. (C-C'): Graphs of combined morpholino data for Slug *in situ* hybridizations. Uninjected Control N=16; Dvl-1MO 72ng N=26; Dvl-2MO 72ng N=10; Dvl-3MO 72ng N=12; Dvl-1MO + Dvl-2MNO 36ng each N=15; Dvl-1MMMO 72ng N=13; Dvl-1MO + Dvl-1MMMO 36ng each N=25; Dvl-2MO + Dvl-1MMMO 36 ng each N=11. (D and D'): Graphs of combined data for Twist *in situ* hybridizations. Uninjected Control N=36; Dvl-1MO 72ng N=84; Dvl-2MO 72ng N=28; Dvl-3MO 72ng N=20; Dvl-1MO + Dvl-2MNO 36ng each N=31; Dvl-1MMMO 72ng N=54; Dvl-1MO + Dvl-1MMMO 36ng each N=18; Dvl-2MO + Dvl-1MMMO 36 ng each N=24.

As a final control, we injected our MO targeted against Dvl3. Consistent with the absence of Dvl3 expression in early neural crest (Fig. 7G, H), injection of a full dose of the Dvl3MO had no effect on Slug expression (Fig. 9C). Dvl3 MO had a very modest effect on the later expression of Twist, consistent with Dvl3's low level expression in the crest at later stages (Fig. 6D). Serendipitously, our Dvl3MO differs from our Dvl1 MO by only 4bps (Table 1), so the Dvl3 MO serves as an important control for specificity. Injection of the Dvl3MO did not disrupt early neural crest induction, but did consistently elicit specific defects in somite development that were not observed with Dvl1MO or Dvl2MO (see below). Thus, dose-dependent MO phenotypes for each Dvl gene correlated with sites of expression for each Dvl, while mismatched MOs had no effect. Taken together, these data suggest that Dvl1 and Dvl2, but not Dvl3, are necessary to mediate the Wnt-dependent signals that control neural crest specification in *Xenopus* (e.g. (LaBonne and Bronner-Fraser, 1998a; Monsoro-Burq et al., 2005)). This result is important, as it highlights the divergent roles of the three vertebrate Dvl genes in the development of different animals. No neural crest-specific expression has been reported for any mouse Dvl. Dvl1 mutant mice do not display neural crest defects (Lijam et al., 1997), but neural crest does contribute importantly to the development of the cardiac outflow tracts, and these are defective in mice lacking Dvl2 (Hamblet et al., 2002).

## **2.4. Dishevelled family genes function during somitogenesis**

### **2.4.1. A conserved role for Dvl1 and Dvl2 in somite segmentation**

*Xenopus* Dvl genes are expressed in divergent patterns in the developing somite and presomitic mesoderm (Fig. 2). In order to study the role of Dvls in somitogenesis while avoiding early morphogenetic defects, we targeted our MOs to a subset of the presumptive somites using ventral-vegetal injections (Moody and Kline, 1990; Afonin et al., 2006). Targeted injections of the Dvl1 or Dvl2 MOs alone or a combination of Dvl1 and Dvl2 MOs resulted in embryos that were short in length and that displayed defects in somite boundary formation. Using Immunostaining for 12/101 and for fibronectin, we observed both failure of boundary formation, and ectopic boundary formation in Dvl1 and Dvl2 morphants (Fig. 10C, D; data not shown). In these morphants, the expression

of MyoD was maintained throughout the somite (Fig. 11B). This phenotype is consistent with studies in mice lacking Dvl1 and Dvl2 (Hamblet et al., 2002).

#### **2.4.2. A novel role for Dvl3 in the maintenance of muscle cell identity in *Xenopus***

The most striking difference between mouse and *Xenopus* Dvls was the strong and specific expression of Dvl3 in the *Xenopus* presomitic and somitic mesoderm (Fig. 2). This unique pattern of Dvl3 expression is interesting given that somite development is highly derived in amphibians in general, and that somitogenesis is highly variable among the anurans, being particularly derived in *Xenopus* (Keller, 2000; Scaal and Wiegrefe, 2006; Handrigan and Wassersug, 2007). It is thought that the derivation of somite development in amphibians is an adaptation to their initially-aquatic lifestyle; the tadpole tail lacks an osseous skeleton and is more flexible than that of most fishes (Hoff and Wassersug, 2000; Handrigan and Wassersug, 2007). To better understand the role of this unique domain of Dvl3 expression in *Xenopus*, we examined the effects of targeted Dvl3 knockdown in the somites.

In contrast to Dvl1 and Dvl2, Dvl3 knockdown had little effect on somite segmentation (Fig. 10). Reflecting their highly derived nature, *Xenopus* somites are formed from mesenchymal, rather than epithelial, cells. These cells are initially oriented perpendicular to the anteroposterior axis; the cells then rotate *en mass* to take on their final orientation parallel to the long axis (Afonin et al., 2006; Handrigan and Wassersug, 2007). However, we observed anteroposteriorly aligned cells in Dvl3 morphants, suggesting no role for Dvl3 in somite rotation (Fig. 10E).

We did however consistently observe an attenuation of MyoD expression in the anterior somites of Dvl3 morphants (Fig. 11C, E). Curiously, this decrease of anterior MyoD expression was not accompanied by a decrease in anterior 12/101 staining (Fig. 11E'), suggesting that somites had been patterned normally, but that MyoD expression was not maintained. We observed a similar phenotype when we examined Myf5. Myf5 expression in the body of the somite was reduced anteriorly, though expression in epaxial and hypaxial muscle was unaffected by these injections (Fig. 11G). As with MyoD, the reduction of Myf5 was not accompanied by loss of 12/101 staining (Fig. 11G').

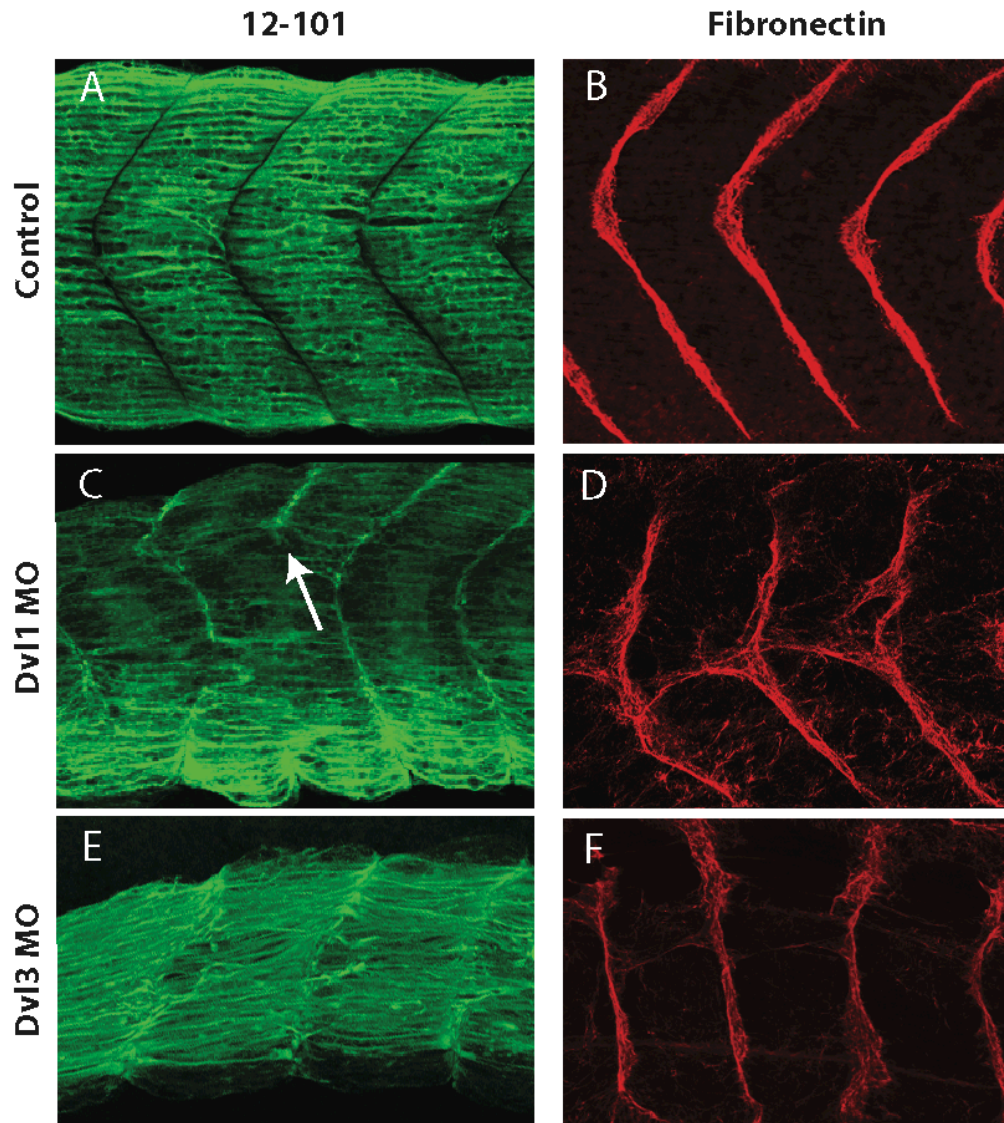


**Figure 10: Divergent, gene-specific somite defects in Dvl morphants.**

Lateral confocal projections displaying somite morphology of Dvl morphants with a muscle specific mouse anti-12/101 antibody (green) and the somite boundaries with a mouse anti-fibronectin antibody (red). (A): Normal morphology of the medial flank of a stage 29/30 embryo (B): Normal fibronectin deposition in somite boundaries stage 29/30 embryo. (C): Dvl1 morphant stage 29/30 embryo displaying segmentation defect (white arrow) (D): Dvl1 morphant stage 29/30 embryo displays defects in the deposition of fibronectin (red) while “chevron” shape is conserved. (E): Dvl3 morphant stage 29/30 embryo displaying un-“chevrone’d” somites and multiple cells are disrespecting the established somite boundaries. (F): Dvl3 morphant stage 29/30 embryo displaying normal deposition of fibronectin between un-“chevrone’d” boundaries.



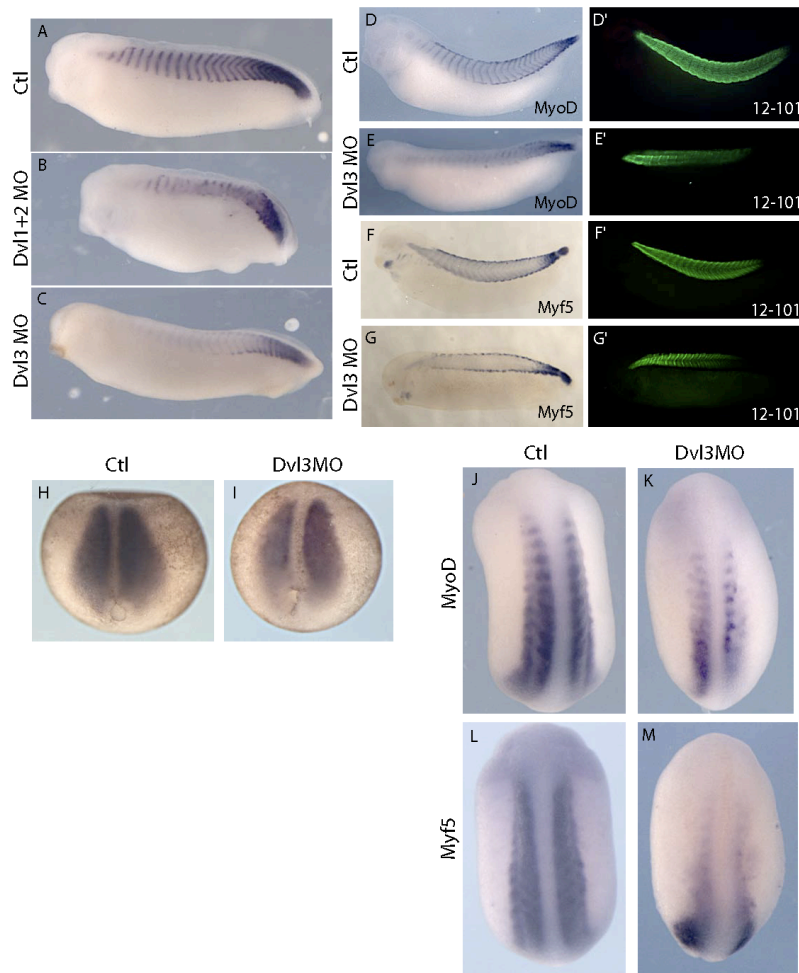


**Figure 11: Knockdown of distinct Dishevelled genes generates distinct somite phenotypes.**

(A): *In situ* hybridization to MyoD at control stage 29/30. (B): Injection of Dvl1+2MO cocktail yields shorter embryos that exhibit a disruption of the normal MyoD pattern. (C): Dvl3 morphants are normal in length, but embryos exhibit diminished anterior MyoD expression. (D): St. 32, normal MyoD (purple) *in situ* hybridization and (D') 12/101 (green) antibody staining. (E): In Dvl3 morphants, MyoD expression is reduced anteriorly but 12/101 (E') is maintained. 12/101 staining is increased at the somite boundaries (red arrows). (F): Normal Myf5 expression (purple) within somites and along both epaxial and hypaxial somite edges and (F') normal 12/101 staining. (G): Myf5 staining of the hypaxial and epaxial somite edges appear unaffected in Dvl3 morphants, but expression is lost within the somites, though 12/101 is maintained (G'). (H): Control stage 13 *in situ* hybridization for MyoD. (I): Sibling stage 13 Dvl3 morphant embryo *in situ* hybridized to MyoD (purple). (J, L): Normal expression patterns of bHLH myogenic transcription factors; MyoD and Myf5 at stage 22. (K, M): Reduced anterior expression of assayed myogenic markers in Dvl3 morphants at stage 22.

Several lines of evidence demonstrate that this somite phenotype was specific for Dvl3. First, we observed the same loss of anterior MyoD expression with a second, independent Dvl3 MO (Table 1; data not shown). Second, a 5bp mismatched MO for Dvl3 had no effect on MyoD expression (data not shown). Third, and most compellingly, our Dvl1 MO differs from the Dvl3 mRNA sequence by only 4bp (Table 1), but injection of Dvl1 MO consistently disrupted somite segmentation and did not attenuate anterior MyoD expression (Fig. 11B; Fig. 10C).

The absence of MyoD expression in the anterior somites of Dvl3 morphants could stem from a failure to initiate or a failure to maintain muscle cell fates. We therefore assessed the expression of myogenic regulatory factors at a variety of stages in Dvl3 morphants. When assessed at stage 13, Dvl3 morphants displayed no significant loss of MyoD or Myf5 (Fig. 11I; data not shown). By contrast, we found that expression of MyoD, Myf5, and also MyoS (another bHLH myogenic regulator) was clearly disrupted in anterior regions at early tailbud stages in Dvl3 morphant embryos (Fig. 11K, M; data not shown). These data reveal a novel, Dvl3-specific function in the maintenance of differentiated somitic muscle in *Xenopus*. We have found no reports of a similar phenotype following manipulation of Wnt signaling in other animals, so this result may reflect the highly derived nature of somitogenesis in *Xenopus*. This *Xenopus*-specific role for Dvl3 in muscle cell fate specification may be related to the delayed multi-nucleation of myocytes in anuran amphibians or to the fact that multi-nucleation in anurans involves nuclear divisions rather than the cell fusions observed in amniotes (Handrigan and Wassersug, 2007).

#### **2.4.3. A novel role for Dvl3 in sclerotome development in *Xenopus***

In addition to the curious mode of myotome development in amphibians, the nature of sclerotome development of amphibian embryos is evolutionarily derived. Though this tissue has received very little attention, it is clear that multiple modes of sclerotome development exist even within the amphibia (Geetha-Loganathan et al., 2006). In contrast to the chick, the sclerotome of amphibians is extremely small and difficult to visualize (Handrigan and Wassersug, 2007). In *Xenopus* the small number of sclerotome

cells segregates from the myotome and takes up a peri-notochordal position (Youn et al., 1980; Handrigan and Wassersug, 2007). The molecular basis of sclerotome development in amphibia is almost entirely unexplored, so we asked if the divergent, specific expression of Dvl3 might be related to sclerotome development. Paraxis is a known Wnt target gene in chick and is involved in sclerotome development (Linker et al., 2005; Takahashi et al., 2007), so we were encouraged to find that Paraxis expression was decreased and disordered in Dvl3 morphants (Fig. 12A, B).

We next examined the expression of Pax-1, which is expressed in the sclerotome of most vertebrates, including *Xenopus* (Handrigan and Wassersug, 2007). Pax-1 was strongly expressed perinotochordally, consistent with the location of *Xenopus* sclerotome cells (Fig. 12C). In Dvl3 morphants, perinotochordal Pax1 expression was almost entirely eliminated, though expression in the branchial arches (not targeted by injection) was unaffected (Fig. 12D). These results suggest that the unique and specific expression of *Xenopus* Dvl3 in the presomitic region is required for the derived mode of sclerotome development in this animal.

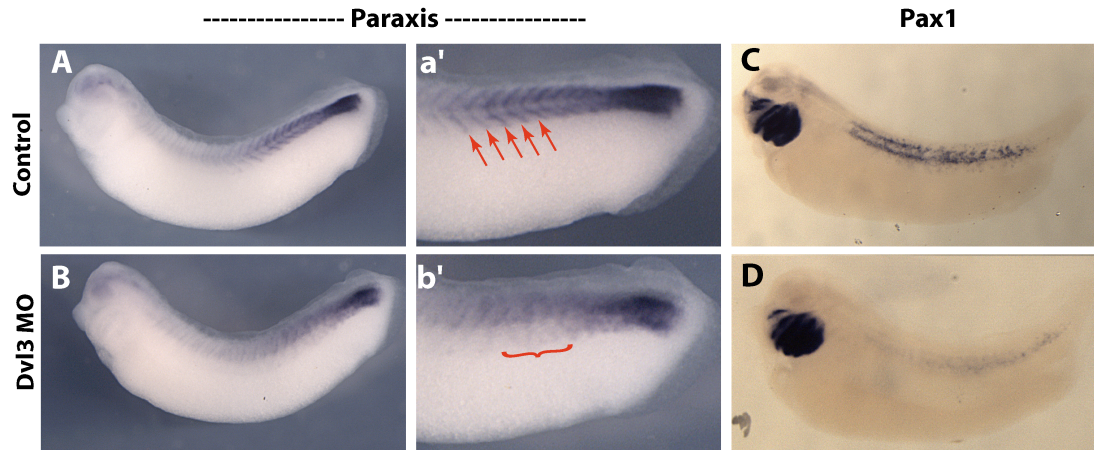


**Figure 12: Knockdown of Dvl3 in presomitic mesodermal tissues disrupts normal expression of both paraxis and Pax-1 genes.**

(A-B): single stage 29/30 tailbud stage embryo. (A): Control uninjected side displays normal paraxis expression in the posterior presomitic mesoderm and within individual somites. (a') A magnified image of posterior half of the (A) side of the embryo. (B): morpholino injected side displays a loss of paraxis expression within individual somites as well as diminished expression in the unsegmented mesoderm. (b') A magnified image of the posterior half of the (B) side of the embryo. (C): Normal expression of Pax-1 in a wild type stage 37 embryo in the branchial arches and perinotochordal region. (D): Dvl3 morphants lack any appreciable Pax-1 staining surrounding the notochord (targeted by injection) while the brachial arches (not targeted by injection) retain Pax-1 expression. Red arrows point to paraxis expression within individual somites. Red bracket highlights defects in both expression and patterning of paraxis transcript expression.

## 2.5 Discussion

Wnts and Frizzleds are members of large gene families, and the developmental functions of these proteins are controlled in part by the restricted expression patterns of the genes that encode them. For example, Wnt11 plays key roles in early dorsal patterning in *Xenopus*, while ventrally-expressed Wnt8 is central to patterning ventral structures (Christian et al., 1991; Tao et al., 2005). Indeed, a role for patterned expression of Wnt genes is conserved from vertebrates (Garriock et al., 2007) to basal metazoans, such as cnidarians and sponges (Kusserow et al., 2005).

By contrast, the Dvls form a three-member gene family in most vertebrates, but the expression patterns and developmental functions of Dvls have received little attention. Here, we have reported detailed expression patterns for all Dvl genes in *Xenopus* and in the chick. We find that in contrast to the mouse, Dvl genes' expression is spatially and temporally dynamic, and remarkably divergent between these two vertebrates. Moreover, we have expanded the comparative scope of the project by investigating Dvl expression outside of vertebrates, during the development of a basally branching deuterostome, the hemichordate *S. kowalevskii*. Dvl expression is also dynamic and tissue-specific in this animal. These data demonstrate that tissue specific, temporal and spatial regulation of Dvl transcription may be a general feature of deuterostomes. Furthermore, our data strongly suggest there was one Dvl gene in the common ancestor of chordates and that this gene was duplicated independently in both cephalochordate and vertebrate lineages.

We have also systematically knocked down the three Dvls in *Xenopus*. Consistent with previous experiments using dominant-negative constructs, we show a role for Dvl in axis elongation and in anteroposterior patterning of the central nervous system in *Xenopus*. Moreover, we show that the specific role for Dvl1 and Dvl2 in somite segmentation identified in the mouse is conserved in *Xenopus*. We also find that Dvl1 and Dvl2 specifically transduce the canonical Wnt signals that specify neural crest in *Xenopus*, a role not conserved in mice. Canonical Wnt signals also specify neural crest in the chick (Garcia-Castro et al., 2002), so in light of the expression data shown here, we would predict that Dvl3 mediates that signal in the chick.

Finally, we report here that the loss-of-function phenotype for Dvl3 in *Xenopus* is entirely divergent from that of Dvl3 in the mouse (Etheridge et al., 2008). We report a novel role for Dvl3 in somite patterning in *Xenopus*, where our data suggest a specific requirement for Dvl3 in mediating Wnt-dependent signals that maintain muscle cell identity and direct sclerotome development. This *Xenopus*-specific function for Dvl3 likely reflects the highly derived mechanism of amphibian somite development (Scaal and Wiegrefe, 2006; Handrigan and Wassersug, 2007). Moreover, the result suggests that evolutionary changes to Dvl paralogue function during vertebrate diversification have resulted in a range of developmental roles for the lineage specific patterns reported here.

This study demonstrates that Dvl gene transcription is, as a general rule, highly regulated during vertebrate development and identifies specific developmental phenotypes resulting from knockdown of Dvl1, Dvl2, and Dvl3 in *Xenopus*. A recent study has found that the different Dvl proteins have subtly differing abilities to transduce Wnt signals (Lee et al., 2008b). However, other studies have suggested that the different Dvl proteins behave interchangeably (Rothbacher et al., 1995). The dramatically different phenotypes we observed following Dvl knockdowns correlate with the temporal and spatial domains of Dvl gene transcription. We think it likely that the result of this study reflect an important, but previously ignored, role for transcriptional control of Dvl gene expression as an important regulator of Wnt-dependent patterning events in vertebrate embryos. Furthermore, it is likely that tight transcriptional regulation of Dvl expression is a common feature of, at least deuterostomes, and possibly all metazoans.

## Chapter 3: Planar Cell Polarity Effector Gene Family

### 3.1. Introduction

Loss of function alleles of a class a PCP effector genes: *fuzzy* (*fy*/Fuz); *inturned* (*in*/Intu); *fritz* (*frtz*/Frtz); and *multiple wing hairs* (*mwh*/Mwh) were classified as epistatic to mutant allele of the core PCP genes; *frizzled* (*fz*/Fz), *dishevelled* (*dsh*/Dvl), and *Van Gogh* (*Vang*/Stbm) (Gene names as *Drosophila*/Vertebrate nomenclature) (Gubb and García-Bellido, 1982; Wong and Adler, 1993; Lee and Adler, 2002; Collier et al., 2005; Taylor et al 1998). More plainly, defects of *frtz*, *fy*, *in*, or *mwh* fly mutant wing hair epidermis, seen as multiple pre-hair initiations and subsequently two or more wing hair outgrowths, where the wild type hair cell has only one wing hair, are not synergistic in any mutant backgrounds of the core PCP genes: Fz, Dsh, or Vang.

Surprisingly, despite additional evidence that the PCP effector genes are required for the intracellular signals downstream of Fz signaling there is paucity biochemical or cell biological information for the mechanisms of these genes. However, recent works wonderfully illustrate the concept that the vertebrate homologues of Intu and Fuz are important for convergent-extension movements in the frog (Park et 2007). Additionally, it was discovered that the loss-of-function Intu or Fuz generates defects of ciliogenesis. Importantly, loss of cilia in the neural tube results in defective hedgehog signaling (Hh) during early mouse development (Huangfu et al., 2003). These results firmly established the importance of understanding the intracellular mechanisms downstream of Fz/Dvl signaling.

### 3.2. Cell biology and embryology of PCP effector genes

The classifications of PCP ‘effector’ genes were made from observations of a screen for genes responsible for the polarity of the wing hair outgrowths (reviewed by Adler and Lee 2001). The resulting defects observed in the fly wings are as follows; Group I comprises the ‘core’ PCP genes: Fz, Dvl, and Prickle. These genes are characterized by apical actin bundles resulting in a wing hair outgrowth near the geometric center of the

cell; Group II comprises the PCP ‘effector’ genes, *in*, *fy*, and *fritz*. This set of mutants exhibit multiple ectopic actin accumulations which result in multiple wing hair outgrowth near the periphery of the cell membranes; While a third Group III contains only one member, the *mwh*. This comprises multiple actin bundles that are late forming and develop multiple wing hairs as seen in group II mutants (Collier et al., 2005). Additionally, *mwh* cells develop multiple very small pre-hair remnants or secondary hairs, not seen in the group II mutants. Additional studies indeed classified the genes: *fuzzy*; *inturned*; *fritz*; and *mwh* among others as epistatic and downstream of Fz/Dvl dependent signaling events in the wing hair epidermis (Adler and Lee, 2001).

### **3.2.1. PCP effector proteins and the cytoskeleton**

These initial observations led to a hypothesis that PCP effector genes are adaptors of the cytoskeleton downstream of Dvl (Lee and Adler 2002). Indeed, the disruption of the microtubules dynamic by tubulin binding drugs, vinblastine and colchicines, generates a multiple wing hair phenotype. However, these perturbations do not affect the polarity of the winghair outgrowth, seen with disruptions of the PCP effector genes (Lee and Adler 2002). Additionally, it was reported that PCP effector mutant did not display any noticeable disruptions with the microtubule networks; as well, micro-injection of vinblastin into *in* or *fy* mutants produced additive wing hair defects; moreover, double mutant combinations of the PCP effector genes are not synergistic (Wong and Adler 1993; Lee and Adler 2002). These data suggest that the defects in wing hair development via mutations in the PCP effectors are independent of defects seen in colchicine or vinblastine treated embryos. Thus, *fy* and *int* are functioning in a single pathway to effect PCP events.

In a solitary study in the frog, no gross defects were observed with microtubules dynamics (Park et al., 2006). However, the formation of the tubulin-rich cilia was affected in overall localization within the cell. The normal deposition of the cilia in the multi-ciliated frog epidermis is well above the apical surface; morpholinos targeted to both *Intu* and *Fuz* displayed defects in the apical extension of cilia resulting in large masses of tubulin staining structures below the apical surface (Park et al 2006). However,



in these same experiments it was observed that the formation of an apical localized actin ‘mat’ was severely disrupted in ciliated cells of both *Intu* and *Fuz* morphant embryos. In contrast, mutants of the *mwh* gene in fly multiple exhibit ectopic actin bundles in the wing epidermis (Strutt et al 2008). This is most likely reflective of multiple differences between the cells type and organisms studied rather than dramatic functional differences.

### **3.2.2. PCP complex subcellular localization**

In both the fly and the frog, *Intu* has been observed to accumulate at the cell membranes (Park et al 2006; Adler et al 2004). At least in the fly, *Intu* is localized at the proximal cell membrane of wing epidermal cell, while a GFP-*Intu Xenopus* fusion protein localizes to cell membranes, as well at diffuse apical foci in ciliated cells of the frog epidermis (Adler 2004; Park 2006). Both *Fritz* and *Multiple wing hairs* protein localizes and is enriched at the proximal cell membranes of the fly wing epidermis using indirect immunofluorescence (Strutt et al 2008). No accounts of *Fuzzy* protein localization have been published; however, this work describes preliminary evidence that *Fuz* is localized to apical structures within ciliated cells as well as cell membranes in all cell types of the frog epidermis (Fig. 13).

The proximal localization of the PCP effector genes is interesting; as they are much removed from the actual wing hair initiation site in the wild type wing; and given these gene products directly affect the wing hair initiation. It has been put forth the *Intu/Fuz/Frtz* complex might be negatively regulating pre-hair initiation in a proximal-distal gradient or the complex is setting up an intracellular polarity that aids in the distal establishment of the pre-hair initiation site (Adler 2004). Recent evidence suggests the former (Strutt 2008), while this work gives some impetus to the latter (Chapters 4 and 5). Additionally, loss-of-function of individual PCP effector genes does not cause dramatic non-autonomous effects on neighboring cells, observed with core PCP genes (Adler 2004; Strutt 2008). This concept may further support a proximally directed mechanism of the PCP effector proteins despite the distal localization in the fly wing epidermis. Finally, either hypothetical mechanism given above need not be mutually exclusive.

As alluded to in the preceding paragraph, it is clear that a Fuz/Intu/Frtz protein complex is localized to the proximal side of the fly wing cell. Indeed, multiple lines of evidence address this issue; Frtz localization is disrupted in both *fy* and *in* mutant clones, this is not the case in *mwh* mutants; Intu is mislocalized in both *fy* and *frtz* clones; Finally, Frtz is localized to apicolateral junctions with enrichment to proximal domains and this proximal localization is dependent on Stbm, a proximal marker accumulating protein (Strutt 2008 and Adler 2004).

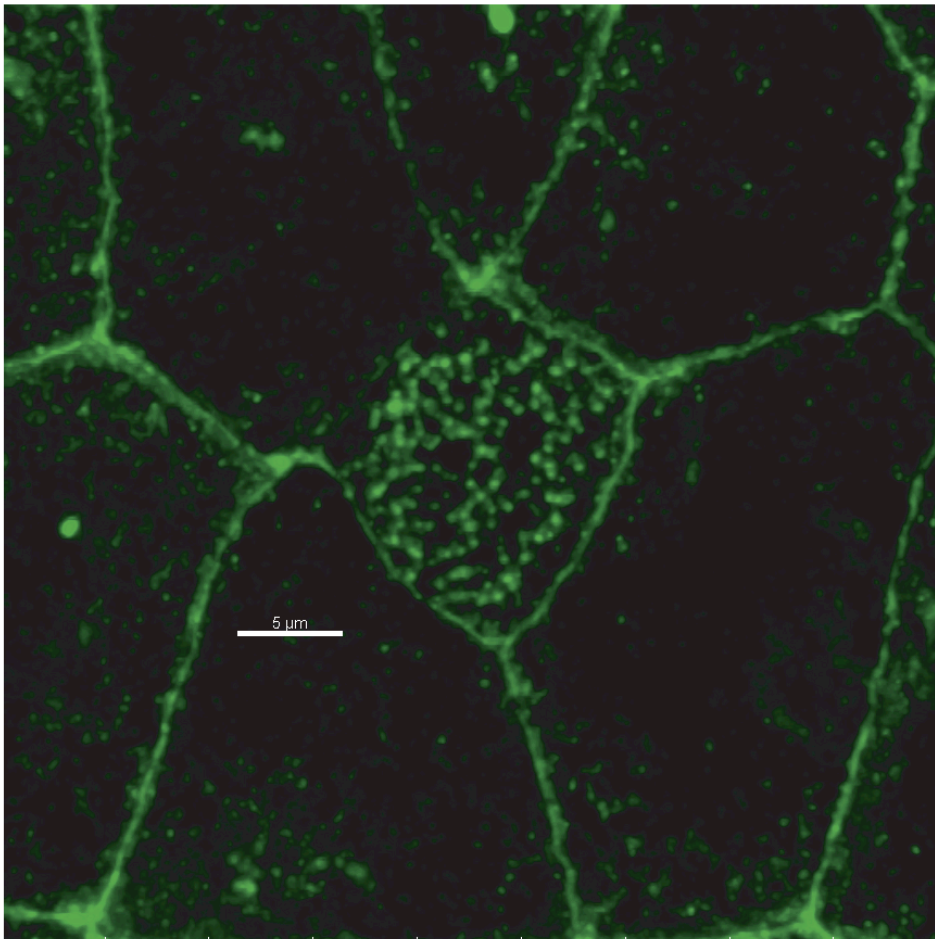


**Figure 13: *Xenopus laevis* Fuz antibody labels cell membranes and rootlet.** A peptide antibody generated in rabbit -PA0983; 1:100 dilution; Dent's Fix- shows localization of endogenous Fuz protein at the cell membranes of all epithelial cells and at the rootlet structure of the multi-ciliated cells.

It has also been reported that both fly Fy/Intu and frog Frtz/Intu physically interact (Lee, H dissertation 2002 and Park, TJ personal communication). It will be interesting to investigate physical interactions of all PCP effector proteins. This will require rigorous deletion mapping biochemistry and finally crystal structure analysis of the PCP effector interactions.

### **3.3. Molecular biology of PCP effectors**

#### **3.3.1. Sequence homologies of PCP effector genes**

Primary sequence homology searches for the PCP effector gene yields the following: Intu is a PDZ domain containing protein; Frtz is a  $\beta$ -propeller containing protein (Chapter 5.3), labeled as a WD-40 repeat contain protein in the fly (Collier et al 2005); Mwh is a formin like protein (Strutt et al 2008); and Fuz was predicted to contain a four-pass transmembrane domain and with both strong and weak alleles corresponding to loss of one or more of these putative membrane spanning motifs (Collier et al 1997). However, this work describes methods that suggest that Fuz may contain a longin-like domain. Longin-like domains are present in multiple proteins important for vesicle trafficking events of diverse proteins including the Sec22b protein (Chapter 4, Chapter 5.2; this work; (Rossi et al., 2004). Mwh have the best predictive sequence similarity to a novel formin like protein, assigning a probable function in actin nucleation (Strutt et al 2008) (Lu et al., 2007).

The remaining family members have yet to be described biochemically or cell biologically to any degree that yield helpful insights into molecular functions. This work again suggests a novel role for Fuz protein in vesicle trafficking events; as well, will attempt to integrate the remaining members in this role using bioinformatics data (Chapters 4 and 5). Clearly, *mwh* is epistatic to *fy*, *frtz*, and *int* (Strutt et al 2008; (Yan et al., 2008). Thus, at least one function of the presumed Fuz/Intu/Fritz interaction in fly wing epithelium is to regulate Mwh function. This is less likely in the vertebrate, given that a *bone fide* orthologue of Mwh does not appear to be present. However, multiple formin-like ORFs are contained in the human and frog genomes (personal observation). As well, there are clear defects of apical actin distribution in both Intu and Fuz morphant

embryos (Park et al., 2006). Lastly, Dvl and DAAM1, a formin-like molecule, are known to interact during C/E processes in the frog (Habas et al., 2001). Clearly, the mechanism of actin polymerization is conserved from the fly to vertebrates, it just does not appear to be conserved by an orthologue of Mwh in the vertebrates.

### **3.3.2. Molecular interactions of PCP effector proteins**

Almost nothing is known of the molecular mechanisms of Fuz/Intu/Fritz proteins. However, There are clear epistatic relationships between groups of PCP genes (Chapter 3.2). One mechanism of how the Fuz/Intu/Fritz complex function is in phosphorylation of Mwh. Endogenous Mwh protein was found to of a higher mobility than predicted by primary sequence. This higher mobility protein is repressible by addition of a phosphatase to wild type protein extracts or diminished in the protein extracts of *fritz* mutant embryos (Strutt et al 2008).

Interestingly, this loss of phosphorylation of Mwh protein is not recapitulated in either *stbm* or *fz* extracts. This suggests that perhaps even when the Intu/Fuz/Fritz complex is mislocalized, it is retaining some ability to positively affect Mwh phosphorylation events. Clearly, much work needs to be done to fully understand the molecular mechanisms of the PCP effector proteins.

### **3.4. Primary cilium: A crossroads of multiple developmental signaling events.**

The primary cilium, was once noted by many biologist to be a ‘vestigial’ organelle, of no functional significance (Federman and Nichols, 1974). Clearly, the past few years have greatly challenged that concept. It is now abundantly clear that the primary cilium of multiple cell types plays crucial roles in the ‘sensing’ and ‘processing’ of both extracellular ligands as well as physical forces. For instance Hh signaling events in a variety of cell types for the former and the mechanosensing abilities of the primary cilium of developing kidney cells and the cartilage and bone cells of the skeleton in the latter (Malone et al., 2007; Kolb and Nauli, 2008). For this, we must begin to integrate our understanding of developmental processes of cells and tissues with the formation and proper functioning of the cilium.

### **3.4.1. To move or not to move**

Cilium and a related organelle the flagella are mostly associated with mobility of diverse eukaryotic organisms and cells: the double cilium/flagella of the *Chlamydomonas reinhardtii* (Pan, 2008); the flagella of the sperm (Inaba, 2003); and the nodal cilia (Essner et al., 2002) to name a few. Most motile cilia are characterized by a 9+2 arrangement of microtubules (9 peripheral doublets surrounding a pair of central single microtubules) within the axoneme of the cilium. This is true of respiratory cilia and the ependymal cilia of the brain. However, the motile cilia of the embryonic node have 9+0 axonemes. Interestingly, rabbit motile nodal cilia are observed to have a 9+4 axonemal arrangement (Blum et al., 2007). Motile cilia generally exhibit a 9+0 axonemal arrangement as observed in renal monocilia and the photoreceptor connecting cilium structure (Adams et al., 2007). Again this is not necessarily indicative of function as observed in the non-motile 9+2 axoneme of the non-motile kinocilia of the inner ear (Nayak et al., 2007). It is generally accepted that non-motile cilia serve as the ‘signaling’ or ‘sensory’ cilia however we provide some indirect evidence that the motile cilia of the *Xenopus* epidermal multi-ciliated cells may serve to signal in some fashion (Chapter 5 this work).

### **3.4.2. The cilia and human disease**

A multitude human disease are now being directly attributed to defects in the formation of cilia (refer to as ciliogenesis) (Badano et al., 2006). A short listing of these ‘ciliopathies’ include: Polycystic kidney disease (PKD); Alstrom syndrome (ALMS); Bardet-Biedl syndrome (BBS); McKusick-Kaufman syndrome (MKKS); Meckel-Gruber syndrome (MKS); Oro-facial-digital type 1 (Odf1) syndrome; Joubert syndrome (JBTS); and Jeune’s asphyxiating thoracic dystrophy (JATD) ((Beales et al., 2007) and excellently reviewed by (Adams et al., 2008)). All of these ciliopathies share one or more developmental defects including: Cystic kidneys; Retinal degeneration and pigmentosa; *Situs inversus*; Anosmia; Respiratory problems; Infertility; Hydrocephalus; Neural tube defects; Polydactyly and skeletal defects; Conotruncal defects; Cognitive impairments;

Obesity; and Diabetes (Inglis et al., 2006). A cross-reference of all the malformations observed in known ciliopathies; Ranked list of these malformations likely to be the result of defective ciliogenesis are as follows: Dandy-Walker Malformation; Agenesis of Corpus Callosum; Situs inversus; Posterior encephalocele; Multicystic renal disease; Post-axial polydactyly; Hepatic disease; Retinitis pigmentosa; and Mental Retardation (Badano et al., 2006).

The phenotypes associated with MKS and JATD are particularly interesting in light of the loss-of-function *Fuz* mouse we report in Chapter 4 of this work. MKS is characterized by defects in renal, hepatic, and nervous systems. Additionally, cleft palate and polydactyly is commonly associated with MKS (Badano et al., 2006). While the *Fuz* mouse does not exhibit cleft palate, this process is known to be the result of defects in convergent-extension a PCP dependent process. Multiple genes have been associated with MKS; however, MKS 1 and MKS3 have been shown experimentally to localize to the cilia (Kyttala et al., 2006; Smith et al., 2006). Interestingly, a disruption of both MKS1/3 genes blocked centriole migration to the apical membrane thereby, completely inhibiting ciliogenesis (Dawe et al., 2007). This might help to explain the severity of defects seen in MKS patients as compared to less severe developmental phenotypes observed in BBS patients.

JATD as well exhibits multi-system disorders including: skeletal dysplasia (e.g. small ribcage) and severe chondrodysplasia; defects with renal, hepatic, pancreatic, and retinal abnormalities; as well, a mild shortening of all long bones (Hall et al., 2009). One cilia specific gene, IFT80, has been implicated in some JATD patients (Beales et al., 2007). Interestingly, we observe severe chondrodysplasia and shortening of the long bones in the *Fuz* loss-of-function mouse (Chapter 4 this work). Importantly, our observations are of a mild effect of the cilia biogenesis defect with a loss-of-function *Fuz*; as well, a loss of the single IFT complex B protein, IFT80 generate mild ciliogenesis defects (Beales et al., 2007).

What is abundantly clear from the preceding is that cilia are important for most tissues and organ systems of vertebrate organisms. As we begin to uncover more genes

necessary for building and maintaining cilia function, more human disease candidates will likely be explained in part by defects of cilia biogenesis and function.

### **3.4.3. Cilia are signaling organelles**

The primary cilium is now considered a crucial organelle for signal receiving and processing events in a variety of cell types. Currently three major developmental signaling pathways are suggested to require a functional primary cilium: Hedgehog (Hh); Wnt; and PDGFa reviewed by (Fliege et al., 2007; Bergmann et al., 2008).

The first major developmental pathway associated with defects in ciliogenesis were uncovered by two mutant alleles of the mouse orthologues of *Chlamydomonas* IFT172 and IFT88 (polaris), uncovered in a mutagenic screen for neural tube closure defects. Interestingly, these mice were observed to have convergent-extension defects associated with neural tube closure defects as well as unpredicted defects such as polydactyl and a loss of ventral cells types of the neural tube, commonly associated with defective Hh signaling (Huangfu et al., 2003). This synergy of both PCP and Hh signals are reminiscent of the developing somites (see review Chapter 1.3.3. this work).

The Hh pathway is characterized by a patched (Ptch) receptor that which inhibits a receptor smoothened (Smo) in the absence of Hh ligand. Transcriptional regulation of Hh target genes is carried out by GLI proteins (GLI 1-3). Wherein, the Ptch/Smo interaction generates a proteolytic dependent GLI3 Repressor (GLI3R) form. The GLI3R then translocates to the nucleus to keep Gli/Hh responsive genes turned off (Wong and Reiter, 2008). The defect in Hh signaling was further shown to be downstream of the Hh receptors, as *ptch/Ift172* and *smo/Ift172* mutants are phenotypically identical to *Ift172* single mutants (Huangfu and Anderson, 2005). This concept suggests that the IFT mechanism is necessary for all GLI processing events both activator and repressor forms (Liu et al., 2005; May et al., 2005).

Interestingly, the IFT122 deletion mutant mouse exhibits ciliogenesis and neural tube closure defects, however an expansion of ventral cell types in the neural tube were observed (Cortellino et al., 2009). However, this mutant mouse allele has a partial deletion of the MED1 gene. While this caveat exists, these experiments suggest that the

cilia are not just simple signaling centers. Rather, the cilium may serve as a processing unit of extracellular signals in a variety of cell types and signaling pathways. In the future, any models of cilia dependent signaling must be tempered by results observed in the IFT122 mutant mouse.

Multiple observations defects in Wnt and PCP signaling pathways have been made with mutant alleles of known cilia protein components (e.g. BBS and IFT proteins) (Quinlan et al., 2008). In addition, multiple mutant alleles of Wnt and PCP proteins have been shown to generate defects in ciliogenesis (Montcouquiol et al., 2003; Park et al., 2006; Deans et al., 2007; Park et al., 2008). This highly suggests that akin to Hh signaling, canonical and PCP Wnt signaling may dependent on functional cilia in order to receive and process these events. This idea is attractive as there are multiple tissues that synergize Hh/Wnt signaling throughout development, for example the development of the ventral neural tube and during somitogenesis ((Lei et al., 2006) and reviewed in Chapter 1.3.3. this work).

$\beta$ -arrestin ( $\beta$ -arr) localizes at primary cilia and mediates Smo localization (Kovacs et al., 2008). It is interesting that both Smo and Fz have structurally similar seven trans-membrane pass domains (7TMS), know to utilize  $\beta$ -arr during endocytic events (See Chapter 1.2.1.). In addition, multiple PCP proteins localize in or near cilium (e.g. Vangl2; Dvl; Fuz; Intu). This is very interesting considering that Wnt/Fz have also been shown to be dependent on  $\beta$ -arr dependent endocytosis (see Chapter 1.2.1.).

Direct evidence of a function of cilia on the canonical Wnt pathway is yet to be adequately given. While elevated  $\beta$ -cat signaling was reported in a conditional Kif3a deletion of the mouse kidney (Lin et al., 2003), this may reflect an inactivation of the PCP pathways of the developing nephrons. Furthermore, if the cilia of the kidney mesenchyme facilitates non-canonical pathway flux, then the cilia defects in these cells leads to ectopic activation of the canonical pathway. In addition, it is clear that Wnt signaling is not fully dependent on cilia, as *wnt3a* mutants die at gastrulation, much earlier than *kif3a* mutants (Yamaguchi et al., 1999; Huangfu et al., 2003).

The development of the kinocilium of the inner ear has been shown to be dependent on PCP signaling. As mutant alleles of Prickle-like 2 (Deans et al., 2007);



Frizzled 3/6 (Wang et al., 2006b); Vangl2 and Scribble (Montcouquiol et al., 2003) exhibit defects in the polarity and development of the inner ear kinocilia.

A model that the cilium constrains the canonical Wnt signaling arises from results of ciliogenesis defective mutants and from the presence of molecule known to inhibit canonical Wnt signals within the primary cilium. Using small interfering RNAs targeting a variety of ciliogenesis, genes (e.g. Kif3, Ift88, and Odf1) in cell culture; it was observed that canonical Wnt signaling was decreased. As well, primary culture of mouse embryonic fibroblasts (MEFs) from homozygous *kif3a* mutant mice showed increased response to Wnt3 using by a TOPFLASH LEF/TCF reporter assay. This increase in canonical signaling was shown *in vivo*, with the homozygous *kif3a* mouse and an extragenic beta-catenin-activated transgene (BATgal) reporter. This increased canonical signaling is correlated by hyper-phosphorylation of Dvl protein, which is dependent on casein-kinase I function (Corbit et al., 2008).

In addition, three molecules have recently been described to aid in the constraint of the canonical pathway: Inversin (Simons et al., 2005); *Seahorse* (Kishimoto et al., 2008); and nephrocystin-3 (Bergmann et al., 2008). Inversin has been shown to localize to the primary cilium and microtubule structure throughout the cell cycle in cell culture (Nurnberger et al., 2004). Moreover, mutations of the Inversin gene are linked to nephronophthisis type II, characterized by renal cysts, *situs inversus* and renal failure (Otto et al., 2003). As well, Inversin is reported to act as a switch between canonical and non-canonical signals; in that Dvl protein is targeted for degradation by Inversin protein. Additionally, Inversin was shown to be crucial for both C/E and gastrulation processes in *Xenopus*, both non-canonical dependent modes of morphogenesis (Simons et al., 2005). Furthermore, studies in the zebrafish showed that Inversin is localized to the primary cilia of kidney tubule cells in response to fluid flow. This conceptually implicates Inversin like molecules, PCP and cilia during specific development events. It will be very interesting to begin to understand the roles of these events during development and throughout the life cycle of the organism using targeted expression and drug inducible methods.

#### **3.4.4. Transit mechanisms of the cilia**

There are two main considerations of cilium directed trafficking of protein complexes or vesicles: how to get proteins and vesicles from the Golgi/ER to the cilia; and how to introduce protein complexes within the cilia. The brunt of the work addressing these questions has taken place in the *Chlamydomonas reinhardtii*. The concept of intraflagellar transport or IFT was first observed by differential interference contrast (DIC) imaging of the two cilia-like flagella of *Chlamydomonas*.

The numerous IFT mutants of *Chlamydomonas* provide a wonderful list of the basic mechanisms of ciliogenesis and ciliary function. I will address a few genes that uncover specific examples of these mechanism, however many wonderful reviews of this process have been reported previously (Rosenbaum and Witman, 2002; Scholey, 2003; Pedersen and Rosenbaum, 2008).

The three basic classes of IFT molecules are defined as follows: anterograde specific; retrograde specific; and Golgi to cilia transport. Of course, these classes are not necessarily mutually exclusive. The IFT genes originally characterized as anterograde are grouped as IFT B complex proteins including the anterograde motor protein kinesin-2 (Wedaman et al., 1996). The retrograde is grouped as the IFT A complex proteins including the retrograde motor protein Dynein-1B (Gibbons et al., 1994). A more recent class was observed by work with IFT20 (Follit et al., 2006). Wherein, IFT20 was shown to dynamically travel between the Golgi complex to the basal body and cilia. In addition, a loss-of-function IFT20 gives both a strong phenotype seen as a loss of cilia, while in some cases only certain proteins were disrupted in cilia localization. This implies a shuttling mechanism of IFT20 for specific cargoes traveling from the Golgi network to a cilium.

Some work has implicated cilia specific proteins as prototypical vesicle trafficking proteins. This interesting concept is supported by a high degree of sequence homology of domains commonly found in vesicle trafficking proteins. For example, both Complex A and B IFT proteins contain multiple examples of WD40/ $\beta$ -propeller (WD) domains and tetratricopeptide repeats (TRP); both domains are thought to act as scaffolds for protein-protein interactions (Cole, 2003). Interestingly, these protein domains are found throughout the vesicle coatomer proteins of the COP I/II and clathrin machinery; as well

as, the nuclear pore complex (Jekely and Arendt, 2006). These data suggest that interesting models for the evolutionary origins of the cilium

### 3.5. Conclusion

While there will be clear similarities in the mechanisms of PCP effector genes of the fly wing epidermis and the frog multi-ciliated cells, I would be remiss to not outline some distinct differences. While the fly wing epidermis exhibits a clear asymmetry of Fz/Dvl at the distal side that initiates the wing hair outgrowth, the multi-ciliated cell of the *Xenopus* epidermis contains a single Dvl foci situated near the basal body in the middle of a structure known as the rootlet (Park et al., 2008). It is currently not known where the “proximal” core PCP protein, Vang/Stbm or Prickle (Pk) reside in the multi-ciliated cells. However, Vangl1 and Vangl2 are present in primary cilia (unpublished personal communication). We will present preliminary evidence that Fuz protein is localized near the basal bodies. As well, a GFP-Intu fusion protein localizes in diffuse patterns at the apical surface of the ciliated cells, while Frtz is localized to cilia and the large secretory vesicles of the *Xenopus* epidermis (Park 2008 and TJ Park unpublished data). This implies that though Intu and Fuz are apically localized they are, like fly wing cell, not directly localized with Dvl. Thus, a similar mechanism may be co-opted in the physiology of the multi-ciliated cell.

Additionally, we have been unable to find a clear orthologue of Mwh in the human, mouse, or frog genome. The closest homologue is in fact a formin-like gene, however it is localized by *in situ* hybridization to a specific myeloid lineage and not in lineages that express other PCP effector gene transcripts (unpublished data). Possibly, vertebrate PCP effector proteins exhibit a conserved function (i.e. Mwh is phosphorylated) for yet to be discovered formin-like gene(s); alternately, the PCP effector gene products might function through non-homologous formin-like proteins (e.g. DAAM1).

## **Chapter 4: The Planar Cell Polarity Effector Fuzzy is Essential for Targeted Membrane Trafficking, Ciliogenesis, and Mouse Embryonic Development**

### **4.1. Introduction**

PCP signaling is essential for a variety of vertebrate developmental events, including morphogenesis of the neural tube, heart, kidney, and ear. Components of the pathway govern a wide array of polarized cellular behaviors, including cell intercalation and migration, cell division, and ciliogenesis (Karner et al., 2006; Wallingford, 2006). In *Drosophila* and *Xenopus*, the “PCP effector” proteins, including Fuz, act downstream of the “core” components such as Dishevelled (Dvl) (Lee and Adler, 2002; Park et al., 2006). The PCP effectors have received little attention, being the subject of only a single study in vertebrate animals (Park et al., 2008), whereas the core proteins have been the subject of intense study (Hamblet et al., 2002; Karner et al., 2006; Wallingford, 2006; Kibar et al., 2007b; Park et al., 2008). Fuz is essential for ciliogenesis in *Xenopus*, but its precise molecular function, like that of all intracellular PCP proteins, remains very poorly understood.

### **4.2. Mice lacking a functional Fuzzy gene display multiple developmental defects**

We asked if PCP effectors were essential for mammalian development by obtaining murine ES cells with a gene-trap inserted into the second of eleven exons in Fuz, the mouse orthologue of *Drosophila* and *Xenopus* Fuz. This gene trap is predicted to disrupt the transcription of the Fuz gene due to the trapping vector’s insertion. These cells were used to generate mice carrying the Fuz gene inactivation. Litters from heterozygous matings produced no viable full-term homozygous mutant pups, as the small litters failed to follow expected genotypic ratios upon analysis. Homozygous fetuses were obtained at E18, and these mice displayed a wide range of developmental defects (Fig. 14-16).

All homozygous mutant mice displayed severe developmental defects that are associated with defective ciliogenesis. Fuz mutant mice displayed defects in craniofacial

development as well as incompletely penetrant rostral neural tube closure defects, including exencephaly and encephaloceles (Fig. 14B, Fig. 16B, C). This spectrum of defects reflects the phenotype of BBS and IFT mutant mice (Huangfu et al., 2003; Ross et al., 2005), and also is reminiscent of the neural tube defects in human patients with the ciliopathic Meckel-Gruber syndrome (Smith et al., 2006). Some Fuz mutant mice displayed normal neural tube closure despite having severe craniofacial and ocular defects (Fig. 16D). However, even mice with mild overt neural tube closure defects displayed severe internal hydrocephalus with enlarged lateral ventricles communicating with the third ventricle of the brain (Fig. 16F).

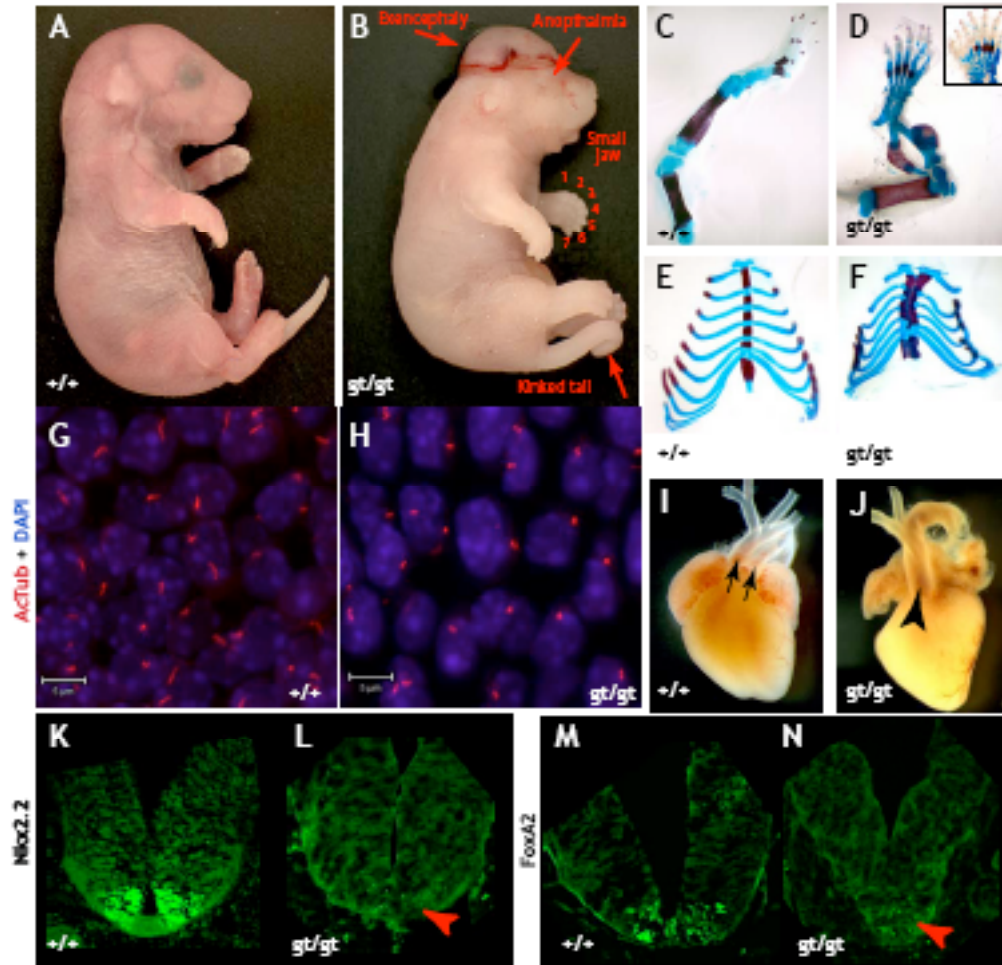


**Figure 14 Mice lacking a functional Fuz gene display multiple developmental defects.** (a) Control mouse, E18.5. (b)  $Fuz^{gt/gt}$  mouse. (c) Skeletal preparation of control hindlimb. (d) Skeletal preparation of  $Fuz^{gt/gt}$  hindlimb. Inset shows a paw with extreme polydactyly from a  $Fuz^{gt/gt}$  mouse. (e) Sternum preparation from control mouse. (f) Sternum preparation from  $Fuz^{gt/gt}$  mouse. (g, h) Confocal projection of Meckel's cartilage stained with acetylated tubulin (red) and DAPI (blue) exhibits diminished primary cilia in  $Fuz^{gt/gt}$  mouse sections. (i) Dissected heart from a control mouse, arrows indicate outflow tracts. (j) Dissected heart from a  $Fuz^{gt/gt}$  mouse, arrowhead indicates single outflow tract. (k, l) Normal expression of Nkx2.2 (green) in the ventral neural tube is lost in  $Fuz^{gt/gt}$  mice sections (red arrowhead). (m, n) Normal expression of FoxA2 (green) in the ventral neural tube is lost in  $Fuz^{gt/gt}$  mice sections (red arrowhead). 50μm scale bar in (g, h). This figure was generated in collaboration with Bogdan J. Włodarczyk, Heather L. Szabo-Rodgers, Karen J. Liu and Richard H. Finnell.

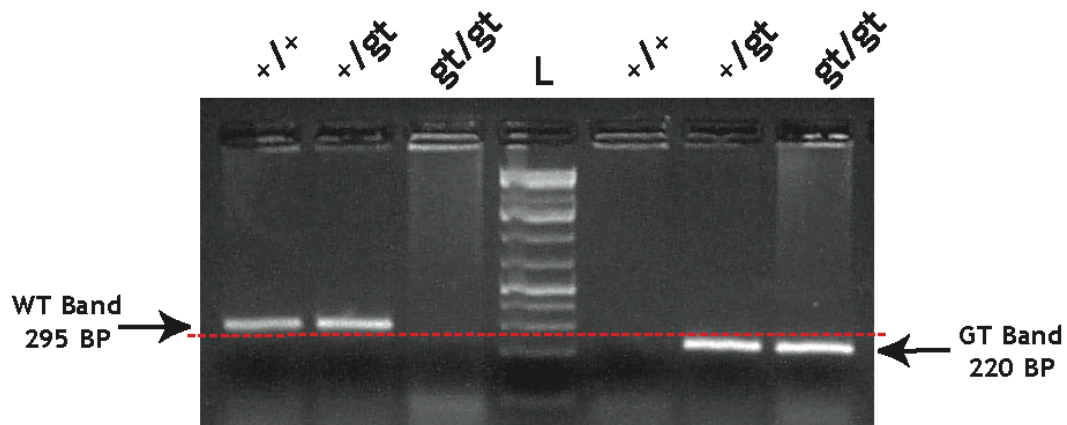


**Figure 15 PCR genotyping of Fuz mutant mice.** Agarose gel electrophoresis results of  $Fuz^{Gtl(neo)}$  knockout mouse PCR genotyping (DNA extracted from tails of fetuses at E18). PCR with primers to detect the wild type allele (Fuz forward and Fuz reverse primers – see Chapter 6 methods) produces a 295 bp product, which was detectable in both +/+ and +/gt mice (left). PCR with primers detecting the mutant allele (Fuz forward and LTR reverse – see Chapter 6 methods) produces a 220 bp product, which was detected in +/gt and gt/gt mice (right). This figure was generated solely by the efforts of Bogdan J. Włodarczyk and Richard H. Finnell.

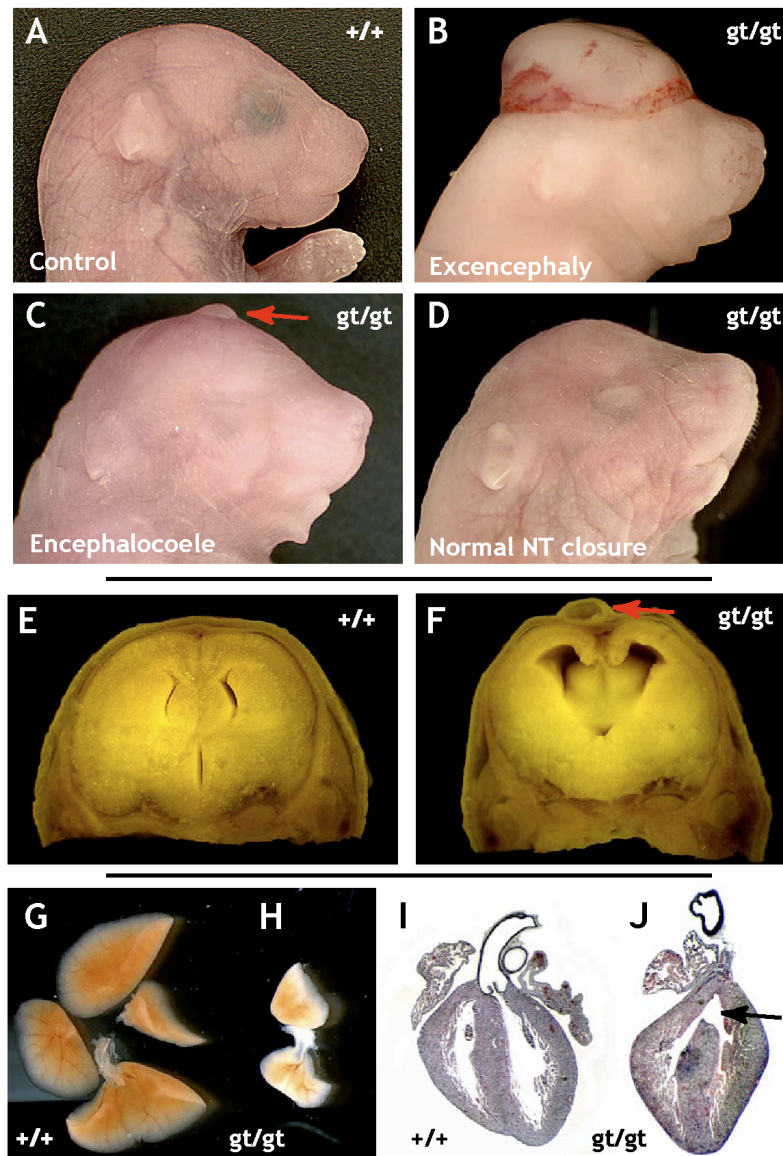


**Figure 16 Variable penetrance neural tube closure defects and organogenesis defects in mice lacking a functional *Fuz* gene.** (a-d) E18.5 mice *Fuz*<sup>gt/gt</sup> showing variable NTDs. (a) Control mouse. (b) *Fuz*<sup>gt/gt</sup> mouse displaying excencephaly. (c) *Fuz*<sup>gt/gt</sup> mouse displaying encephalocoele (red arrow). (d) *Fuz*<sup>gt/gt</sup> mouse displaying normal neural tube closure (note reduced eyes and jaw). (e) Thick section of control brain. (f) Thick section of *Fuz*<sup>gt/gt</sup> brain from a fetus with an encephalocoele (red arrow). (g, h) *Fuz*<sup>gt/gt</sup> mice display severely hypoplastic lungs. (i) Section through control heart. (j) Section through *Fuz*<sup>gt/gt</sup> heart with ventriculoseptal defect (arrow). This figure was generated solely by the efforts of Bogdan J. Wlodarczyk and Richard H. Finnell.



In addition to these craniofacial and neural defects. Fuz mutant mice consistently displayed polydactyly on all limbs, with some limbs containing up to nine digits (Fig. 14D). Moreover, we also observed widespread defects in skeletal development and organogenesis, including malformed sternum, ribs, and long bones, as well as severely hypoplastic lungs (Fig. 14C-F; Fig. 16H). These latter attributes resemble those in human patients with the ciliopathic Jeune's asphyxiating thoracic dystrophy(Beales et al., 2007).

Collectively, these malformations are consistent with a failure of cilia-mediated Hedgehog signaling in Fuz mutant mice, so we next examined the expression of known Hedgehog target genes in the spinal cord(Huangfu et al., 2003; Park et al., 2006). We found that while *Nkx2.2* and *FoxA2* were robustly expressed in the ventral spinal cord of control mice, these expression domains were almost entirely absent in Fuz mutant mice (Fig. 14 K-N). Finally, we found that Fuz mutant mice displayed defects in primary ciliogenesis. Immunostaining for acetylated tubulin revealed that primary cilia in the Fuz mutant mice were significantly shorter than those in wild-type mice (Fig. 14G-H and Fig17; WT = 1.73 $\pm$ 0.06mm (n=70) and Fuz<sup>gt/gt</sup> = 0.87  $\pm$ 0.04mm (n=52); p<0.001). Despite the extremely significant difference in average length, the effect on cilia length was variable, and some cilia of nearly normal length were observed in Fuz mutant mice (Fig. 17). This variable defect in ciliogenesis reflects the result of Fuz knockdown in *Xenopus*(Park et al., 2006), and moreover, the finding is consistent with the Fuz mutant mouse embryonic phenotypes. Fuz mutants resemble single BBS mutations or hypomorphic alleles of IFT genes, in which cilia are present but defective. By contrast,

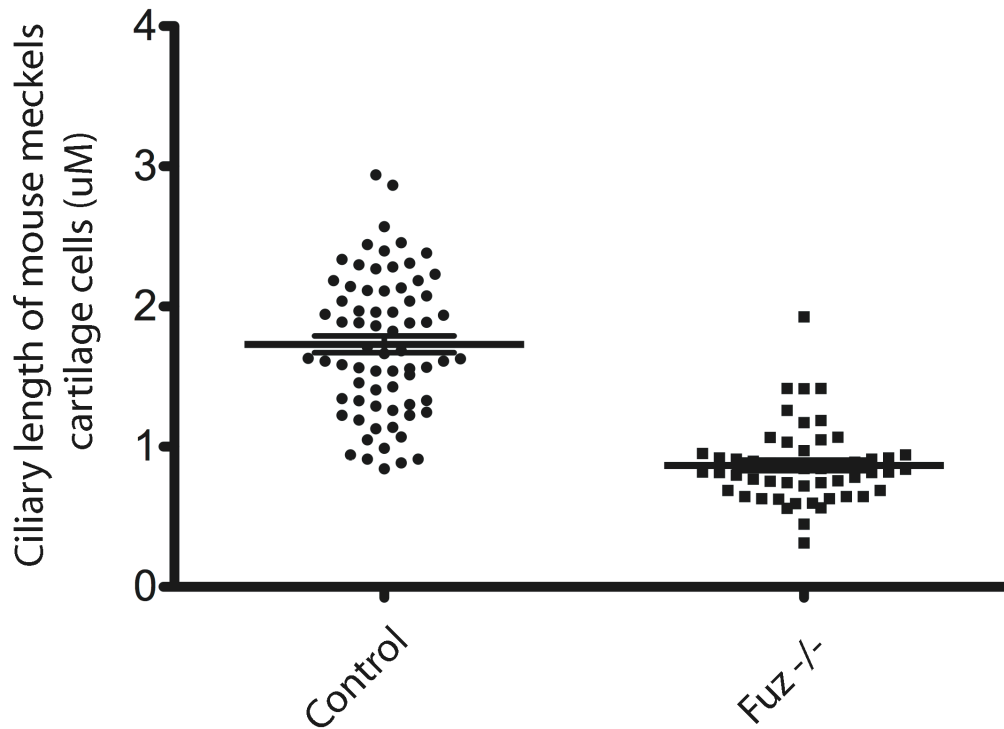


**Figure 17: Individual measurements of actylated tubulin signal of mouse Meckels cartilage mesechyme.** The Fuz<sup>gt/gt</sup> exhibits significant defects in primary cilia of the cell of the Meckels' cartilage. A scatter plot showing cilia length measured by acetylated-tubulin staining. Fuz<sup>gt/gt</sup> were frequently measured as length between two acetylated tubulin dots no commonly observed in controls. Bars indicate mean and SEM. This figure was generated in collaboration with Heather L. Szabo-Rodgers and Karen J. Liu.

Kif3a null mice, which lack cilia entirely, display far more severe embryonic phenotypes (Takeda et al., 1999).

In addition to these defects in Hedgehog signaling, Fuz mutant mice also displayed defects consistent with a failure of PCP signaling (Huangfu et al., 2003; Park et al., 2006). For example, the homozygous Fuz mutant mice displayed a kinked or curly tail (Fig. 14B), a phenotype that is consistently associated with heterozygous mutations in core PCP proteins such as Dvl or Vangl2 (Kibar et al., 2001; Hamblet et al., 2002). The homozygous Fuz mutant mice also display cardiac defects, including single outflow tracts and ventral septal defects (Fig. 14J; Fig. 16J), similar to those observed in mouse models lacking core PCP genes such as Vangl2 and Dvl (Hamblet et al., 2002; Karner et al., 2006). The pattern of congenital malformations in the Fuz mutant mice is thus entirely consistent with that found in *Xenopus* embryos following Fuz knockdown (Park et al., 2006). Fuz morphant *Xenopus* embryos and Fuz mutant mice each display comparatively mild PCP defects together with more severe defects in cilia-mediated developmental events.

#### **4.3. Homology modeling and network predictions suggest fuzzy involvement with vesicle trafficking**

Our bioinformatic approach successfully revealed novel aspects of the genetic network in which Fuz functions, so we extended this approach to investigate the cell biological function of the novel protein encoded by the Fuz gene. We first turned to mouseFUNC, a large-scale community effort to systematically predict mouse gene function using the consensus of diverse computational approaches (Pena-Castillo et al., 2008). MouseFUNC predicted a central role in vesicle trafficking for Fuz (Table 2). This suggestion was supported by results of iterative BLAST searches (PSIBLAST), which identified a modest similarity between Fuz and the yeast vacuolar fusion protein Mon1 (data not shown).

We next used homology modeling (Ginalski, 2006) to predict the structure of the Fuz protein. Using mGENTHREADER (see supplemental methods), we predicted that the C-

terminus of the *Xenopus* Fuz protein should fold into a series of five  $\beta$ -sheets flanked by  $\alpha$ -helices (Fig. 20A, B; Fig. 18). This structure, known as a longin domain (Rossi et al., 2004), is consistent with a vesicle trafficking function for Fuz. Indeed, the longin domain is present in the structure of SEDL, a subunit of the vesicle-tethering TRAPP complex that is associated with skeletal dysmorphogenesis (Gedeon et al., 1999; Jang et al., 2002). Moreover, the longin domain is shared by several other vesicle trafficking proteins, including subunits of the AP clathrin adaptor complexes (Collins et al., 2002) and the membrane-fusing SNARE proteins, sec22b, VAMP7, and Ytk6p (Refs. (Rossi et al., 2004; Pryor et al., 2008)).

These longin domain containing proteins are all tightly linked to one another in probabilistic networks of human, mouse, and yeast genes, and this node within the gene networks is tightly linked to other core vesicle-trafficking proteins (Supp. Fig. 19; and see Supplemental Methods). However, the scale of these linkages was too large to generate easily testable hypotheses. We therefore returned to the physical interactome data, looking this time for relationships between longin domain containing proteins with structural similarity to the Fuz C-terminus. We found that the longin-domain proteins AP2s, AP1s, and SEDL were all linked by physical associations to the PCP protein Dvl2 (Fig. 20C), which interacts genetically with Fuz (Lee and Adler, 2002; Park et al., 2006). More importantly, AP2s, AP1s, SEDL and Dvl2 were all linked by physical association to CLAMP (Fig. 20C), a microtubule-bundling protein that is a known component of cilia and flagella (Chan et al., 2005; Dougherty et al., 2005; Park et al., 2008).

GO id	Description	Type	Combined Score	B	C	C*	D	E	F	G	H
GO:0031988	membrane-bound vesicle	CC	0.226	0.00512	0.81	0.897	I	0.0334	0.128	0.00447	0.612
GO:0031982	vesicle	CC	0.22	0.00547	0.798	0.838	I	0.0334	0.183	0.00315	0.603
GO:0031410	cytoplasmic vesicle	CC	0.214	0.00549	0.792	0.867	I	0.000473	0.171	0.00301	0.614
GO:0016023	cytoplasmic membrane-bound vesicle	CC	0.204	0.0133	0.778	0.893	I	0.102	0.14	0.00387	0.624
GO:0006886	intracellular protein transport	BP	0.13	0.0188	0.601	0.735	I	0.0353	0.0407	0.00897	0.56
GO:0008104	protein localization	BP	0.129	0.0123	0.6	0.686	I	0.000426	0.13	0.01	0.559
GO:0016192	vesicle-mediated transport	BP	0.129	0.00592	0.597	0.85	I	0.000457	0.109	0.00676	0.552
GO:0046907	intracellular transport	BP	0.127	0.011	0.595	0.741	I	0.0163	0.0965	0.0105	0.537
GO:0045184	establishment of protein localization	BP	0.126	0.0328	0.593	0.739	I	0.00441	0.0684	0.00913	0.563
GO:0051641	cellular localization	BP	0.125	0.0394	0.591	0.738	I	0.000356	0.168	0.0106	0.543
GO:0015031	protein transport	BP	0.124	0.024	0.587	0.723	I	0.000874	0.0611	0.00901	0.552
GO:0051649	establishment of cellular localization	BP	0.124	0.0403	0.588	0.74	I	0.349	0.0978	0.0106	0.54
GO:0009628	response to abiotic stimulus	BP	0.00729	0.0207	0.0706	0.0171	0.122	0.0352	0.109	0.00847	0.293
GO:0006952	defense response	BP	0.00708	0.0147	0.0687	0.0215	0.00211	0.00137	0.306	0.0101	0.304

**Table 2 MouseFUNC predicts a vesicle trafficking function for Fuz.** The description column defines the Gene Ontology descriptors for Fuz function ranked in order of combined score (blue column). Specific Gene Ontology identifiers (GO id's) are listed in the leftmost column. The combined score represents the overall prediction of GO id by all algorithms generated in the MouseFUNC competition. The columns at right (B-H) are the relative scores for each GO id that were predicted by individual algorithms. The Type column indicates the parent GO hierarchy for the annotations (cc, cellular compartment; bp, biological process). This figure was generated in collaboration with Insuk Lee, Greg Weiss and Edward M. Marcotte.

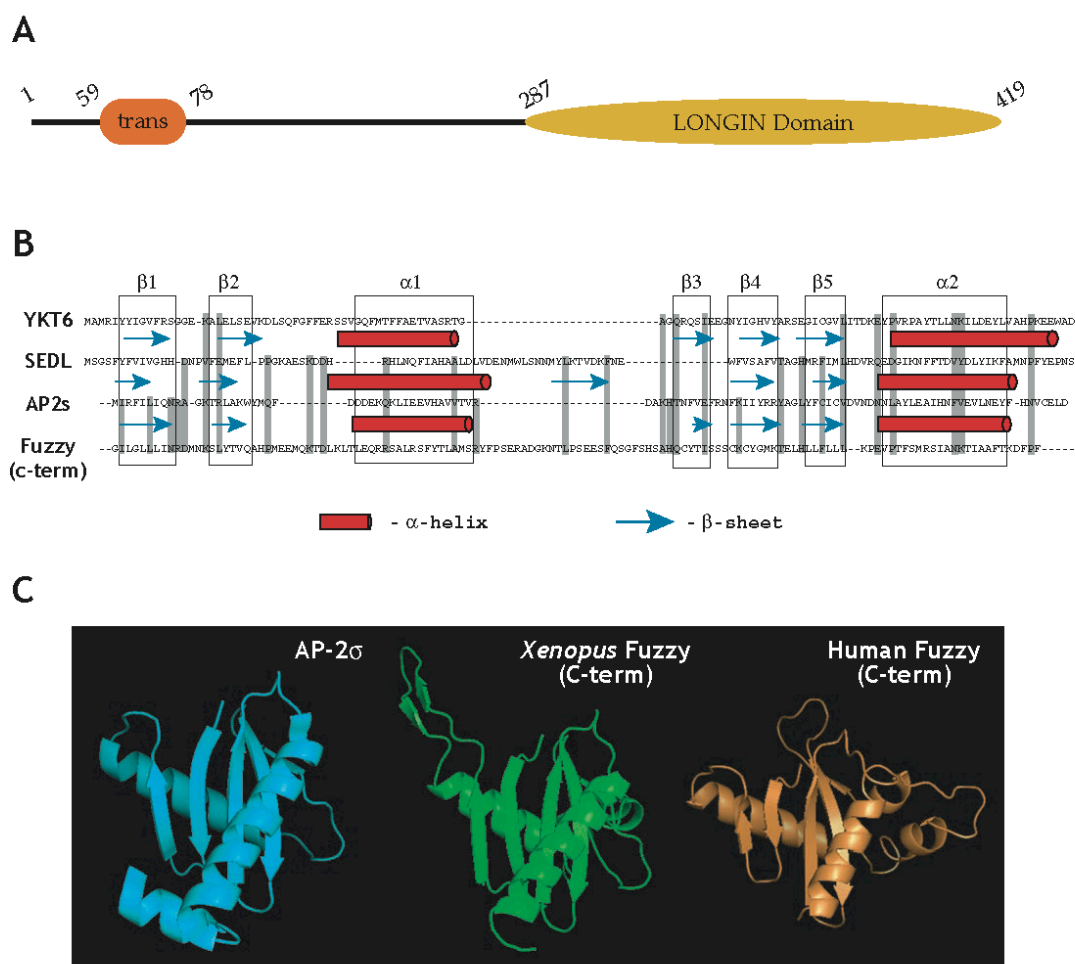


**Figure 18 Structure modeling of the Fuz protein.** (a) The primary sequence of Fuz is predicted to contain a single transmembrane-spanning domain in the N-terminus (MEMSAT3) and a putative longin domain in the C-terminus (mGENTHREADER). (b) Comparison of secondary structures for *Xenopus* Fuz and three longin domain-containing proteins, Ykt6 (3bw6A0), SEDL (1hgA0), and AP2s (1vg1S0). The b-sheets and a-helices predicted for *Xenopus* Fuz are indicated by the boxes (see labels above each box). The sheets and helices of the other three proteins are indicated by blue arrows and red barrels, respectively. Critical residues in the Fuz C-terminus, which are conserved in the other proteins, are indicated by the vertical grey bars. (c) Rendered protein models of AP-2s (left), and homology threaded model of the C-terminus of *Xenopus* Fuz (middle) and homology-threaded model of the C-terminus of human Fuz (right).

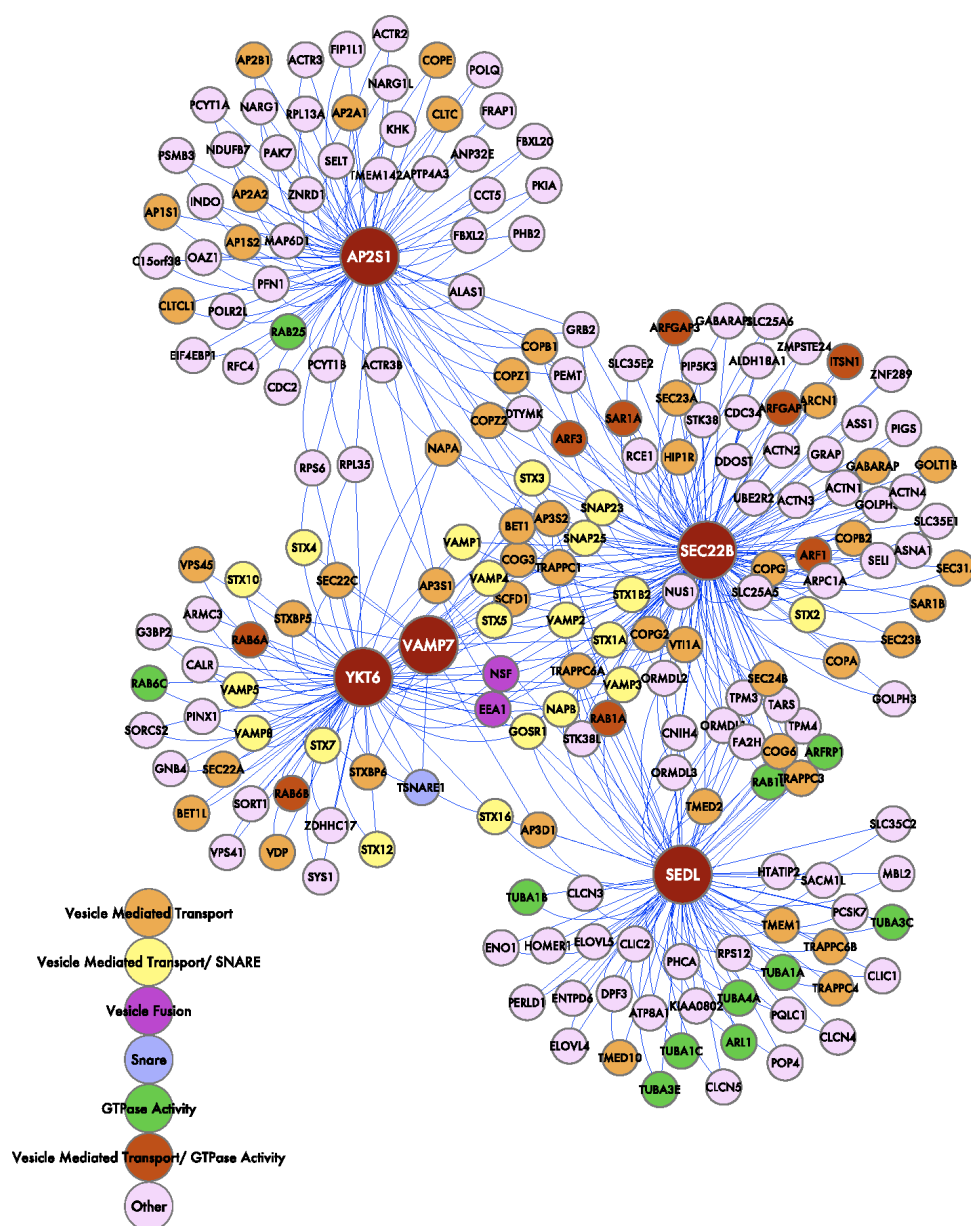


**Figure 19 Network diagram of functional interactions between other structurally related Fuz like longin-domain containing proteins. SEDL, YKT6, SEC22B, VAMP7 and AP2s (PDB id: 1H3Q, 3BW6, 1IFQ, 2VX8 and 1VGL respectively). This figure was generated by Greg Weiss.**

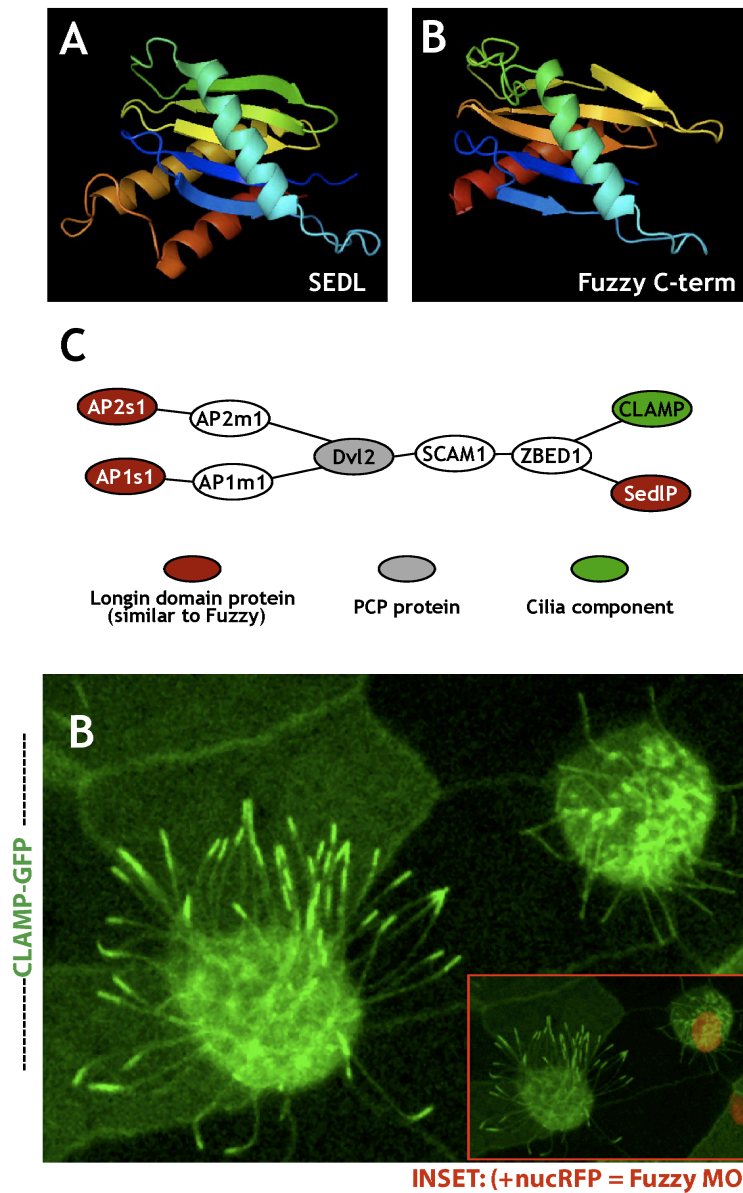


**Figure 20 Homology modeling and network predictions suggest a vesicle trafficking function for Fuz.** (a, b) Rendered protein models (Open-Source PyMOL 0.99rc6 software). (a) Sedl N-terminal domain (pdb:1H3Q). (b) 1H3Q based homology threaded model of the C- terminal aa(s) 287-419 of *Xenopus* Fuz protein. (c) Illustration of experimentally-derived protein-protein interactions linking Dvl2 with longin-domain proteins AP1/AP2 subunits (m/s) and SedlP (longin domains) and CLAMP (component of the ciliary rootlet). (d) Mosaic imaging of live agarose embedded embryo. CLAMP-GFP highlights a variety of epidermal structures. RFP-Histone2B (nuc-RFP) marks the nuclei as well serves as a lineage tracer for morpholino containing cells. Confocal slice - exhibiting a loss of apical localized CLAMP-GFP to ciliary tips in FUZMO cells (inset shows merge of (e) and more basal slice to display nucRFP signal).



#### **4.4. A novel fuzzy binding partner, RSG1**

The essential developmental requirement for Fuz is thus conserved from frogs to mammals. This finding allows us now to exploit the tremendous wealth of bioinformatics data in mammalian systems to help us elucidate the functions of the novel Fuz protein. We first queried the human interactome for potential Fuz-interacting proteins. We noted that high-throughput yeast two-hybrid screening (Rual et al., 2005) had suggested a weak interaction between human Fuz and the protein encoded by Chromosome 1 Open Reading Frame 89. BLAST predicted this gene to encode a small GTPase similar to REM2 and the vesicle-targeting Rab proteins (Fig. 21A). Based on this homology, we propose renaming C1orf89 as Rem/Rab-Similar GTPase 1, RSG1. Co-immunoprecipitation confirmed that RSG1 associates with Fuz (Fig. 21B).

To assess the function of RSG1, we designed an antisense morpholino-oligonucleotide (MO) to block translation of the protein. Injection of this MO resulted in defects in rostral neural tube closure (Fig. 22A-C), similar to the defects observed in Fuz morphants (Park et al., 2006) and in Fuz mutant mice. Co-injection of GFP-RSG1 mRNA suppressed the open neural tube phenotype of RSG1 morphants in a dose-dependent manner (Fig. 22A, D), demonstrating that the effect of the MO was specific. In addition, we assessed a loss of ventral cell fates of the RSG1 morphant embryos by *in situ* hybridizations of Nkx2.2 (Fig. 23). The results are similar to a loss-of-function of fuzzy in the frog and multiple cilia mutants in the mouse (Huangfu et al., 2003; Huangfu and Anderson, 2005; Park et al., 2006).

##### **4.4.1. RSG1 morphants exhibit general defects in ciliogenesis and of cytoplasmic ciliary components**

Because RSG1 GTPase binds to Fuz and is essential for ciliogenesis, we would expect to observe a similar CLAMP trafficking phenotype following interference with RSG1 function. Indeed, in mosaic embryos, nucRFP-positive RSG1 morphant cells displayed defects in the trafficking of CLAMP-GFP to the apical cell surface, while nearby control cells displayed no such defects (Fig. 24C, D). In addition, expression of RSG1<sup>T65N</sup> also severely disrupted apical trafficking of CLAMP-GFP, though expression

of wild-type RSG1 had little effect. (Fig. 25). Finally, RSG1 knockdown also eliminated the accumulation of CLAMP-GFP to the apical tips of cilia in multi-ciliated cells (Fig. 24E).

RSG1 contains the invariant serine/threonine residue whose mutation to asparagine has been shown in other GTPases to alter the guanine nucleotide binding affinity and to generate a dominant-negative protein (Fig. 21C, D; yellow/pink residues). To test the significance of RSG1 GTPase activity, we mutated this residue and expressed high levels of RSG1<sup>T65N</sup> in *Xenopus* embryos. Overexpression of RSG1<sup>T65N</sup> resulted in defective ciliogenesis in multi-ciliated cells of the epidermis, though we observed no effect from overexpression of wild-type RSG1 (Fig. 26E, F).

Finally, we examined RSG1 subcellular localization by expression of low levels of GFP-RSG1, and we observed that it localized strongly to the vicinity of basal bodies in multi-ciliated cells (Fig. 26G). This localization is very likely accurate, since GFP-RSG1 can rescue the phenotype of RSG1 morphants (Fig. 22). By contrast, the GFP-RSG1<sup>T65N</sup> localized only very poorly to basal bodies (Fig. 26H). Together, the results of knockdown, expression of the dominant-negative, and localization of the GFP-fusion proteins, suggest a role for the RSG1 GTPase in ciliogenesis. These results are consistent with a role for this protein in mediating Fuz function.

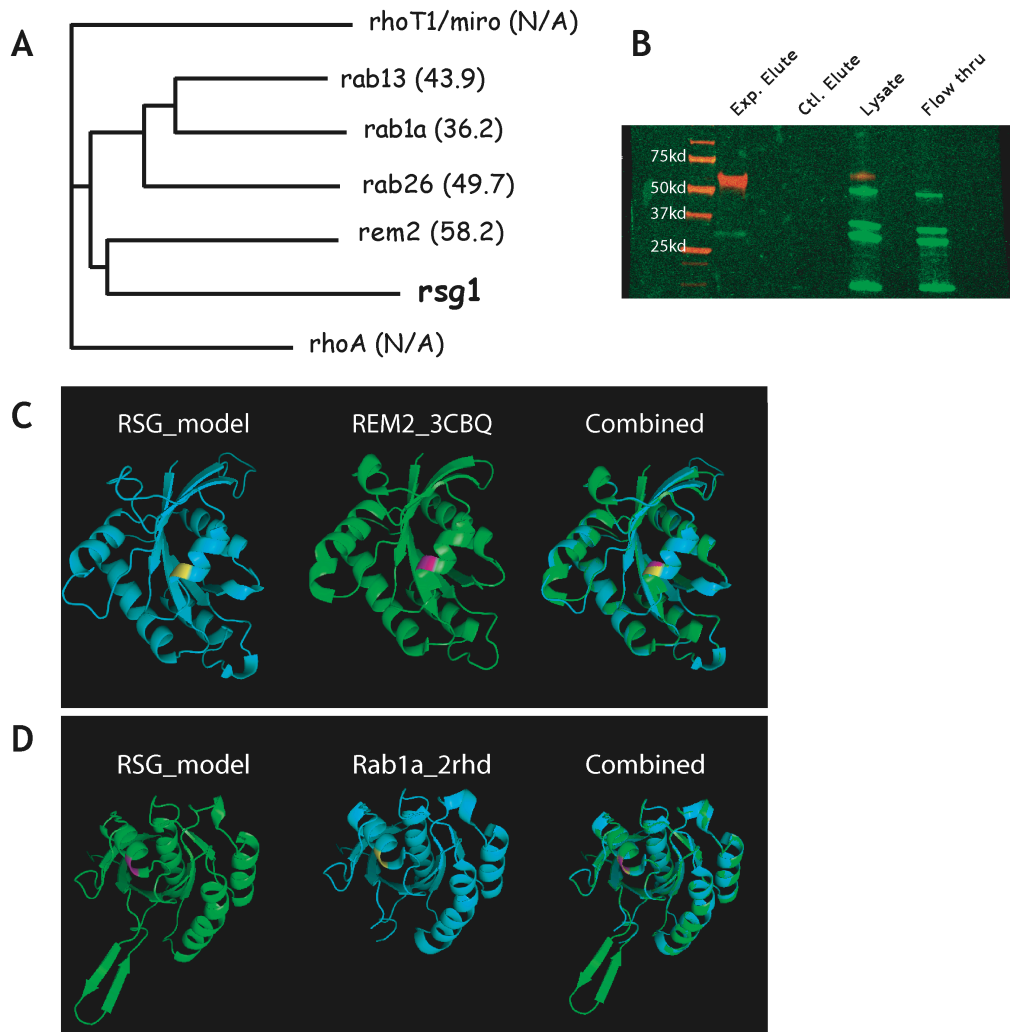


**Figure 21 Human chromosome 1 open-reading frame 89 encodes a novel Rab-Similar GTPase (RSG) that is a Fuz interacting protein.** (a) Neighbor joining tree of human GTPase proteins with RhoT1 and RhoA serving as outgroups. RSG1 forms a clade with REM2 as its closest protein homolog. Parenthesis indicate percent amino acid identities to RSG1. (b) Co-immunoprecipitation of FLAG-RSG protein by pull-down of MYC-FUZ with anti-MYC beads (Exp. Elute). Whereas embryo lysates expressing only FLAG-RSG protein exhibit no interactions with anti-MYC beads (Ctl. Elute). White asterisk demark anti-FLAG background seen in *Xenopus* whole embryo lysates. (c, d) Rendered protein models (Open-Source PyMOL 0.99rc6 software). (c) Predicted model of RSG1 (cyan) threaded on the REM2 structure (green) (pdb:3CBQ). (d) Predicted model of RSG1 (green) threaded on the Rab1a structure (cyan) (pdb:2RHD). Contrasting colored amino acid (i.e. yellow or magenta) in each structure reflects the location of the conserved threonine residue mutated in our study (T65 in RSG, mutated to N; see main text for discussion). This figure was produced in collaboration with Otis Blanchard.

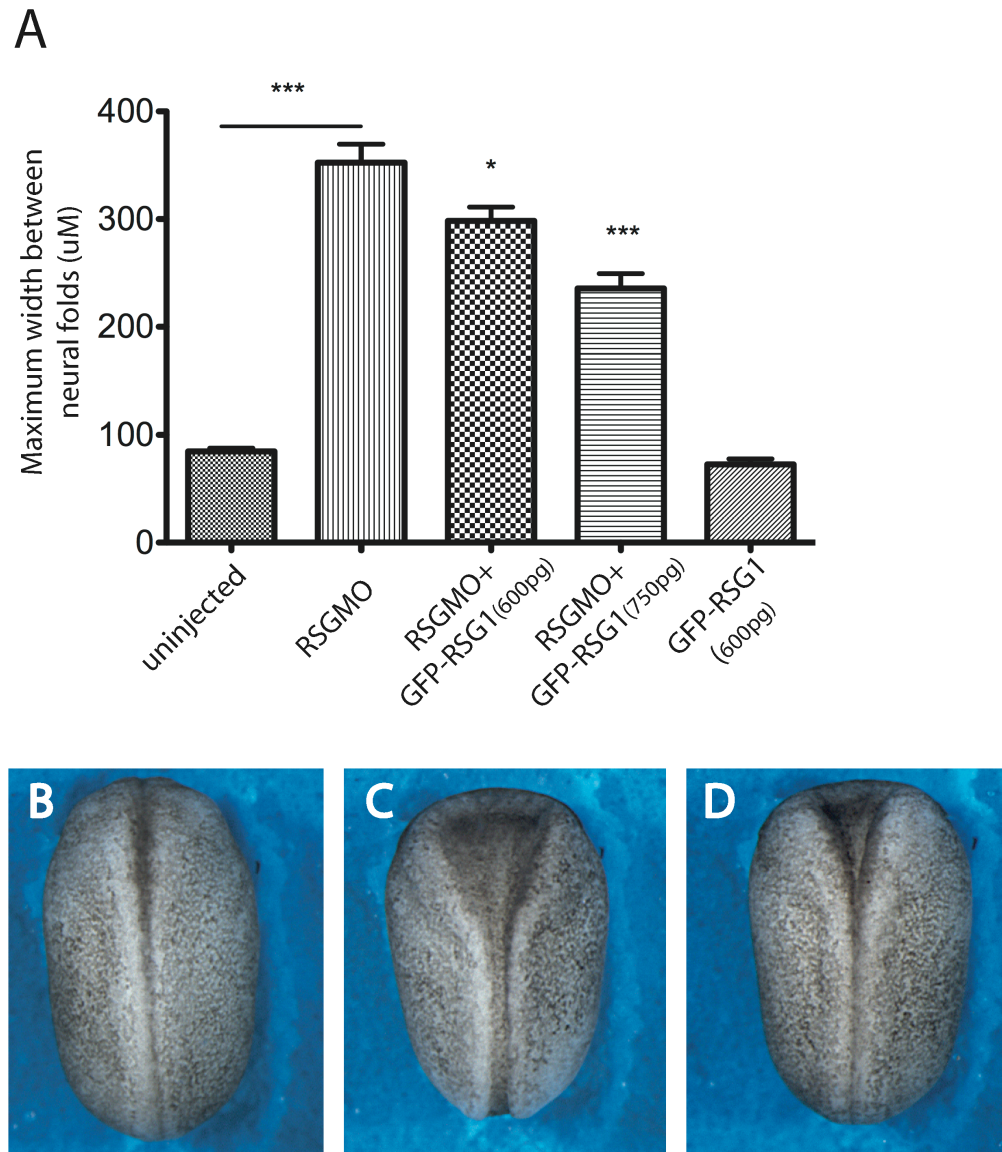


**Figure 22 Dorsally targeted RSG1 MO displays anterior neural tube closure defects that is rescued by co-injection of a GFP-RSG mRNA. (A)** RSG morphants exhibit significant defects in anterior neural tube closure compared to uninjected or RSGGFP injected sibling embryos ( $P < 0.001$ ). **(B)** Representative uninjected stage 20 embryo. **(C)** Representative RSG1 morphant embryo displaying a severe anterior neural tube closure defect. **(D)** Representative RSGGFP (750pg) rescue embryo displaying a subtle but significant decrease in severity of the anterior neural tube defect. \*  $P < 0.05$  and \*\*\*  $P < 0.001$  versus RSG morpholino injection embryos or control as indicated by linebar.  $n = 3$  independent replicate experiments. All  $P$  values were analyzed by one-way ANOVA with Bonferoni correction. Data are shown as means  $\pm$  SEM.

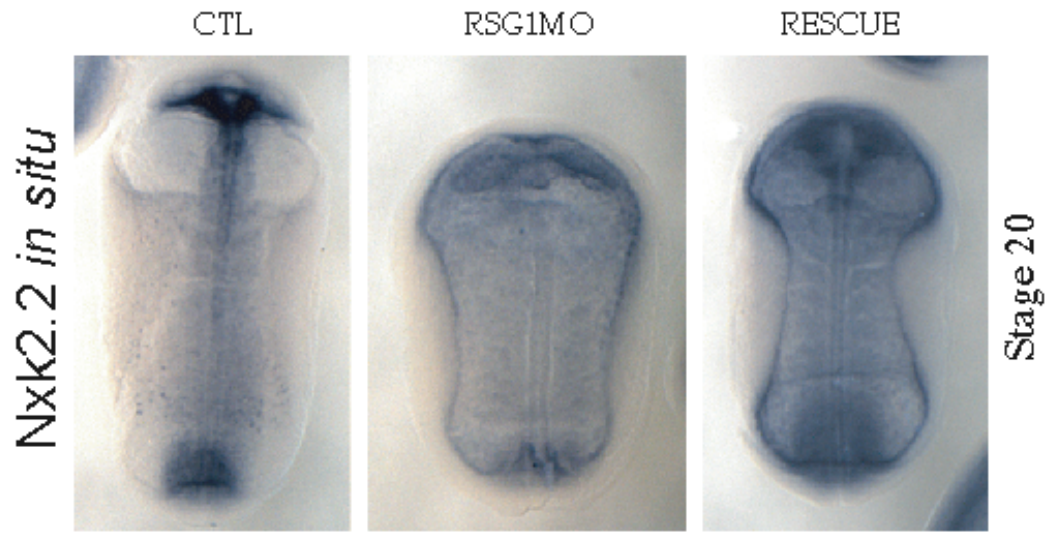


**Figure 23 Loss of *Nkx2.2* in *Xenopus* RSG morphants.** The induction of *Nkx2.2*, a ventral neural tube cell marker is disrupted by dorsal expression of the RSG1 morpholino. This affect is subtly rescued by co-expression of a non-targetable GFP-RSG1 fusion protein.

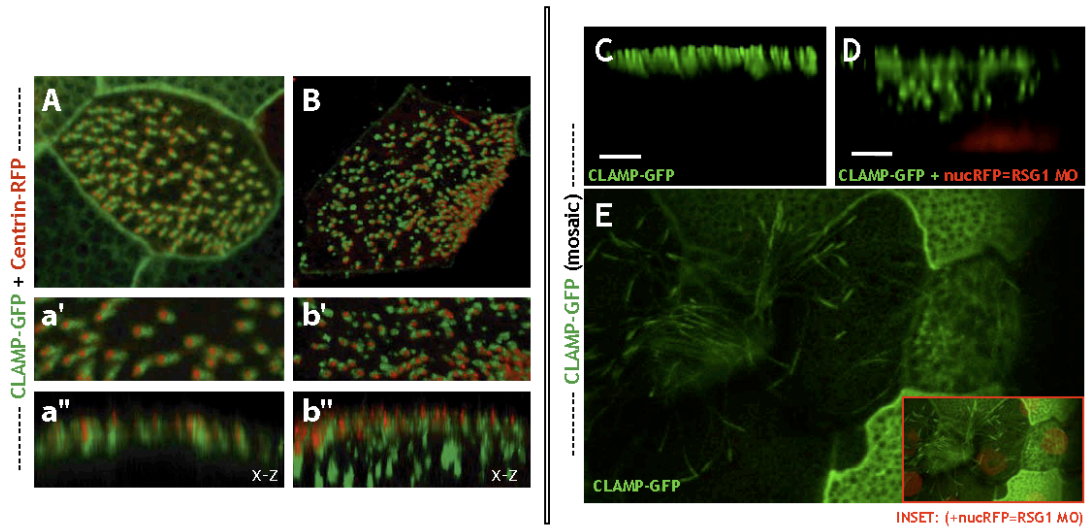


**Figure 24 Fuzzy and RSG1 function in multiple vesicle trafficking events in the *Xenopus* epidermis.** (a, b) Fuz knockdown disrupts ciliogenesis and localization of CLAMP-GFP to the ciliary rootlet. Confocal stacks of formaldehyde fixed stage 29 *Xenopus* epidermis injected with centrin-RFP and CLAMP-GFP mRNAs. (a) Multi-ciliated cell x-y view of uninjected control embryo exhibits elongated CLAMP-GFP signal extending from relatively evenly spaced basal bodies (centrin-RFP). (a') Thin x-y section from [a]. (a'') Z projection of section [a'] displays apical alignment of centrin-RFP and CLAMP-GFP. (b) Ciliated cell x-y view of Fuz morphant exhibits defects in the spacing of centrin-RFP signal and defects in elongated CLAMP-GFP signal. Additionally CLAMP-GFP signal is not localized with a centrin-RFP signal in many cases. (b') Thin x-y section from [b] (b'') Z-projection of section of [b'] displays apical alignment of the centrin-RFP signal however in many cases the CLAMP-GFP signal is below the apical surface in large punctae. (c-e) Mosaic imaging of live agarose embedded embryo. CLAMP-GFP highlights a variety of epidermal structures. RFP-Histone 2B (nuc-RFP) marks the nuclei as well serves as a lineage tracer for morpholino containing cells. (c, d) 3D rendered IMARIS projections (x-z). RSG1 MO (+ nucRFP cells) display defects in normal CLAMP-GFP localization along the apical surface. (e) Confocal slice (x-y) exhibiting a loss of apical localized CLAMP-GFP to ciliary tips in RSG1 MO cells (inset shows merge of (e) and more basal slice to display nucRFP signal).



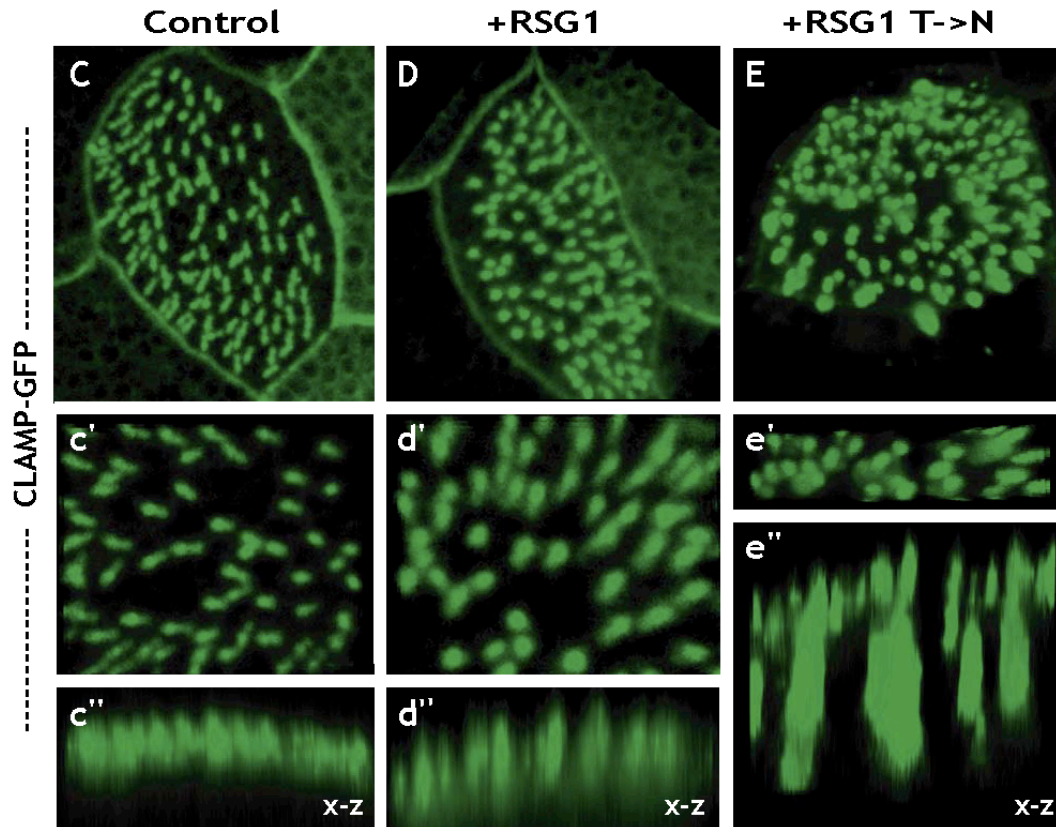


**Figure 25 Localization and function of RSG1 in formaldehyde fixed multi-ciliated epidermal cells.** (c) Multi-ciliated cell view (x-y) of uninjected control embryo exhibits elongated CLAMP-GFP signal. (c') Thin x-y section from [c]. (c'') Z-projection of section [c'] displays apical alignment of CLAMP-GFP. (d) Multi-ciliated cell view (x-y) of wild type RSG1 mRNA injected embryo exhibits subtle defects in the elongation of the CLAMP-GFP signal. (d') Thin x-y section from [d]. (d'') Z-projection of section [d'] displays apical alignment of CLAMP-GFP with a subtle defect in the resolution of apical punctae. (e) Multi-ciliated cell view (x-y) of RSG1<sup>T65N</sup> mRNA injected embryo exhibits dramatic defects in the elongation of the CLAMP-GFP signal. (e') Thin x-y section from [e]. (e'') Z-projection of section [e'] displays dramatic loss of the apical alignment as well as aberrant cytoplasmic punctae of CLAMP-GFP signal.

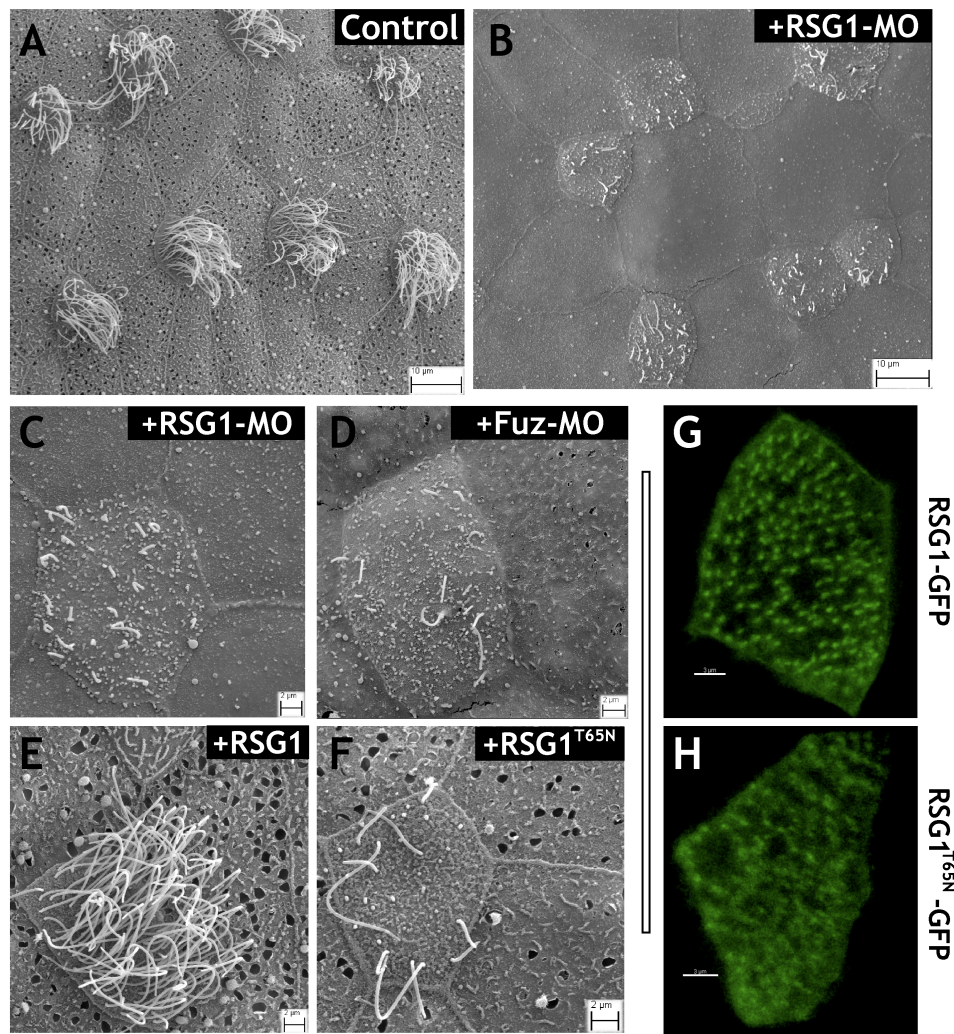


**Figure 26 Fuzzy and RSG1 control mechanisms of ciliogenesis and mucous secretion.** (a) SEM of control epidermis exhibits multi-ciliated cells. The surrounding mucous secreting cells are characterized by apical mucous granules and exocytic pits. (b) SEM of RSG1 MO displays defects in ciliogenesis and near complete loss of mucous granules and exocytic pits. (c) Loss of function RSG1 (RSG1 MO), display diminished cilia numbers and lengths and a decrease in exocytic pits in secretory cells. (d) Loss of function Fuz (Fuzzy MO), display diminished cilia numbers and lengths and a decrease in exocytic pits in secretory cells. (e, f) Epidermal targeted over-expression of RSG1<sup>T65N</sup>, but not wild type RSG1, displays defects in ciliogenesis as well as decreases in mucous granules and exocytic pits in secretory cells. (g) GFP-RSG1 localizes to the basal body region of multi-ciliated cells. (h) GFP-RSG1<sup>T65N</sup> expression in multi-ciliated cells is diffuse and not tightly associated with basal bodies. Observations of fluorescence levels following expression of GFP-RSG1 and GFP-RSG1<sup>T65N</sup> mRNA were comparable, suggesting similar rates of translation for the two proteins. This figure was produced in collaboration with Phillip B. Abitua.



#### **4.5. *Xenopus*, loss of function fuzzy (morphant) experiments display multiple developmental defects**

##### **4.5.1. Fuzzy morphants exhibit general defects in ciliogenesis and of cytoplasmic ciliary components**

Since Fuz is essential for ciliogenesis, we asked if Fuz may play a role in CLAMP localization. In living *Xenopus* embryos, CLAMP-GFP labelled the axonemes of cilia in multi-ciliated cells (Fig. 20D, left), as has been reported previously for sperm flagella(Chan et al., 2005). In addition to the axonemal labelling, however, we also observed an obvious enrichment at the apical tips of cilia (Fig. 20D, left). To test the effect of Fuz knockdown, we used targeted injection to generate *in vivo* mosaic epidermis, where control and morphant cells are intermingled. In these mosaics, the morphant cells are indicated specifically by co-injected mRNA encoding nuclear-RFP (nucRFP; Fig. 20D, inset). In nucRFP-positive Fuz morphant cells, CLAMP-GFP was visible in the the shortened and dysmorphic cilia, but the normal accumulation of CLAMP-GFP at the apical tips was entirely absent (Fig. 20D, right).

This role for Fuz in CLAMP localization was of particular interest because we previously found that CLAMP also co-localizes with Dvl2 in the vicinity of the ciliary rootlet<sup>5</sup>, which is a known nexus for vesicle trafficking to cilia(Fariss et al., 1997; Yang and Li, 2005; Park et al., 2008). In control embryos fixed with formaldehyde, CLAMP-GFP is restricted to the apical cell surface, where it formed a well-defined, linear structure adjacent to the apically-docked basal bodies indicated by co-expressed centrin-RFP (Fig. 4A, a', a'' and see Refs. (Hayes et al., 2007; Park et al., 2008).). By contrast to controls, the CLAMP-GFP signal in Fuz morphant embryos was present in larger, irregularly-shaped foci. Z-projections revealed that many of these irregular foci were well below the apical cell surface (Fig. 4B, b', b''), though centrin-RFP formed an even line at the cell surface of these cells. This result indicates that Fuz, unlike Dvl (Park et al., 2008), is not essential for apical docking of basal bodies, but is essential for apical trafficking of CLAMP. The dual localization of CLAMP-GFP at the basal apparatus and at the apical tip is reminiscent of IFT88 and IFT52 in mammalian cells(Follit et al.,

2006), and our data suggest that Fuz is required for the normal accumulation of CLAMP at both at the apical basal body localization and the distal cilia tip localization.

#### **4.5.2. Fuzzy and RSG1 morphant embryos display secretory defects of *Xenopus* epidermis**

Our data thus demonstrate that Fuz and RSG1 act to regulate trafficking during ciliogenesis. Because longin-domain proteins participate in many fundamental vesicle trafficking events (Rossi et al., 2004), we next asked if Fuz might play a broader role in trafficking than is reflected by the phenotype in multi-ciliated cells. We examined the mucus-secreting goblet cells that surround the multi-ciliated cells in the *Xenopus* epidermis (Hayes et al., 2007). Scanning electron microscopy (SEM) demonstrated that the apical surface of the goblet cells in controls were decorated with numerous open exocytic vesicles, many of which were actively releasing mucus granules (Fig. 27A). By contrast, open exocytic vesicles were extremely rare and few mucus granules were visible on goblet cells in Fuz morphants (Fig. 27B). SEM revealed severe defects in ciliogenesis in the epidermal multi-ciliated cells of RSG1 morphants (Fig. 26A-C). This phenotype was very similar to that of Fuz knockdown (Fig. 26D). We also observed that either knockdown of RSG1 or overexpression of RSG1<sup>T65N</sup> elicited defects in exocytosis in mucus-secreting cells (Fig. 26C, F), indicating that this GTPase is a key effector of Fuz function in multiple cell types.

To confirm the failure of secretion in Fuz morphant goblet cells, we turned again to mosaic epidermis and we examined immunostaining for Intelectin2, a major component of the secreted *Xenopus* epidermal mucus (Nagata et al., 2003; Hayes et al., 2007). In control cells of these mosaics (indicated by an absence of membrane-RFP co-injected with the MO), Intelectin2 in exocytosing mucus granules was visible as discrete foci, at or above the apical surface (Fig. 27D, d'). By contrast, Intelectin2 signal was present only below the apical cell surface in neighboring morphant cells (indicated by the presence of co-injected membrane-RFP in Fig. 5D, d'). The failure of exocytosis in morphant cells in these mosaic epithelia was also confirmed by SEM (Fig. 27C).

The joining of membrane compartments proceeds through discrete steps of transport, tethering, and fusion(Cai et al., 2007). Our bioinformatic analyses suggested a possible relationship between Fuz and either vesicle tethering or membrane fusion precesses (Fig. 19), and electron microscopy of Fuz morphants supports such a relationship. TEM revealed that morphant goblet cells often were decorated by large apical membrane blebs atop putative exocytic vesicles (Fig. 27F, green arrowhead), and this phenotype was also obvious in SEM (Fig. 27B, green arrowheads). Such apical membrane blebs were also apparent in RSG1 morphants (Fig. 26B, C). Many mucus-filled vesicles in Fuz morphants appeared to be tethered to the apical plasma membrane, though very few had fused.

The finding that mucus-filled vesicles in Fuz morphant cells appear to tether to, but fail to fuse with, the apical plasma membrane might suggest a general role for Fuz in governing vesicle fusion. However, secretion in *Xenopus* goblet cells can proceed by compound exocytosis, in which secretory vesicles fuse with one another as they approach the plasma membrane(Billett and Gould, 1971). We frequently observed such homotypic fusion of mucus-containing vesicles in Fuz morphants, despite the failure of nearby, apparently-tethered, vesicles to fuse with the plasma membrane (Fig. 27F, red arrow; Fig. 28B, C). In some cases, vesicles were observed that had fused to one another, but had not yet tethered to the apical plasma membrane (Fig. 28B, arrows). These data demonstrate that Fuz is essential for mediating only a specific subset of membrane fusion events.

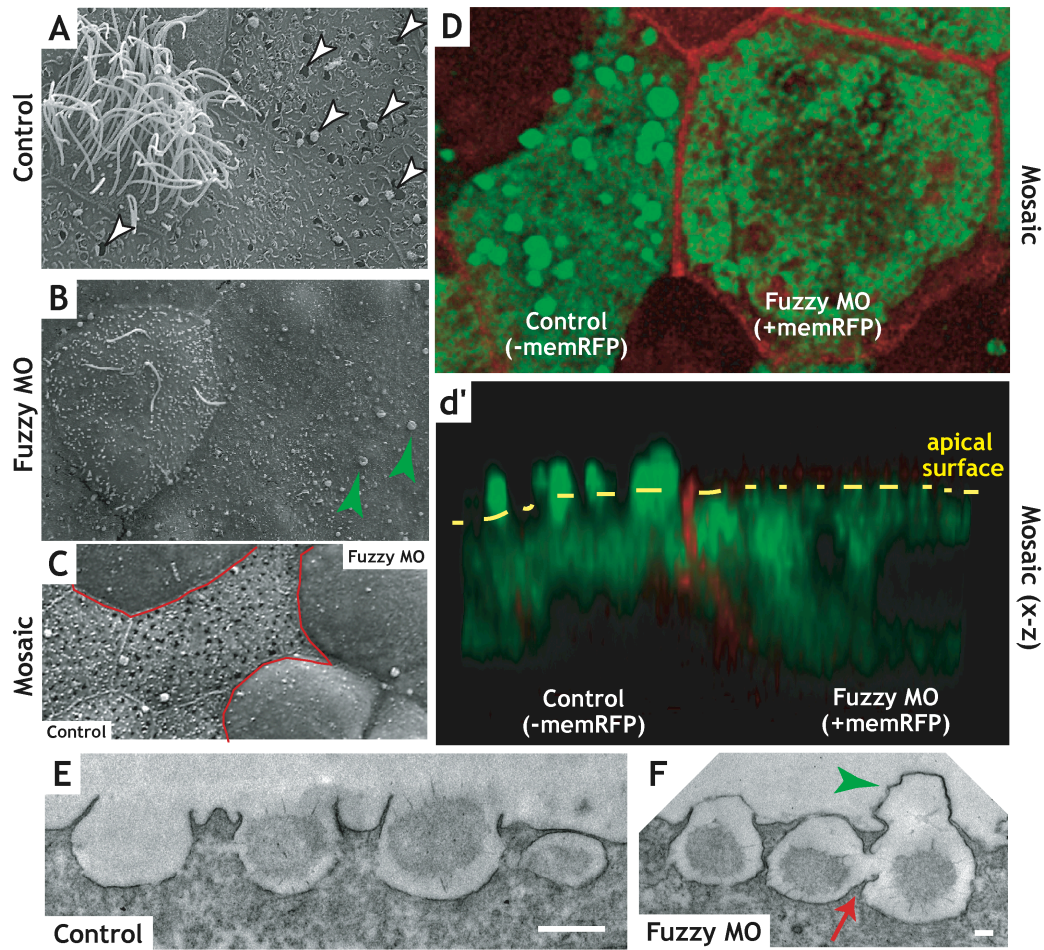


**Figure 27 Knockdown of Fuz disrupts exocytosis in mucus-secreting cells.** *Xenopus* epidermis as viewed by (a-c) SEM, (d, d') Confocal, and (e, f) TEM. (a) Wild type multi-ciliated cell (left) flanked by secretory cells. (b) Fuz morphants display defects in ciliogenesis of multi-ciliated cell (left) and of mucous granules as well as the “pock-marked” character of the epidermis (white arrowheads in [a]). (c) Mosaic epidermal tissue outlined by the red line. (d) Confocal section (x-y) of RFP-CAAX (memRFP) mRNA and Fuz morpholino injected embryo and processed for Xeel (interlectin-2) antibody (green). Cell expressing a high level memRFP (right) lacks apical Xeel antibody staining comparable to the neighboring cell (right). (d') Confocal section (x-z) of [d] illustrates the loss of apical (yellow dotted line) Xeel staining (green) in the Fuz morphant cell correlated with apical memRFP expression (right). (e) Thin section TEM of epidermis shows empty and mucous granule containing vesicles docked at the apical surface whereas Fuz morphants (f) display a general defect of vesicle content release as illustrated by large membrane protrusions (green arrows in [b, f]). Additionally frequent lateral vesicle fusion events are observed in secretory cells of Fuz morphants (red arrow). This figure was generated with Phillip Abitua.

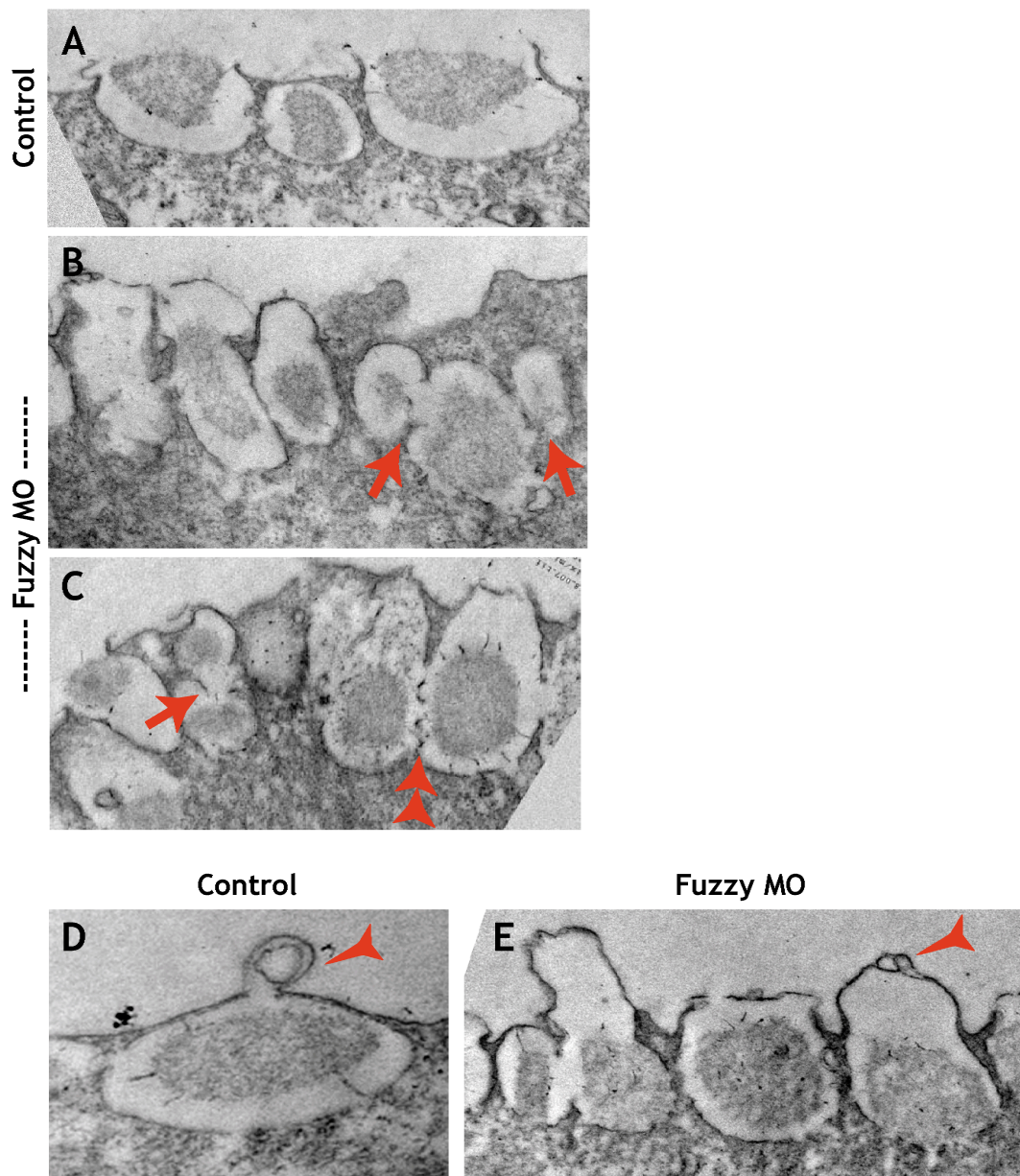


**Figure 28 Additional TEM analysis of mucus secreting cells in Fuz morphants.** (a) Control image showing representative *Xenopus* thin section epidermis. Generally the vesicles display even spacing of vesicles with no lateral mixing. (b, c) Fuz morphants display multiple lateral mixing events (red arrows and double red arrowheads [b, c] ) as well as uneven spacing of the vesicles. (d) Wild-type secretory granule. Red arrowhead indicates a membrane signature that maybe indicative of hemifusion. (e) Fuz morphant secretory granule. Membrane blebs out significantly indication a lack of full fusion, but a hemifusion signature similar to that in controls cells is present (red arrowhead). This figure was produced in collaboration with Phillip B. Abitua.



#### 4.6. Discussion

The PCP signaling cascade is broadly required for development of vertebrate embryos. However, studies to date have focused on only a small number of the known PCP genes, such as Dvl and Vangl2 (Refs. (Hamblet et al., 2002; Karner et al., 2006; Kibar et al., 2007b; Park et al., 2008).). Here, we have demonstrated that the largely unstudied PCP effector protein Fuz is fundamentally necessary for mouse embryonic development. Our data suggest a central role for Fuz in regulating targeted membrane fusion events, and this cellular function can explain the phenotype of embryos lacking Fuz function.

First, failure of trafficking to the basal body and within axonemes is essential for ciliogenesis (e.g. Refs. (Fariss et al., 1997; Yang and Li, 2005; Follit et al., 2006; Park et al., 2008)), and the phenotypes observed in *Xenopus* or mouse embryos lacking Fuz function reflect those observed in mice lacking key ciliogenesis factors, such as the BBS or IFT proteins (Huangfu et al., 2003; Ross et al., 2005). A key role of the cilium in development is thought to be the transduction of Hedgehog signaling (Huangfu et al., 2003; Huangfu and Anderson, 2005), so it is relevant that Hedgehog target gene expression is lost in Fuz morphant *Xenopus* embryos (Park et al., 2006) and in Fuz mutant mice (Fig. 14). Secondly, defective secretion in cells lacking Fuz function may also contribute to the embryonic phenotype. We observed severe skeletal defects in vertebrate embryos lacking Fuz function (Fig. 14 and Ref (Park et al., 2006)); skeletal defects are likewise observed humans or zebrafish with mutations in Sec23A, a subunit of the COPII complex (Boyadjeiev et al., 2006; Lang et al., 2006; Fromme et al., 2007) and in humans with mutations in the TRAPP complex subunit, SEDL (Ref. (Gedeon et al., 1999)). Our data therefore place Fuz and the interacting GTPase RSG1, at the interface of developmental regulatory systems (e.g. PCP signaling) and fundamental cell biological processes (e.g. ciliogenesis, secretion). In combination with the finding that Dvl mediates vesicle association with basal bodies in ciliated cells (Park et al., 2008), the data here suggest that coordination of vesicle trafficking may be a unifying mechanism by which PCP signaling can control so many diverse cellular behaviors during embryonic development.

## Chapter 5: Future Directions

### 5.1 Introduction

#### 5.1.1. Wnt signaling: To PCP or not to PCP

Several studies suggest a functional link between Wnt signaling events and vesicle trafficking events. Both the canonical Wnt/ $\beta$ -catenin pathway, as well as the non-canonical planar cell polarity (PCP) pathway appear to require endocytic events downstream of a Frizzled (Fz)/Wnt (ligand/receptor) interaction (reviewed by (Gagliardi et al., 2008)). In addition, there is no unifying mechanism to explain how PCP signaling controls such diverse processes as convergent extension and ciliogenesis. We and others have suggested that proteins classified genetically as downstream PCP effectors of the *drosophila* wing hair epithelium (e.g. fuzzy, fritz, and inturbed) may in fact serve to function as or interact with *bone fide* vesicle trafficking proteins (Adler and Lee, 2001; Classen et al., 2005). Furthermore, we suggest that PCP effector proteins aid in the fidelity of vesicle sorting within the general milieu of the cellular cytoplasm. Thus, a unifying mechanism of PCP might be explained by directed vesicle trafficking events.

Specification of the Wnt/ $\beta$ -catenin pathway versus the PCP pathways is activated downstream of specific Wnt/Fz interactions; for example Wnt3a in *Xenopus* in the former and Wnt5a in *Xenopus* for the latter. Downstream of Wnt/Fz interactions multiple proteins serve to generate pathway flux towards a canonical versus a non-canonical signal. For instance, phosphorylation of dishevelled (Dvl) protein by casein kinase 1 (CK1) and GSK3 $\beta$  shifts Dvl's protein function towards the inhibition of the  $\beta$ -catenin ( $\beta$ -cat) destruction complex and subsequently upregulate  $\beta$ -cat/LEF/TCF dependent transcription (Bryja et al., 2008). While multiple Wnts have been classified to function in canonical  $\beta$ -cat or PCP signaling, multiple lines of evidence suggest strongly that specific tissue environments in addition to Fz receptors provide additional regulation of Wnt pathway decisions (Mikels and Nusse, 2006). In addition, LRP5-a Fz co-receptor- seems to provide a switch at the level the Fz receptor in order to generate flux towards the

canonical pathway (He et al., 2004); as well, Ryk –a Fz co-receptor- has been shown to perform a similar function for the PCP pathway (Kim et al., 2008a). While these examples exhibit a degree of fidelity of Wnt signaling at the plasma membrane, a reductionist approach suggests we seek the intracellular mechanisms that cells utilize to generate a bifurcation of the Wnt pathway within the cytoplasm. This will serve to both, generate a deeper understanding of the cytoplasmic mechanisms generating pathway flux and strengthen assays for the pathway specificity of the upstream Wnt/Fz/co-receptor interactions.

### **5.1.2. Dishevelled is a multi-potential protein downstream of Wnt signaling**

Dishevelled proteins (Dvls) are multi-functional ‘scaffolding’ protein controlling both canonical Wnt signaling and PCP signaling, but a unifying mechanism for Dvl function has yet to be established. Given, Dvl proteins serve at least a dual role in Wnt dependent intracellular signaling; first principles suggest that one might explore Dvls role in the bifurcation of the Wnt signaling pathway. Domains of Dvl have been shown to be necessary or dispensable for both PCP and the Wnt/ $\beta$ -catenin pathway (Rothbacher et al., 2000; Wallingford and Harland, 2002). Canonical signaling assayed in frog as secondary axis induction, requires the DIX and PDZ domains as well the most N-terminal portion seems to contribute somewhat to canonical Wnt signaling (Rothbacher et al., 2000). Furthermore, the DIX domain is thought to self-polymerize akin to the self-polymerization of Axin protein; also this polymerization is necessary for Dvl-Axin interaction (Schwarz-Romond et al., 2007). Interestingly, this mechanism of polymerization may aid in the explanation of over-expression of Dvl which generates a secondary-axis (Sokol et al., 1995). This point is bolstered by Dvl DIX domain mutants, that inhibit the self-polymerization of Dvl protein and which disrupt the canonical signaling (Bilic et al., 2007).

The PCP pathway utilizes the PDZ and DEP domains. The DEP domains is known to directly interact with both DAAM1 and Prickle (Pk) two regulators of convergent-extension and gastrulation two non-canonical processes in the frog (Habas et al., 2001; Takeuchi et al., 2003). The *dsh1* allele; a lysine to methionine mutation in the DEP domain of Dvl protein, was the first mutant of Dvl that did not effect canonical Wnt



signaling but disrupted PCP signaling. This mutant, originally described in fly, was thought to disrupt the membrane localization in response to Fz signaling in *Xenopus* animal cap assays (Axelrod et al., 1998; Boutros et al., 1998). Moreover, a sodium/proton pump protein, Nhe2, regulates the pH at the plasma membrane aiding in the stabilization of a negatively charged membrane that facilitates DEP domain interaction (Simons et al., 2009). Conversely, the crystal structure of the DEP domain suggests that this crucial lysine residue is not on a face of the domain that is positively charged (polybasic region) and thus more likely to associate with the plasma membrane (Wong et al., 2000). This suggests that the lysine residue instead interacts with additional protein partners that facilitate membrane interaction in response to Fz signals. It would be prudent to screen for protein interactions partners of the Dvl DEP domain that interact with the wild type and not with the *dsh1* allele Dvl DEP domain. In light of new evidence that Dvl form large polymers via self-interaction of the DIX domain, any screen should attempt to exclude this domain (Schwarz-Romond et al., 2007).

A role of Dvl during endocytosis is supported by experiments, which mutated a canonical tyrosine-based YXX $\Phi$  motif, where  $\Phi$  represents a residue with a bulky hydrophobic side chain. This motif (YHEL in XDvl2) is known for multiple proteins to be important for binding the C-terminal region of  $\mu$ 2-adaptin of the AP-2 complex (Collins et al., 2002). The binding of  $\mu$ 2-adaptin to Dvl-2 was inhibited by mutation in the YHEL region. Additionally, these YHEL Dvl-2 mutants were defective in the endocytosis Frizzled 4 in Wnt-activated cultured cells (Yu et al., 2007). These YHEL mutants are defective in planar cell polarity but not canonical signaling; thus, the role of clathrin-based endocytosis of Dvl might generate flux in the direction of PCP signaling. As well,  $\beta$ -arrestin is implicated in flux towards non-canonical signaling (reviewed in Chapter 1.2.1. this work).

Clearly, there is need to further investigate the functions of Dvl dependent pathway bifurcation of Wnt signaling. In the case of canonical Wnt/ $\beta$ -cat, we understand a great deal of the cytoplasmic mechanisms. One could posit that a greater understanding of PCP signaling should begin with an understanding of the cytoplasmic events of cells

undergoing convergent-extension, wing hair outgrowths or multi-ciliated cell (Shimada et al., 2006; Shindo et al., 2008).

Cilia are polarized membrane protrusions, important for diverse function such as: motility, fluid flow, and more recently found to be crucial for at least some developmental signaling events (Fliegauf et al., 2007). The structures of cilia are highly divergent, however the mechanisms of cilia biogenesis seem well conserved. We have utilized a specialized cilia that is present as large tufts of ~100 cilia which are highly motile and are thought to be important for the generation of fluid flow over the epidermis of the developing tadpole embryo (Mitchell et al., 2007). A speculative explanation for the relevance of this mechanism follows that flow increases the accessibility of dissolved oxygen and decreases the ability of microorganism invasion. Importantly, this epidermal tissue provides a highly tractable model of ciliogenesis and is likely to uncover many mechanisms well conserved in the similar tissue types of the airway epithelium of the respiratory system or the ependymal cilia of the brain. As well as, at least minimal conservation of function throughout a range of ciliated cell types.

## **5.2. Integrating trafficking defects with fuzzy function during development**

The presence of a predicted Longin-like domain in Fuzzy (Fuz) suggests some interesting hypothesis about the molecular mechanisms of Fuz protein (see Chapter 4 this work).

Multiple longin domain containing proteins have been shown to be involved in vesicle trafficking: Ykt6; Sec 22 isoforms; VAMP7; SEDL; and  $\sigma$ 2 adaptin of the AP2 complex (Rossi et al., 2004). I would be remiss to not caution the reader we use this classification of a longin-like fold when speaking of Fuz protein for good reason. True longin domain were so named in *bone fide* SNARE proteins to describe the N-terminal ‘long’ domains in contrast of the N-terminal ‘brevin’ or ‘short’ domains found in other SNAREs. The primary sequence of Fuz protein does not suggest any canonical SNARE motif.

Moreover, the longin-like fold is the last 132 amino acids of the *Xenopus laevis* protein. While all cases of the SNAREs, the longin domains are located at the N-terminal of the protein. In addition, multiple proteins functional in all aspects of vesicle trafficking events exhibit longin-like folds (Rossi et al., 2004). Most importantly, we observed

multiple defects in our manipulations of Fuz that in addition suggests a role for vesicle trafficking.

In Chapter 4, we argue that vesicle or protein complex trafficking to and within the ciliary axoneme is affected by a loss-of-function Fuz or RSG1; as loss-of-function Fuz morpholino containing embryo (Fuz morphants) exhibit, in MEMFA fixative, sub-apical accumulations of CLAMP-GFP foci near normally structured accumulations of basal bodies as imaged with centrin-RFP (Fig. 24). During live imaging of mosaic Fuz-morpholino/HistoneRFP (FuzMO/nucRFP) *Xenopus* multi-ciliated epithelium we observed an increase in sub-apical CLAMP-GFP spots in some cases near the basal layer of the nucleus (data not shown). We also observed a decrease of distally localized CLAMP-GFP at the tips of cilia in the same analysis (Fig. 19). The same analysis using in RSGMO embryos recapitulated all loss-of-function phenotypes of the FUZ morphant embryos where analysed. However, we observed in all an increased incidence of the sub-apical CLAMP-GFP foci during live mosaic RSG1MO/nucRFP multi-ciliated cells. This may reflect a non-specific morpholino dependent efficacy of knockdown; alternately, this might reflect a promiscuity of RSG1 protein for a Fuz-like protein(s) functioning in parallel during cilia biogenesis and function. As dose dependence of morpholino injections are problematic with these kinds of assays; these experiments would be hard to interpret. A deeper understanding of this caveat will be better addressed by genetic ablations and/or elucidation of binding partners for RSG1.

The multi-ciliated frog epithelium also contains a large numbers of cells that function to secrete large granules of mucous. In a loss-of-function Fuz embryo, we observed a loss of normal exodermal secretory granules as assayed by antibody staining of anti-Xeel (intelectin-1) (Nagata et al., 2003). Furthermore, TEM analysis of frog epidermis showed that vesicles were significantly increased in apically docked yet unfused vesicles, at times exhibiting homotypic fusion, not observed significantly in wild type uninjected control sibling embryos. While, SEM analysis shows Fuz morphants significantly lack exocytic pits seen in *Xenopus* secretory epithelium (Hayes et al., 2007). As well, our SEM analysis observed defects in mucous secretion and ciliogenesis in RSG1 morphants reflecting a conservation of function between Fuz and RSG1.

A loss of CLAMP-GFP fusion protein at the distal tips of cilia is highly reminiscent of results with IFT20 mutants in both *Chlamydomonas* and the mouse (Pedersen et al., 2003; Jonassen et al., 2008). This mutant displayed defects: in the length cilia which did not phenocopy the defects seen with retrograde IFT mutants (e.g. bulbous tip); in the trafficking of a distal EB1 signal; and of trafficking of polycystin-2 to the cilia (Follit et al., 2006). In attempts to test a hypothesis that Fuz loss-of-function might be controlling SNARE sorting, we explored the localization of a SNARE dependant of most fusion events SNAP-25. Indeed, SNAP-25 is localized to cilia however this localization is concentrated at the distal tips of cilia (Fig. 29). Interestingly, we observed that SNAP-25 is lost from most distal ends of the cilia in Fuz mosaic cells (Fig.30). It will be crucial to parse out if our defects in trafficking to cilia in both Fuz and RSG1 loss-of-function experiments are acting in a pathway with or parallel to the IFT20 mechanisms.

Additional observations of Fuz loss-of-function embryos may be analogous to a loss of COPII function. As disruption of COPII exhibits collagen secretion defects essential for normal craniofacial development (Townley et al., 2008). We have evidence of severe defect in cranial development in the Fuz gene trap mouse (Chapter 4). It might be interesting to explore a role of Fuz/RSG1 in the export of collagen from the endoplasmic reticulum.

Localization data using a Fuz peptide antibody generated in rabbit shows specific localization to the area of the rootlet (Fig. 13). It may be that Fuz is crucial for pre-initiation of vesicle traffic from the basal area in order to retrieve/ recycle SNARES for proper secretory events at the transition zone of the cilia; this mechanism may explain the defects seen with secretion of the large mucus granules. Furthermore, it is possible that vesicle trafficking to the cilia is defective as represented by the aberrant localization of a CLAMP-GFP fusion protein and a loss of the distally localized endogenous SNAP-25 assayed by anti-body staining (Fig. 29-30).

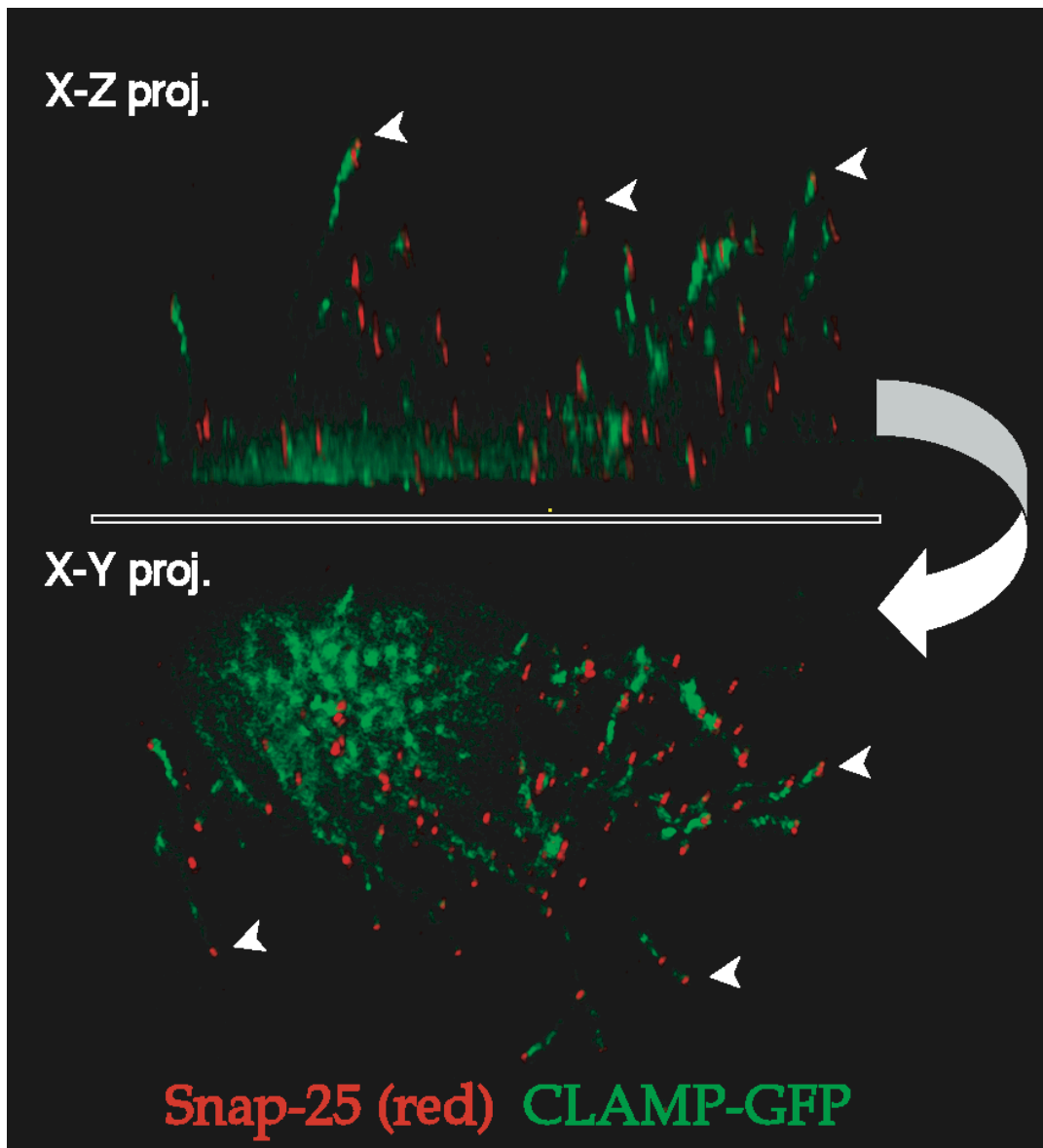


**Figure 29 SNAP-25 localizes to the distal tips of epithelial cilia.** Confocal projection of *Xenopus* multi-ciliated cell expressing a CLAMP-GFP fusion protein and antibody stained for anti-mouse SNAP-25 (red). MEMFA fixed.

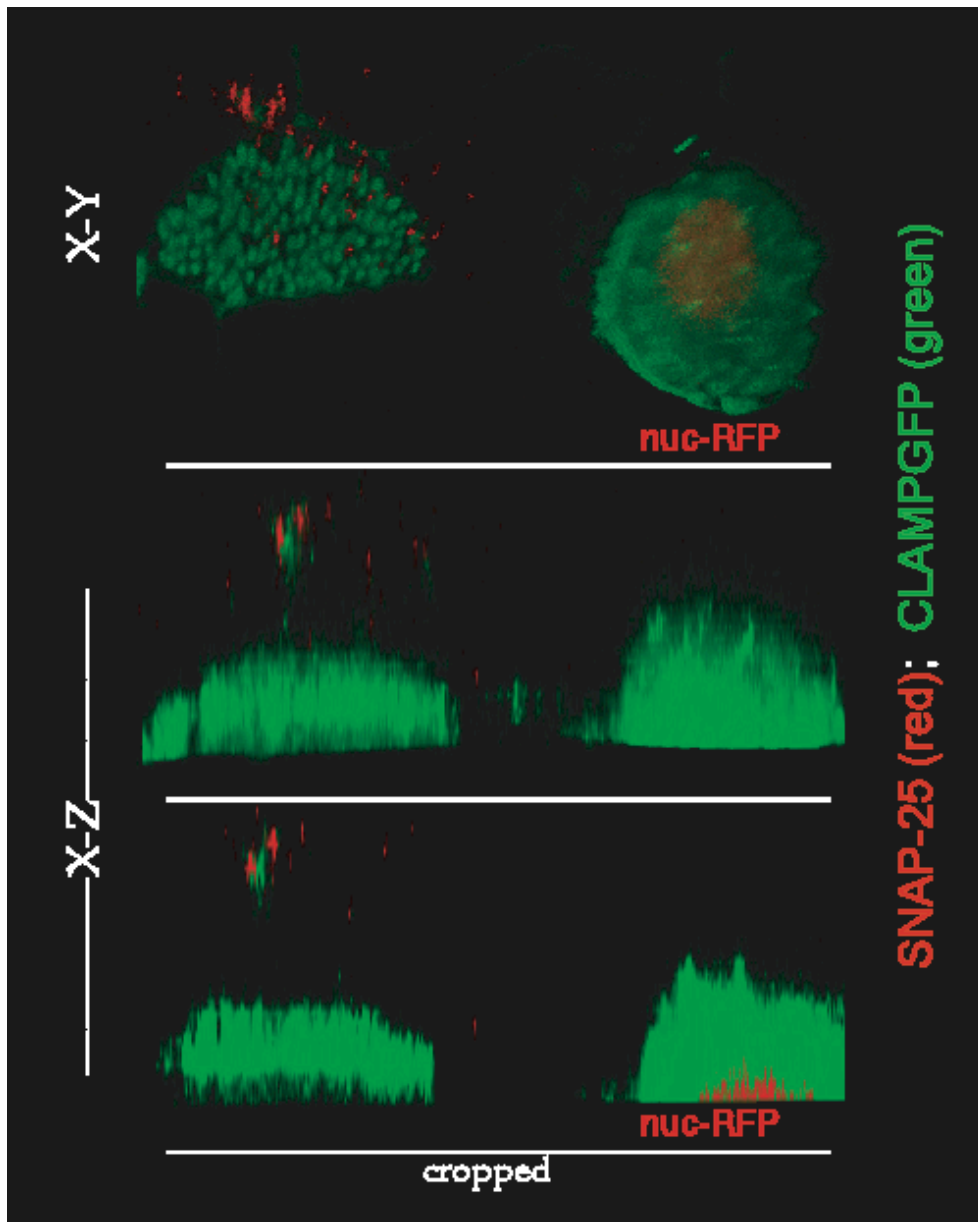


**Figure 30 SNAP25 localization to the distal tips of cilia is disrupted in Fuz mosaic multiciliated cells.** Confocal projection of mosaic *Xenopus* multi-ciliated epithelia expressing a CLAMP-GFP fusion protein and histone-RFP (nucRFP) tracing a co-expression of the Fuz morpholino. Processed with an anti-mouse SNAP-25 (red). MEMFA fixed. The cells expressing the nucRFP signal lack apically extended cilia (green) as well as absence of SNAP-25 antibody staining.

### **5.2.1. The C-terminal domain of Fuz: A Longin-like fold domain is a dominant negative molecule during *Xenopus* development**

Over expression of the C-terminal (AA 287-419) of *Xenopus laevis* Fuz in the dorsal tissues of the developing tadpole generates defects in the formation of normal craniofacial development. Seen as defects in cranial cartilage development, loss or reduction normal eye development, as well as a phenotype associated with loss of function Fuz, a delay in the closure of the anterior neural tube (Fig. 31-32 and reference (Park et al., 2006)). This may imply a squelching mechanism of inhibition on the normal function of fuzzy, which we predict acts to inhibit the mechanics or localization/retrieval of SNAREs *in vivo*. The similar dominant negative effects were observed with the over-expression of the longin-domain of TI-VAMP (Proux-Gillardeaux et al., 2007). Interestingly, these experiments exhibited defects in the polarized secretion of lysosomal proteins, necessary for membrane repair, and general cell migration in wound-healing assay in cell culture. This is further supported by observations that polarized secretions of matrix proteins and/or matrix dissolving proteins (e.g. matrix metalloproteases) are necessary for cell migrations *in vivo* (Davidson et al., 2004; Davidson et al., 2006; Masckauchan et al., 2006).

In the case of Ykt6, the longin domain auto-inhibits its SNARE domain. This provides fidelity of interaction between multiple compartments of the cytoplasm. Such that the solubility of a lipid-modified form of Ykt6 protein is enhanced by self-interaction with its longin-domain as well may prevent promiscuous interactions with inappropriate SNAREs (Hasegawa et al., 2003).

Additionally, the longin domain of Sec22 was recently shown to provide a sorting mechanism for this SNARE (Mancias and Goldberg, 2007). As such, the binding of the N-terminal longin-domain of Sec22 to a NIE amino acid region within the SNARE domain of Sec22 allows the association with the COPII coatomer proteins Sec23/24. Thus, the longin domains of two proteins Sec22 and Ykt6 provide a fidelity of sorting within the cytoplasm that is likely dependent on conformational changes of the protein which facilitates binding of coatomer proteins such as COPII.

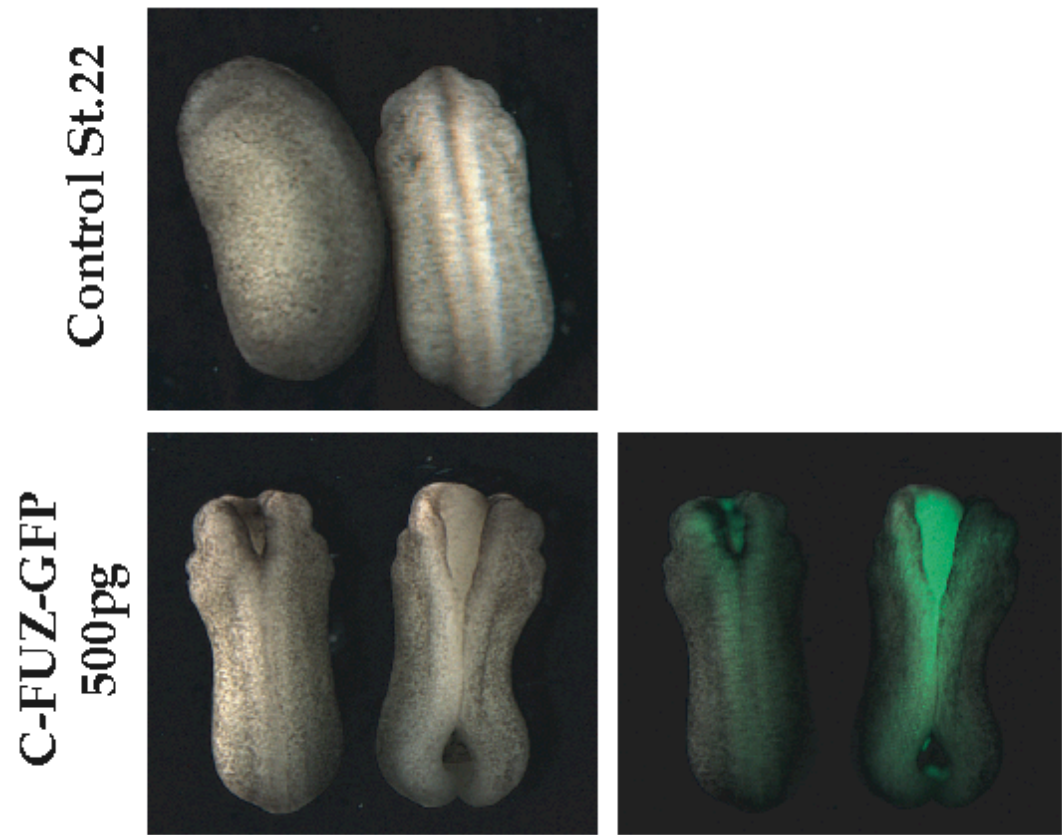


**Figure 31 C-Fuz acts as a dominant-negative for anterior neural tube closure.**  
Dorsally targeted expression of C-Fuz generates delayed anterior neural tube closure defects (bottom panels) as compared to sibling un-injected embryos (top).



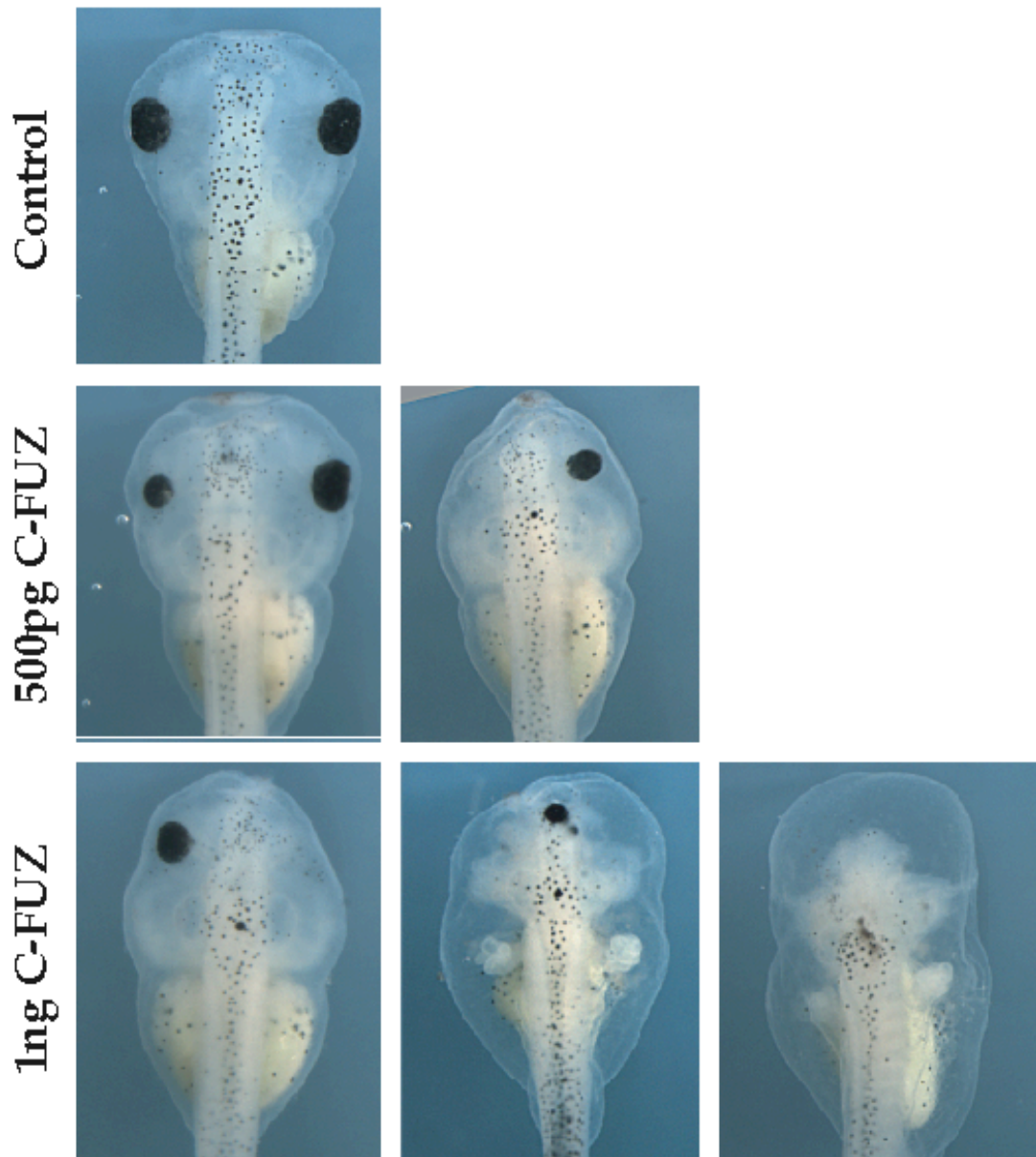


**Figure 32 C-Fuz generates dose-dependent defects of cranio-facial development.**  
 The expression of 1ng C-Fuz generates increased observations of cranio-facial defects such as loss of eyes structures as compared to either 500pg injection or uninjected sibling embryos.

The regulation of vesicle transport is regulated by the combinatorial interactions of multiple SNARE proteins, tethers, and Rab-like GTPases (Cai et al., 2007). Importantly, the appearance of a longin-like fold occurs in multiple proteins that exhibit divergent roles in these processes. For instance, the longin domains of the SNARE proteins: Sec22b, Ykt6, and Nyv1p (Rossi et al., 2004); the longin-like folds of the endocytic adaptin protein subunits  $\sigma$  and  $\mu$  {Collins, 2002 #3206}; and the SEDL subunit of the TRAPP tethering complex (Jang et al., 2002; Fan et al., 2009). This commonality of the longin domains in vesicle trafficking proteins suggests at least some mechanistic or functional conservation. One mechanism is clear from the observations of the longin domains of the SNARE protein mentioned previously; longin domains provide fidelity of interactions and prevent promiscuity of interaction. The longin-like domain,  $\mu 2$  of the AP2 complex are known to link clathrin to specific membrane cargo during vesicle budding (Collins et al., 2002). In addition, the  $\mu 2$  and  $\sigma 2$  subunit of the same complex have been shown to stabilize the AP2 tetrameric complex; via interactions with all three corresponding subunits (Collins et al., 2002). While, observations of the Srx longin domain (Kinch and Grishin, 2006); the C-terminal helix of Arf1 a GTPase interacts with a putative longin domain of delta-COP (Sun et al., 2007); and the longin-like fold of the C-Fuz implicate functional interactions with a small GTPases ( Chapter 4 this work).

Another speculative model of the PCP effector proteins and the GTPase RSG1 is highlighted by a model of coat nucleation of the COPII complex with its GTPase, Sar1. Wherein, GTP hydrolysis was increased *in vitro* by addition of Sec 23/24 and further increased by addition of Sec 31 (Bi et al., 2007). This increase in GTP hydrolysis is indirect evidence that the COPII complex proteins are GTPase Activation Proteins (GAP) for Sar1. This model beautifully, explains the coupling of coat assembly to disassembly. It would be interesting to explore the role, if any, of PCP effector genes on the GAP activity of RSG1.

In light of our observations that RSG1 and Fuz display a conservation of function and that we observed that these proteins bind one another, we have begun to test what domain of Fuz are necessary for binding of RSG1. In fact, we observe the binding of a GFP-RSG1 fusion construct to myc-Fuz and myc-C-Fuz fusion proteins (Fig. 33). The C-

fuz construct represents the predicted longin-like fold domain. In the future test we will test if this interaction is conserved for the N-terminus as well though are hypothesis is that the N-terminus will not be sufficient for an interaction.

In addition, we hope to begin to explore if the N-terminus of Fuz might bind the C-terminus of Fuz. In effect, an auto-inhibition function akin to observations of the longin-domain protein Ykt6 (Tochio et al., 2001). As well, given our results that the dominant-negative GFP-RSG1 T64N fusion protein displays a defect in localization to the rootlet in multi-ciliated cells we will explore the effects of a loss-of-function Fuz on the localization of a GFP-RSG1 fusion protein. Lastly, we plan on exploring if the binding of RSG1 to Fuz is dependent on GTP by attempting to immunoprecipitate the dominant negative RSG1 T64N protein, which should be constitutively GDP bound. Our hypothesis is that Fuz will not pull-down a RSGT64N fusion protein.

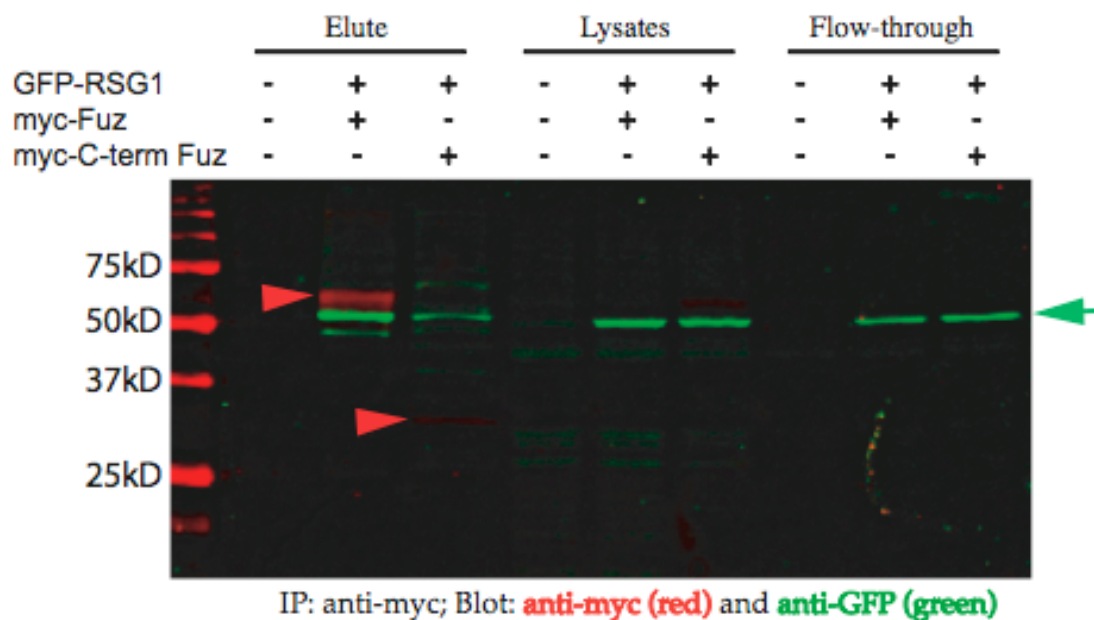


**Figure 33 The predicted longin-like fold of Fuz binds GFP-RSG1** A Li-COR double anti-processed for anti-myc (red) and anti-GFP (green). Embryos were co-injected with fusion construct as indicated and immunoprecipitated with anti-myc beads.

### 5.3. Are PCP family effector proteins inherently vesicle trafficking proteins?

Because we observe multiple line of evidence that Fuz protein serves a role in vesicle trafficking events; moreover, as all PCP effector proteins seem to have conservation of function both in fly; frog; and likely mouse (Chapter 4 this work and (Park et al., 2006)); we employed similar bioinformatics technique to investigate the function of Inturned (Intu) and Fritz (Frtz).

We find that Fritz is a  $\beta$ -propeller containing protein as predicted by both structural homology modeling and primary BLAST search. We do not prescribe these domain be referred to as WD repeats as the canonical WD sequences are not conserved in our models or in the primary sequence (Fig. 34 and not shown). In addition, Fritz protein has multiple clathrin binding motifs: a strong conservation of a well-defined D/ExxxLL motif (aa 457-462 human Fuz), known to bind both  $\beta 2$  and  $\mu 2$  subunit of the AP2 complex (Olesen et al., 2008). In addition, we observe a well-conserved FxDxF motif, known to bind specifically to the  $\alpha$ -adaptin protein, in both *Xenopus* species (138-142 *Xenopus* Fritz) while in other vertebrate species this motif appears as LxDxF. We are currently unsure whether these motifs are functional in binding AP2 subunits.

We find that Inturned (Intu) displays a large PDZ domain modeled as amino acids 143-272 of *Xenopus* Intu. In addition, a primary sequence BLAST search predicts this data. Structurally, we also predict a large solenoid structure of  $\alpha$ -helices between amino acids 281-559 of *Xenopus* Intu (Fig. 34). This large solenoid prediction can be modeled on the protein database (pdb) structure 2vgl of the adaptin core complex 2 (AP2). This is interesting, given that Fuz resembles both the  $\mu 2$  and  $\sigma 2$  subunits in terms of the longin-like fold and that fly Intu and Fuz have been shown to interact genetically as well as physically bind one another (Lee and Adler, 2002; Collier et al., 2005). In addition, Intu protein has multiple clathrin binding motifs observed three well-defined D/ExxxLL motifs, known to bind both  $\beta 2$  and  $\mu 2$  subunit of the AP2 complex (Olesen et al., 2008).

The structural relatedness of Fritz protein to Sec13 is of great interest due to the fact we observe vesicle fusion defects in the large secretory cells that are likely downstream of a mis-sorting of SNAREs. In addition, the chondrodysplasia of both the Fuz and Intu loss-of-function frog and the Fuz knockout mouse embryos might suggest a

role similar to COPII vesicle trafficking events (Fromme et al., 2007). This is also interesting due to our predictions of the Fritz structure. At least in mapping the Fritz structure on the Sec13 crystal structure results in correlation of the mechanism of Sec13 (Fig. 34 Fritz pred. red) binding to Sec31 (Fig 34 Fritz pred. gray) (Fath et al., 2007). Importantly, the  $\alpha$ -solenoid structure that binds to Sec13 is somewhat conserved by our predicted structure of Intu. However, attempts to model Intu on a Sec31 structure using the mGENTHREADER algorithms were unsuccessful (data not shown).

Clearly, much work remains to be done to better understand the PCP effector complex of Fuz/Intu/Fritz. We suggest a role in vesicle trafficking with the Fuz protein and by equivalence the other PCP effector protein Intu and Fritz. Descriptive loss-of-function data from both frog and mouse as well suggest the above hypothesis (Chapter 4 this work). In addition, we describe how all three PCP effector proteins possess structural domains and sequence motifs that are found in vesicle trafficking proteins. In addition, as transport is disrupted to the cilia of the multi-ciliated epithelium that mirrors multiple defects observed with the intraflagellar transport proteins (IFTs) we believe a similar or parallel mechanism is functioning with the PCP effector proteins. Additionally, multiple lines of evidence have generated a hypothesis that the IFT proteins are evolved from proto-coatomer like proteins (Jekely and Arendt, 2006). This hypothesis is supported by the presence of multiple WD repeats domain and tetratricopeptide repeats (TRP) shared by multiple vesicle trafficking proteins of the COP I/II coats and the nuclear pore complex proteins. It will be exciting to test a hypothesis that PCP effector proteins are possibly of proto-coatomer or vesicle trafficking in origin.

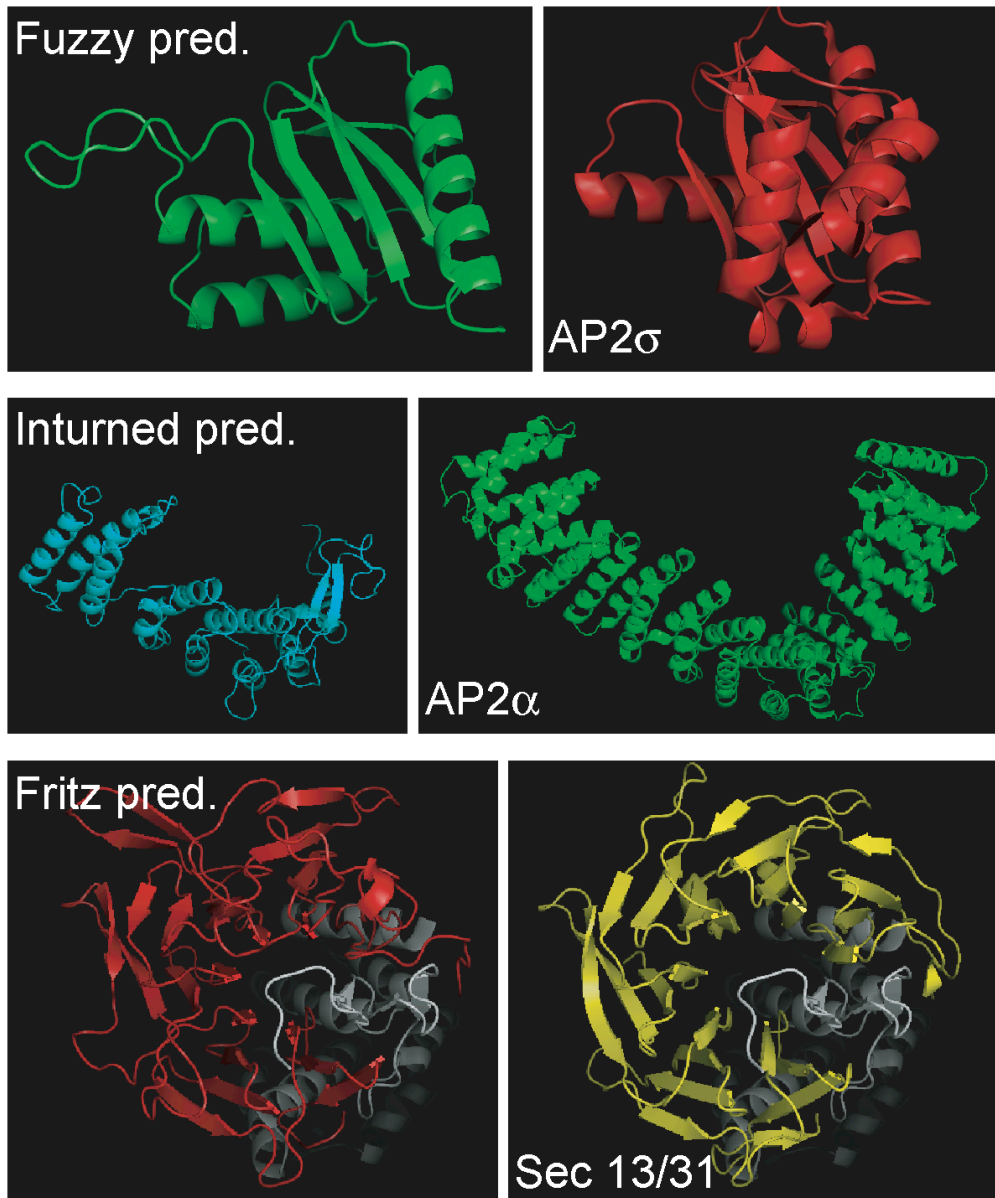


**Figure 34 Modeling of PCP-effector protein domains.** All modeled protein domains were compiled by PSI-PHRED assumptions of secondary structure and mGENTHREADER searching of the PDB database in attempts to model tertiary structure of PCP effector protein domains. Fuzzy prediction modeled on AP2s subunit (pdb: 2vgl). Inturned prediction modeled on AP2a subunit (pdb: 2vgl). Fritz prediction modeled on Sec13 structure (pdb: 2pm7).

## **Chapter 6: Methods and Materials**

### **6.1. Embryo Manipulations**

#### ***Xenopus* embryo manipulations:**

Female adult *Xenopus laevis* were ovulated by injections of human chronic gonadotropin, and eggs were fertilized in vitro and dejellied in 3% cysteine (pH 7.8-7.9) and subsequently reared in 0.3X Marc's Modified Ringer's (MMR). For microinjections, embryos were placed in a solution of 3% Ficoll in 0.3X MMR, injected using forceps and an Oxford universal manipulator, reared in 0.3X MMR + Ficoll to stage 9, then washed and reared in 0.3X MMR alone. Embryo culture, solutions, in vitro transcription were performed using standard methods (Sive et al., 2000).

#### **Chicken embryology:**

Fertilized Leghorn eggs (Ideal Poultry, Texas) were incubated at 38°C in a forced draft-humidified chamber. Embryos were staged according to Hamburger and Hamilton (Hamburger and Hamilton, 1951). Embryos were harvested between embryonic day 2 and 3 and immersion-fixed in 4% paraformaldehyde.

#### **Mouse embryology:**

##### **Generation of experimental animals:**

The Fuz<sup>Gt1(neo)</sup> mutant mice were housed in the Institute of Biosciences and Technology Vivarium, which is fully accredited by the AAALAC. The animals were maintained in clear polycarbonate microisolator cages and were allowed free access to food and water (Harlan Teklad Rodent Diet no. 8606, Ralston Purina, St. Louis, MO). The mice were maintained on a 12-h light/dark cycle. Nulligravid heterozygous Fuz<sup>Gt1(neo)</sup> females, 50-70 days of age, were mated overnight with heterozygous Fuz<sup>Gt1(neo)</sup> males and examined for the presence of vaginal plugs the following morning. The onset of gestation was considered to be 10 p.m. of the previous night, the midpoint of the dark cycle (Snell et al., 1948); thus observation of a plug was determined to be embryonic day

(E) 0.5. Pregnant females were euthanized by CO<sub>2</sub> asphyxiation on gestation day 18.5, the offspring were collected by caesarian section and evaluated for external malformations. Animal experimentation was approved by the IBT Institutional Animal Care and Use Committee.

**Generation and genotyping the knockout Fuz<sup>Gt1(neo)</sup> mice:**

The Fuz<sup>Gt1(neo)</sup> mutant mice were generated by the Texas A&M Institute for Genomic Medicine from ES cells generated by Lexicon Pharmaceuticals Inc. (The Woodlands, TX, USA) that corresponded to clone OST180427 (OmniBank sequence tag), that were targeted by gene trapping. The gene trapping vector was inserted at the second of 11 exons of the Fuz gene in ES cells. This gene trap is predicted to disrupt the transcription of the Fuzzy homolog gene due to the nature of the trapping vector. Specifically, the vector contains a splice acceptor (SA) site followed by a neomycin resistance cassette (NEO). The fused transcript thereby allows antibiotic selection by splicing of the endogenous Fuz promoter and upstream exons (E1 and E2) with the NEO cassette. The vector used for producing the Fuz homolog ES cells also contains mouse phosphoglycerate kinase (PGK) promoter sequence, an exon from Burton's Tyrosine Kinase (BTK), and a splice donor (SD) site. Splicing of this transcript with downstream exons thereby allows for the identification and localization of the trapping vector within the Fuz gene.

Targeted ES cells were selected for blastocyst microinjection into C57BL/6 mice to produce chimeric mice. In order to check for germline transmission of the targeted allele, chimeric males were mated with C57BL/6N females. Heterozygous Fuz<sup>Gt1(neo)</sup> males were then mated with heterozygous Fuz<sup>Gt1(neo)</sup> females to obtain homozygous Fuz<sup>Gt1(neo)</sup> mice. All experimental mice used in this study were of mixed background 129/C57.



## 6.2. Biochemistry

### Co-ImmunoPrecipitation:

30-50 of Co-IP embryos and 30-50 Control embryos are required for procedure. Co-IP embryos are injected with both a RNA to express a tagged protein which can be eluted (protein 1) with ab specific to the tag which are conjugated to agarose beads. If no ab to the second protein is available, then RNA to express second protein must be injected. This protein must have a tag different to the first. The tag will allow for visualization after blotting, not precipitation. In hypothesis, if the second protein binds to the first tagged protein, then the second protein will be precipitated. The control embryos should be the same as the experimental except the lacking of the first tagged protein to be eluted. This control ensures that the second protein does not interact with the beads and ab's.

#### Review:

- Co-IP sample is the embryo homogenate with pull-down tag and target constructs injected. i.e. myc tagged protein pulled down with myc beads targeting a protein tagged with flag tag.
- Control is embryo homogenate injected only with the target construct. (if precipitating with myc tag, then control is the target alone without myc)

#### Lysis

\*Do this for both the sample and the control.

All steps should be performed on ice (4C).

1. Lyse ~30 embryos in 600ul of lysis buffer by pipetting. (approx 20ul per embryo of lysis buffer.)

General NP-40 lysis buffer (that is good for IP)

Tris (pH7.4): 20mM

NaCl: 150mM

NP-40: 0.1-1% (higher concentrations are better for solubilization, but may interfere with protein binding. NP-40 is not good for M2 anti-FLAG ab, so in this case substitute NP-40 with M2)

Glycerol: 0-10% (reduces not specific antibody and bead interactions, but may also interfere with protein interaction.

Protease inhibitor cocktail: 1/100 dilution

PMSF: 1/100 dilution

A good start for optimizing the procedure would be 0.1% NP-40 and 5% Glycerol

TBSGT has been used in the Wallingford lab as a lysis buffer.

2. Incubate for 5 minutes on neurator at 4C.
3. Spin for 15 minutes at max RPM at 4C.
4. There should be three layers after centrifugation. A pellet, the lysate (the sample), and a layer of lipid on the top. Remove as much of this layer as possible, not to demise your sample. Not all of the lipids will be removed. Carefully transfer the supernant to a new tube.

5. This is a good stopping point for the day. To save the sample, freeze the supernant at  $-70^{\circ}\text{C}$ .

### **Immunoprecipitation**

- DO NOT USE HIGH SPEED CENTRIFUGE when working with ab conjugated beads!
- 1. Take 20ul of lysate from embryos injected with myc and flag constructs (supernant) and save for input lane.
- 2. Into two appropriately labels ependorph tubes, transfer 40-60ul of Ab conjugated beads to a tube for the sample and 40-60ul into a tube for the control.

Beads are larger than the p200 pipette tip openings. To transfer from vial, cut the pipette tip. Do this for both the sample and the control.

3. Wash the 40-60ul of beads in the 1ml of the lysis buffer. Spin the beads down with the table top C'fuge. DO NOT USE HIGH SPEED CENTRIFUGE. Discard as much buffer as much as you can without discarding the beads.
4. Add the lysate to the beads and incubate on the neurator or rotator at 4 degrees for more than 3hr.

The lysate can be pre-cleared by incubating with ab-conjugated bead for 30 minutes to reduce non-specific binding.

5. Spin the beads down. From the Co-IP tube, remove 24ul of supernant. This is the Flow-through sample. This sample, when visualized, will prove that both proteins are being expressed in the sample.
6. Carefully remove the remaining supernant from each of the tubes.
7. Rinse the beads with 1ml of lysis buffer. This is essential to remove the flow through in the volume between the beads. Without this step, there will be false positives. Rinse by inverting the tube ~10 times. Spin the beads down and remove the rinse.
8. Repeat rinse with 1ml of lysis buffer.
9. One last wash with 1ml of lysis buffer.

If excessive non-specific binding is seen, then increase each rinse time to 5min on the neutator @  $4^{\circ}\text{C}$ .

### **Elution of the Samples**

There are two methods to elute the Co-IP.

\*Do not use DTT or B-Me in contact with the beads. DTT or B-ME will reduce the antibody from the bead making it hard to see overlapping proteins, and destroying the beads.

#### **Loading buffer method #1**

1. Boil on 30ul of 2x SDS Sample buffer WITHOUT B-ME or DTT for 5 min.
2. After spinning beads down, transfer sample to fresh/labeled tube. Add 50mM of DTT (1/20 dilution of 1M aliquot) and boil for 5min. 15-30ul of sample should give sufficient signal on a western blot.

#### **Loading buffer method #2**

\*Glycine elution will give less background but more steps are needed (dialyze).

1. add 30ul of 100mM Glycine (pH2.5).
2. Elute twice and pool the sample together.
3. Immediately add 1/20 volume of 1M Tris (pH9.5) to neutralize the sample.
4. Dialyze sample to remove glycine to prevent very wide bands on the SDS-page gel. We use pierce mini dialysis units with 10kDa membrane, and incubate in lyses buffer for 2-3 hours. (200 to 300 times the volume of sample)

### **6.3. Cloning and PCR**

**Morpholino antisense oligonucleotides were obtained from GeneTools, LLC:**

*Dvl1*MO, 5'-GGTAGATGATTTTGGTCTCAGCCAT-3'

5mis *Dvl1*MMMO, 5'-GcTAGATcATTTTcGTCTgAGCgAT-3'

*Dvl2*MO, 5'-TCACTTTAGTCTCCGCCATTCTGCG-3'

As described previously (Lee et al., 2006).

*Dvl3*MO, 5'-GGTAGATGACCTTGGTCTCCCCCAT-3'

*Dvl3* Alternate MO, 5'-GGCTTAGCCCCAAAATCTGTCATAC-3'

5mis *Dvl3* MMO, 5'-GcTAGATcACCTTcGTCTgCCCgAT-3'

**Chicken *DVL1* and *DVL3* probe synthesis:**

Probe fragments for chick *DVL1* and *DVL3* were generated by polymerase chain reaction from a pool of E2 whole embryo cDNA and then subcloned into the pCR-TOPO II vector (Invitrogen).

Primers were designed using MacVector based on sequences submitted to NCBI (chick *Dvl1*: NM001030873 gi-71894888 and chick *Dvl3*: XM422756 gi-118095208). The primer pairs are as follows:

**Chick *DVL1***

Forward: 5'-GGATTGGACAACGAAACAGGAAC-3'

Reverse: 5'-TGTGGAAGTGGAGCAAGGGTATC-3'

**Chick *DVL3***

Forward: 5'-AATACTGGGGGGAGTCGGGAAAAC-3'

Reverse: 5'-TTCACGGTGTGTCTGGATGTAGC-3'

**Mouse genotyping:**

Genomic DNA was extracted from the tail samples using the DirectPCR-tail (Viagen Biotech Inc. Los Angeles, CA) and used for PCR-genotyping. The product for the wild type (wt) allele was 295bp long. Primers sequence:

Fuz forward 5'-AGTAGAGGCTCGGAGCCTTTAGG-3'

Fuz reverse 5'-TCACCTAAGCCAGGAACCACTGC-3'

and for the mutant allele (Gt1) was 216 bp. primers sequence:

Fuz forward 5'-AGTAGAGGCTCGGAGCCTTTAGG-3'

LTR reverse 5'-ATAAACCTCTTGCAGTTGCATC-3'.

The following plasmids have been described previously: CLAMP-GFP, CENTRIN-RFP and MIG12-GFP (Ref. (Hayes et al., 2007; Park et al., 2008)); Fuzzy Morpholinos

(translation blocking 1, 2 and splice blocking) (Ref. (Park et al., 2006)); RSG1 (IMAGE:5571542; Unigene ID: 501682) was purchased from Open Biosystems (Huntsville, AL) and cloned into the CS107 vector. RSG1<sup>T→N</sup> was generated by Mutagenex, Inc; a single point mutant in the 65th codon as ACC to AAC yielding a Threonine to Asparagine mutant. To generate Flag-tagged RSG and RSG1<sup>T→N</sup> fusion proteins, GFP tagged RSG and RSG1<sup>T→N</sup>, and myc tagged Fuzzy, cDNAs were amplified using Vent polymerase (NEB) and subcloned into CS107-flag-3Stop vector, CS107-GFP vector and CS-MT+ vectors, respectively. All constructs were verified by sequencing.

### **Example of a generic VENT polymerase protocol:**

#### **Morpholino and mRNA injections:**

Capped mRNA was synthesized using mMessage Machine kits (Ambion). mRNA or antisense morpholino oligonucleotide (MO) was injected into two ventral blastomeres at the four-cell stage to target epidermis. FuzMOs were injected at 40ng per blastomere. Both splice and translation blocking anti-sense oligonucleotide for Fuzzy were described previously (Park et al., 2006). *Importantly, we find that resuspending morpholinos in molecular grade water at 65 degrees for 5mins and subsequent storage in a dark drawer at room temperature is better than constantly freeze-thawing your aliquots of the morpholino.*

#### **Mosaic Analysis in *Xenopus* using Morpholinos:**

##### **CLAMPGFP and H2BRFP/morpholino mosaics**

CLAMPGFP [ 100ng/injection] was injected into both ventral blastomeres of the 4-cell stage embryo. After these embryo reach the 8-cell stage one animal ventral blastomere was injected with a mixture of FuzzyMO or RSGMO [40ng/injection] and Histone RFP [100ng/injection]. Embryos were chosen at stage 26-27 for mosaic expression of the H2BRFP signal in a field of cells that were evenly expressing the CLAMPGFP signal.

#### **6.4. *In situ* hybridizations and Histology**

##### ***Xenopus* embryos:**

Embryos were allowed to develop until desired stage and then fixed for 2 h in MEMFA, except for the fibronectin antibody where embryos fixed in Dent's fixative. *In situ* hybridizations were carried out with RNA probes labeled with digoxigenin-UTP by using the technique previously described (Sive et al., 2000). Probes used were *Pax3*, (Mariani et al., 2001); *XMyoD*, (Hopwood and Gurdon, 1990); *Dvl1*, CD362087(ATCC); *Dvl2*, (Sokol et al., 1995); *Dvl3*, XL190g16 (NIBB); *XMyf5*, (Hopwood et al., 1991); *XSlug*, (Mancilla and Mayor, 1996); *XTwist*, (Hopwood et al., 1989b); *Myoskeleton*, (Zhao et al., 2007); *XParaxis*, (NIBB); and *XPax1*, XL085n23 (NIBB).

##### **Example *in situ* probe reaction protocol:**

3ul Ethanol precipitated probe template [~1ug/ul]

2.5ul transcription buffer [5X] (promega)

1.5ul Digoxigenin labeled nucleotide mix (Roche)

0.5 ul DTT 100mM (promega)

0.25ul RNasin (promega)

1ul T7 polymerase (promega)

6.25ul molecular grade H<sub>2</sub>O

Vt-15ul

##### **Wallingford lab *in situ* protocol:**

Fix embryos at appropriate stage in 1X MEMFA for 2 hrs rotating at room temp or O/N on nutator at 4 degrees

Wash out MEMFA (all washes 5 minutes each):

PTW washes

Dehydrate in MeOH (all washes 5 minutes each):

MeOH washes

\*continue MeOH washes until NO SCHLERIN LINES!

O/N at -20 in MeOH, or at least 4 hours (*dehydration removes lipids which will absorb stain if still in embryo*)

### **DAY 1 of in-situs** (turn on 60°C bath)

Rehydration (all washes 5 minutes each): (Chanjae transfers to baskets here)

MeOH

75% MeOH/25% PTW

50% MeOH/50% PTW

25% MeOH/ 75% PTW

*(Rehydration into PTW from MeOH is done gradually to prevent the formation of bubbles in embryos, which will damage them. PTW is used because the detergent (Tween) prevents the embryos from sticking to each other and aids in solubilizing cell membranes which assists in penetration. Furthermore, PTW is a phosphate buffered saline solution that helps to neutralize the negative charge of mRNA so that the probe can bind better to it. - (JBW transfers embryos to baskets after first PTW wash because embryos are brittle in MeOH.)*

Proteinase K (1ul/ml of 10mg/ml solution)

Envelopes on embryos = 1 min. in PK

Envelopes off of embryos = 45 seconds in PK

*(This step is to permeabilize the embryo by removing some of the outer proteins, which allows better probe penetration for deeper tissues. **This is not a good time to transfer to baskets!**)*

Rinse 2 x 5 minutes in 0.1M triethanolamine pH 7-8

*(The triethanolamine is a buffer without free amines which is necessary for the next step).*

Add 12.5ul acetic anhydride/5mls: 5 minutes

Repeat acetic anhydride addition; 5 minutes

*(Acetic anhydride acetylates free amines to neutralize positive charge so that the probe will bind specifically to mRNA rather than nonspecifically due to electrostatic interactions.)*

Wash 2x 5 minutes in PTW

Refix for 20 minutes with 1X MEMFA

*(Reduces the permeabilizing step done with PK, but helps keep the embryo intact)*

Wash 5 x 5 minutes in PTW

*(Washes out fix)*

Wash in Prehybridize Buffer for 6 hours at 60°C

(save prehyb solution for use @ step #12)

*(Prehyb buffer has many different components to help keep RNA denatured so that it is linear and can bind to probe effectively. It also has other components that minimize non-specific binding.)*

Replace prehyb buffer with 0.5ml probe solution (1ug/ml probe), hybridize O/N @ 60°C

*(probe binds RNA in embryo)*

### **DAY 2 in-situs**

Remove probe and **keep** (probe can be used several more times)

Replace probe with saved prehyb solution (from step #9),

wash 10 minutes @ 60°C

Washes:

Three times, 20 minutes each in 2x SSC, 60°C

*(Remove excess hybridization buffer and excess probe.)*

2xSSC with Rnase A 20ug/ml & Rnase T<sub>1</sub>

10,000u/ml (5ul T + 10ul A/5ml), 30 minutes

@37°C with shaking (~35 rpm)

*(RNase A and T<sub>1</sub> degrade mismatched double stranded RNA.)*

2xSSC 10 minutes rm. Temp.

Twice in 0.2xSSC, 30 minutes @ 60°C

*(2X SSC is a stringent wash to remove unspecific binding, 0.2X SSC same purpose, more stringent, also washes away RNase)*

**Start thawing Block**

Twice in MAB 10-15 minutes, rm. temp.

Wash in MAB + 2% BMB Blocking Reagent (10% Block stock in freezer), 1 hour or more on nutator @ RT.

*(block keeps Ab binding specific by putting protein blanket on embryo)*

Replace with MAB + 2% BMB Blocking reagent + Ab, O/N at 4°C (1/2000 dilution of anti-dig AP antibody, 1/5000 dilution will work)

*(Ab binds to DIG in probe)*

### **DAY 3 in-situs**

Wash embryos at least 5X, 1 hr each with MAB

*(Washes are necessary in order to wash off excess antibody.)*

You can transfer to vials here using a **glass** pipette (embryos won't stick to glass) or wait until after AP buffer wash.

Wash twice, 5 minutes each @ rm. Temp. with AP buffer + Levamisol

*(levamisol is an endogenous AP inhibitor, AP buffer to get embryos to right pH for staining chromogenic reaction)*

Transfer embryos from baskets to vials carefully using a 5ml plastic pipette cut slanted (slant allows greater area for embryos to enter pipette reducing the chance of damaging them). You need AP buffer beneath the baskets to do this properly!

Remove AP buffer from vials, then add 0.5ml BMPurple/vial (shake BMPurple first!) – watch embryos at least every 30 minutes. Stop staining when background is just beginning to come up.

*(The anti-DIG antibody is labeled with alkaline phosphatase which removes a phosphate from BMPurple and turns the substrate purple.)*

To stop staining remove BMPurple from vials



5 min. PTW wash

(Reaction is stopped by change in pH.)

Fill vial with 1 – 2ml Bouin's fix, nutator @ rm. Temp. O/N  
(bouin's can reduce background)

#### **DAY 4 *in-situ***

Wash with buffered EtOH until solution is clear (no more yellow tint). Start with several 5 minute washes, then change out every 1/2 hour.

Bleach or clear as necessary

#### **Chick embryos and *in situ* hybridization:**

Digoxigenin-conjugated antisense riboprobes were prepared from chick cDNAs for chick *DVL1* and *DVL3*. Whole-mount *in situ* hybridizations were conducted using NBT (Roche) tetrazolium histochemistry according to previously established protocols (Agarwala et al., 2001; Agarwala and Ragsdale, 2002).

#### **Hemichordate embryos and *in situ* hybridization:**

*In situ* hybridizations were done according to (Lowe et al., 2004), but post-fixation was done in formaldehyde rather than in Bouin's fixative.

#### **Morphological analysis of mouse embryos:**

18.5 day old fetuses were harvested and subjected either to internal organs analysis or bone and cartilage staining. Fetuses were fixed in Bouin's solution and examined for internal organ malformation by Wilson sectioning technique (Wilson, 1965). Some fetuses were fixed in 10% formalin in PBS. Thoracic and abdominal cavities in these fetuses were opened by ventral incision in order to inspect the main organs and their topography *in situ*. From these animals, hearts were harvested and processed for standard histological analysis. The remaining fetuses were subjected to double staining with Alizarin Red S and Alcian blue and examined for skeletal abnormalities (Kimmel and Trammel, 1981).

## **6.5.Immunohistochemistry**

### ***Xenopus* embryos:**

#### **Chapter 2:**

The muscle-specific 12/101 monoclonal antibody was used to visualize differentiated somites (Kintner and Brockes, 1984) (Developmental Studies Hybridoma Bank, University of Iowa). 12/101 was used at 1:5, as described (Sive, 2000), along with anti-mouse 2° Alexafluor 488 (Molecular Probes). For combined *in situ* hybridization and immunostaining, *in situ* staining was performed first.

#### **Chapter 4:**

For immunostaining embryos were fixed in 1X MEMFA (1hr), washed in TBST for 30 min at room temperature, then blocked in 10% FBS and 90% TBST (0.1% Triton X-100 in TBS). Primary antibodies were diluted in 10% FBS and 90%TBST. Antibodies used were monoclonal anti Xeel (Interlectin-2) (1:1000 dilution as per Ref. (Hayes et al., 2007)). A monoclonal rabbit  $\alpha$ -SNAP-25 (Stressgen VAM-SV012) (1:600 dilution). A polyclonal rabbit anti-Fuz (peptide antibody OpenBiosystems project PA0983) (1:100 dilution in Dents fix). Primary antibodies were detected with Alexa Fluor-488 or -555 goat anti mouse immunoglobulin G (IgG) diluted 1:300 in FBS/TBST solution.

## **6.6.Bioinformatics, Image analysis, and Modelling**

### ***Xenopus* Imaging and image analysis:**

Immunohistochemistry and mRNA injected embryos were imaged in TBST on an inverted Zeiss LSM5 Pascal confocal microscope. Confocal images were processed and cropped in Imaris software (BITPLANE scientific solutions) and Adobe Illustrator and Adobe Photoshop for compilation of figures.

### **Mouse imaging:**

All fetuses were examined and photographed under the dissection stereoscopic microscope (Leica MZ95) with attached digital camera (Leica DFC480 Wetzlar, Germany) controlled by Image-Pro Plus software (Media Cybernetics MD, USA)

**Genomic sequence analyses:**

Sequence alignment was performed using ClustalX (Jeanmougin et al., 1998). Neighbor-joining trees were constructed using PAUP\* (Poe and Swofford, 1999; Rogers and Swofford, 1999). Non-parametric bootstrap proportions for clades were assessed with 1000 pseudo-replicates.

**Prediction of gene function:**

For MouseFunc-based computational predictions of Fuzzy function, we employed the unified MouseFunc predictions (i.e., the composite predictions across MouseFunc participants)(Pena-Castillo et al., 2008) for the most probable Gene Ontology biological process and cellular component annotations, ranking likely functions by p-value. For gene network-based computational predictions of Fuzzy function, we examined network neighbors of the Fuzzy structural homologs Sedl, AP2s1, AP1s1, sec22, and YTK6 in three probabilistic functional networks: a network of yeast genes(Lee et al., 2007a), a network of mouse genes(Kim et al., 2008b), and a network of 470,217 links among 16,375 human genes calculated using the methods previously described for yeast(Lee et al., 2007a) and worm(Lee et al., 2008a) and derived from 22 publicly available genomics datasets including DNA microarray data, protein-protein interactions, genetic interactions, literature mining, comparative genomics, and orthologous transfer of gene-gene functional associations from fly, worm, and yeast (I.L., E.M.M., manuscript in preparation). For each network, likely association partners of Fuzzy structural homologs were rank ordered by the sum of the pairwise association scores, corresponding to the *naïve* Bayesian estimate of the probability for the linked genes to participate in the same biological processes as the Fuzzy structural homologs. Additional human protein interaction data were analyzed from the BioGRID database(Stark et al., 2006; Breitkreutz et al., 2008).

**Structure modeling:**

All homology predictions were performed using the open access PSIPRED protein structure prediction server <http://bioinf.cs.ucl.ac.uk/psipred/> as described in Refs. (McGuffin et al., 2000; McGuffin and Jones, 2003). Homology models were built using the Swiss-Model server <http://swissmodel.expasy.org/> (Ref. (Arnold et al., 2006)). All models were rendered using MacPyMol software (<http://pymol.sourceforge.net/>). Transmembrane domain of Fuzzy was predicted by MEMSAT3) accessed via the PSIPRED server (McGuffin et al., 2000) , additionally by SPOCTOPUS (<http://octopus.cbr.su.se/index.php?about=SPOCTOPUS>

## References:

- Adams M, Smith UM, Logan CV, Johnson CA. 2008. Recent advances in the molecular pathology, cell biology and genetics of ciliopathies. *J Med Genet* 45:257-267.
- Adams NA, Awadein A, Toma HS. 2007. The retinal ciliopathies. *Ophthalmic Genet* 28:113-125.
- Adler PN. 2002. Planar signaling and morphogenesis in *Drosophila*. *Dev Cell* 2:525-535.
- Adler PN, Lee H. 2001. Frizzled signaling and cell-cell interactions in planar polarity. *Curr Opin Cell Biol* 13:635-640.
- Adler PN, Zhu C, Stone D. 2004. Inturned localizes to the proximal side of wing cells under the instruction of upstream planar polarity proteins. *Curr Biol* 14:2046-2051.
- Afonin B, Ho M, Gustin JK, Meloty-Kapella C, Domingo CR. 2006. Cell behaviors associated with somite segmentation and rotation in *Xenopus laevis*. *Dev Dyn* 235:3268-3279.
- Ahmad-Annuar A, Ciani L, Simeonidis I, Herreros J, Fredj NB, Rosso SB, Hall A, Brickley S, Salinas PC. 2006. Signaling across the synapse: a role for Wnt and Dishevelled in presynaptic assembly and neurotransmitter release. *J Cell Biol* 174:127-139.
- Amit S, Hatzubai A, Birman Y, Andersen JS, Ben-Shushan E, Mann M, Ben-Neriah Y, Alkalay I. 2002. Axin-mediated CKI phosphorylation of beta-catenin at Ser 45: a molecular switch for the Wnt pathway. *Genes Dev* 16:1066-1076.
- Arnold K, Bordoli L, Kopp J, Schwede T. 2006. The SWISS-MODEL Workspace: A web-based environment for protein structure homology modelling. *Bioinformatics* 22:195-201.
- Axelrod JD, Miller JR, Shulman JM, Moon RT, Perrimon N. 1998. Differential recruitment of Dishevelled provides signaling specificity in the planar cell polarity and Wingless signaling pathways. *Genes Dev* 12:2610-2622.
- Aybar MJ, Nieto MA, Mayor R. 2003. Snail precedes slug in the genetic cascade required for the specification and migration of the *Xenopus* neural crest. *Development* 130:483-494.
- Badano JL, Mitsuma N, Beales PL, Katsanis N. 2006. The ciliopathies: an emerging class of human genetic disorders. *Annu Rev Genomics Hum Genet* 7:125-148.
- Baltzinger M, Mager-Heckel AM, Remy P. 1999. Xl erg: expression pattern and overexpression during development plead for a role in endothelial cell differentiation. *Dev Dyn* 216:420-433.
- Beales PL, Bland E, Tobin JL, Bacchelli C, Tuysuz B, Hill J, Rix S, Pearson CG, Kai M, Hartley J, Johnson C, Irving M, Elcioglu N, Winey M, Tada M, Scambler PJ. 2007. IFT80, which encodes a conserved intraflagellar transport protein, is mutated in Jeune asphyxiating thoracic dystrophy. *Nat Genet* 39:727-729.
- Bergmann C, Fliegauf M, Bruchle NO, Frank V, Olbrich H, Kirschner J, Schermer B, Schmedding I, Kispert A, Kranzlin B, Nurnberg G, Becker C, Grimm T, Girschick G, Lynch SA, Kelehan P, Senderek J, Neuhaus TJ, Stallmach T, Zentgraf H, Nurnberg P, Gretz N, Lo C, Lienkamp S, Schafer T, Walz G, Benzing

- T, Zerres K, Omran H. 2008. Loss of nephrocystin-3 function can cause embryonic lethality, Meckel-Gruber-like syndrome, situs inversus, and renal-hepatic-pancreatic dysplasia. *Am J Hum Genet* 82:959-970.
- Bi X, Mancias JD, Goldberg J. 2007. Insights into COPII coat nucleation from the structure of Sec23.Sar1 complexed with the active fragment of Sec31. *Dev Cell* 13:635-645.
- Bilic J, Huang YL, Davidson G, Zimmermann T, Cruciat CM, Bienz M, Niehrs C. 2007. Wnt induces LRP6 signalosomes and promotes dishevelled-dependent LRP6 phosphorylation. *Science* 316:1619-1622.
- Billett FS, Gould RP. 1971. Fine structural changes in the differentiating epidermis of *Xenopus laevis* embryos. *J Anat* 108:465-480.
- Blum M, Andre P, Muders K, Schweickert A, Fischer A, Bitzer E, Bogusch S, Beyer T, van Straaten HW, Viebahn C. 2007. Ciliation and gene expression distinguish between node and posterior notochord in the mammalian embryo. *Differentiation* 75:133-146.
- Borycki A, Brown AM, Emerson CP, Jr. 2000. Shh and Wnt signaling pathways converge to control Gli gene activation in avian somites. *Development* 127:2075-2087.
- Boutros M, Paricio N, Strutt DI, Mlodzik M. 1998. Dishevelled activates JNK and discriminates between JNK pathways in planar polarity and wingless signaling. *Cell* 94:109-118.
- Boyadjiev SA, Fromme JC, Ben J, Chong SS, Nauta C, Hur DJ, Zhang G, Hamamoto S, Schekman R, Ravazzola M, Orci L, Eyaid W. 2006. Cranio-lenticulo-sutural dysplasia is caused by a SEC23A mutation leading to abnormal endoplasmic-reticulum-to-Golgi trafficking. *Nat Genet* 38:1192-1197.
- Boyles AL, Hammock P, Speer MC. 2005. Candidate gene analysis in human neural tube defects. *Am J Med Genet C Semin Med Genet* 135C:9-23.
- Breitkreutz BJ, Stark C, Regulj T, Boucher L, Breitkreutz A, Livstone M, Oughtred R, Lackner DH, Bahler J, Wood V, Dolinski K, Tyers M. 2008. The BioGRID Interaction Database: 2008 update. *Nucleic Acids Res* 36:D637-640.
- Brent AE, Tabin CJ. 2002. Developmental regulation of somite derivatives: muscle, cartilage and tendon. *Curr Opin Genet Dev* 12:548-557.
- Bryja V, Cajanek L, Grahn A, Schulte G. 2007a. Inhibition of endocytosis blocks Wnt signalling to beta-catenin by promoting dishevelled degradation. *Acta Physiol (Oxf)* 190:55-61.
- Bryja V, Gradl D, Schambony A, Arenas E, Schulte G. 2007b. Beta-arrestin is a necessary component of Wnt/beta-catenin signaling in vitro and in vivo. *Proc Natl Acad Sci U S A* 104:6690-6695.
- Bryja V, Schambony A, Cajanek L, Dominguez I, Arenas E, Schulte G. 2008. Beta-arrestin and casein kinase 1/2 define distinct branches of non-canonical WNT signalling pathways. *EMBO Rep* 9:1244-1250.
- Cai H, Reinisch K, Ferro-Novick S. 2007. Coats, tethers, Rabs, and SNAREs work together to mediate the intracellular destination of a transport vesicle. *Dev Cell* 12:671-682.

- Capdevila J, Tabin C, Johnson RL. 1998. Control of dorsoventral somite patterning by Wnt-1 and beta-catenin. *Dev Biol* 193:182-194.
- Carl TF, Dufton C, Hanken J, Klymkowsky MW. 1999. Inhibition of neural crest migration in *Xenopus* using antisense slug RNA. *Dev Biol* 213:101-115.
- Chan SW, Fowler KJ, Choo KH, Kalitsis P. 2005. Spef1, a conserved novel testis protein found in mouse sperm flagella. *Gene* 353:189-199.
- Chen W, ten Berge D, Brown J, Ahn S, Hu LA, Miller WE, Caron MG, Barak LS, Nusse R, Lefkowitz RJ. 2003. Dishevelled 2 recruits beta-arrestin 2 to mediate Wnt5A-stimulated endocytosis of Frizzled 4. *Science* 301:1391-1394.
- Chien AJ, Conrad WH, Moon RT. 2009. A Wnt Survival Guide: From Flies to Human Disease. *J Invest Dermatol*.
- Christ B, Huang R, Scaal M. 2004. Formation and differentiation of the avian sclerotome. *Anat Embryol (Berl)* 208:333-350.
- Christian JL, McMahon JA, McMahon AP, Moon RT. 1991. Xwnt-8, a *Xenopus* Wnt-1/int-1-related gene responsive to mesoderm-inducing growth factors, may play a role in ventral mesodermal patterning during embryogenesis. *Development* 111:1045-1055.
- Classen AK, Anderson KI, Marois E, Eaton S. 2005. Hexagonal packing of *Drosophila* wing epithelial cells by the planar cell polarity pathway. *Dev Cell* 9:805-817.
- Cohen AW, Hnasko R, Schubert W, Lisanti MP. 2004. Role of caveolae and caveolins in health and disease. *Physiol Rev* 84:1341-1379.
- Cole DG. 2003. The intraflagellar transport machinery of *Chlamydomonas reinhardtii*. *Traffic* 4:435-442.
- Collier S, Lee H, Burgess R, Adler P. 2005. The WD40 repeat protein fritz links cytoskeletal planar polarity to frizzled subcellular localization in the *Drosophila* epidermis. *Genetics* 169:2035-2045.
- Collins BM, McCoy AJ, Kent HM, Evans PR, Owen DJ. 2002. Molecular architecture and functional model of the endocytic AP2 complex. *Cell* 109:523-535.
- Corbit KC, Shyer AE, Dowdle WE, Gaulden J, Singla V, Chen MH, Chuang PT, Reiter JF. 2008. Kif3a constrains beta-catenin-dependent Wnt signalling through dual ciliary and non-ciliary mechanisms. *Nat Cell Biol* 10:70-76.
- Cortellino S, Wang C, Wang B, Bassi MR, Caretti E, Champeval D, Calmont A, Jarnik M, Burch J, Zaret KS, Larue L, Bellacosa A. 2009. Defective ciliogenesis, embryonic lethality and severe impairment of the Sonic Hedgehog pathway caused by inactivation of the mouse complex A intraflagellar transport gene Ift122/Wdr10, partially overlapping with the DNA repair gene Med1/Mbd4. *Dev Biol* 325:225-237.
- Coskun A, Kiran G, Ozdemir O. 2009. Craniorachischisis Totalis: A Case Report and Review of the Literature. *Fetal Diagn Ther* 25:21-25.
- Curtin JA, Quint E, Tsipouri V, Arkell RM, Cattanaach B, Copp AJ, Henderson DJ, Spurr N, Stanier P, Fisher EM, Nolan PM, Steel KP, Brown SD, Gray IC, Murdoch JN. 2003. Mutation of *Celsr1* disrupts planar polarity of inner ear hair cells and causes severe neural tube defects in the mouse. *Curr Biol* 13:1129-1133.
- Darken RS, Wilson PA. 2001. Axis induction by wnt signaling: Target promoter responsiveness regulates competence. *Dev Biol* 234:42-54.

- Davidson LA, Keller R, DeSimone DW. 2004. Assembly and remodeling of the fibrillar fibronectin extracellular matrix during gastrulation and neurulation in *Xenopus laevis*. *Dev Dyn* 231:888-895.
- Davidson LA, Marsden M, Keller R, Desimone DW. 2006. Integrin  $\alpha 5 \beta 1$  and fibronectin regulate polarized cell protrusions required for *Xenopus* convergence and extension. *Curr Biol* 16:833-844.
- Dawe HR, Smith UM, Cullinane AR, Gerrelli D, Cox P, Badano JL, Blair-Reid S, Sriram N, Katsanis N, Attie-Bitach T, Afford SC, Copp AJ, Kelly DA, Gull K, Johnson CA. 2007. The Meckel-Gruber Syndrome proteins MKS1 and meckelin interact and are required for primary cilium formation. *Hum Mol Genet* 16:173-186.
- De Calisto J, Araya C, Marchant L, Riaz CF, Mayor R. 2005. Essential role of non-canonical Wnt signalling in neural crest migration. *Development* 132:2587-2597.
- Deans MR, Antic D, Suyama K, Scott MP, Axelrod JD, Goodrich LV. 2007. Asymmetric distribution of prickly-like 2 reveals an early underlying polarization of vestibular sensory epithelia in the inner ear. *J Neurosci* 27:3139-3147.
- Dehal P, Boore JL. 2005. Two rounds of whole genome duplication in the ancestral vertebrate. *PLoS Biol* 3:e314.
- del Barrio MG, Nieto MA. 2002. Overexpression of Snail family members highlights their ability to promote chick neural crest formation. *Development* 129:1583-1593.
- Doudney K, Ybot-Gonzalez P, Paternotte C, Stevenson RE, Greene ND, Moore GE, Copp AJ, Stanier P. 2005. Analysis of the planar cell polarity gene *Vangl2* and its co-expressed paralogue *Vangl1* in neural tube defect patients. *Am J Med Genet A* 136:90-92.
- Dougherty GW, Adler HJ, Rzadzinska A, Gimona M, Tomita Y, Lattig MC, Merritt RC, Jr., Kachar B. 2005. CLAMP, a novel microtubule-associated protein with EB-type calponin homology. *Cell Motil Cytoskeleton* 62:141-156.
- Essner JJ, Vogan KJ, Wagner MK, Tabin CJ, Yost HJ, Brueckner M. 2002. Conserved function for embryonic nodal cilia. *Nature* 418:37-38.
- Etheridge SL, Ray S, Li S, Hamblet NS, Lijam N, Tsang M, Greer J, Kardos N, Wang J, Sussman DJ, Chen P, Wynshaw-Boris A. 2008. Murine dishevelled 3 functions in redundant pathways with dishevelled 1 and 2 in normal cardiac outflow tract, cochlea, and neural tube development. *PLoS Genet* 4:e1000259.
- Fan S, Wei Z, Xu H, Gong W. 2009. Crystal structure of human synbindin reveals two conformations of longin domain. *Biochem Biophys Res Commun* 378:338-343.
- Fariss RN, Molday RS, Fisher SK, Matsumoto B. 1997. Evidence from normal and degenerating photoreceptors that two outer segment integral membrane proteins have separate transport pathways. *J Comp Neurol* 387:148-156.
- Farlie PG, McKeown SJ, Newgreen DF. 2004. The neural crest: basic biology and clinical relationships in the craniofacial and enteric nervous systems. *Birth Defects Res C Embryo Today* 72:173-189.
- Fath S, Mancias JD, Bi X, Goldberg J. 2007. Structure and organization of coat proteins in the COPII cage. *Cell* 129:1325-1336.
- Federman M, Nichols G, Jr. 1974. Bone cell cilia: vestigial or functional organelles? *Calcif Tissue Res* 17:81-85.



- Filali M, Cheng N, Abbott D, Leontiev V, Engelhardt JF. 2002. Wnt-3A/beta-catenin signaling induces transcription from the LEF-1 promoter. *J Biol Chem* 277:33398-33410.
- Fliegeauf M, Benzing T, Omran H. 2007. When cilia go bad: cilia defects and ciliopathies. *Nat Rev Mol Cell Biol* 8:880-893.
- Follit JA, Tuft RA, Fogarty KE, Pazour GJ. 2006. The intraflagellar transport protein IFT20 is associated with the Golgi complex and is required for cilia assembly. *Mol Biol Cell* 17:3781-3792.
- Fromme JC, Ravazzola M, Hamamoto S, Al-Balwi M, Eyaid W, Boyadjiev SA, Cosson P, Schekman R, Orci L. 2007. The genetic basis of a craniofacial disease provides insight into COPII coat assembly. *Dev Cell* 13:623-634.
- Gagliardi M, Piddini E, Vincent JP. 2008. Endocytosis: a positive or a negative influence on Wnt signalling? *Traffic* 9:1-9.
- Galceran J, Farinas I, Depew MJ, Clevers H, Grosschedl R. 1999. Wnt3a<sup>-/-</sup>-like phenotype and limb deficiency in Lef1<sup>(-/-)</sup>Tcf1<sup>(-/-)</sup> mice. *Genes Dev* 13:709-717.
- Gammill LS, Bronner-Fraser M. 2003. Neural crest specification: migrating into genomics. *Nat Rev Neurosci* 4:795-805.
- Garcia-Castro MI, Marcelle C, Bronner-Fraser M. 2002. Ectodermal Wnt function as a neural crest inducer. *Science* 297:848-851.
- Garriock RJ, Krieg PA. 2007. Wnt11-R signaling regulates a calcium sensitive EMT event essential for dorsal fin development of *Xenopus*. *Dev Biol* 304:127-140.
- Garriock RJ, Warkman AS, Meadows SM, D'Agostino S, Krieg PA. 2007. Census of vertebrate Wnt genes: isolation and developmental expression of *Xenopus* Wnt2, Wnt3, Wnt9a, Wnt9b, Wnt10a, and Wnt16. *Dev Dyn* 236:1249-1258.
- Gedeon AK, Colley A, Jamieson R, Thompson EM, Rogers J, Sillence D, Tiller GE, Mulley JC, Gecz J. 1999. Identification of the gene (SEDL) causing X-linked spondyloepiphyseal dysplasia tarda. *Nat Genet* 22:400-404.
- Geetha-Loganathan P, Nimmagadda S, Huang R, Christ B, Scaal M. 2006. Regulation of ectodermal Wnt6 expression by the neural tube is transduced by dermomyotomal Wnt11: a mechanism of dermomyotomal lip sustainment. *Development* 133:2897-2904.
- Gibbons BH, Asai DJ, Tang WJ, Hays TS, Gibbons IR. 1994. Phylogeny and expression of axonemal and cytoplasmic dynein genes in sea urchins. *Mol Biol Cell* 5:57-70.
- Ginalski K. 2006. Comparative modeling for protein structure prediction. *Curr Opin Struct Biol* 16:172-177.
- Gomez C, Ozbudak EM, Wunderlich J, Baumann D, Lewis J, Pourquie O. 2008. Control of segment number in vertebrate embryos. *Nature* 454:335-339.
- Guo N, Hawkins C, Nathans J. 2004. Frizzled6 controls hair patterning in mice. *Proc Natl Acad Sci U S A* 101:9277-9281.
- Habas R, Dawid IB. 2005. Dishevelled and Wnt signaling: is the nucleus the final frontier? *J Biol* 4:2.
- Habas R, Dawid IB, He X. 2003. Coactivation of Rac and Rho by Wnt/Frizzled signaling is required for vertebrate gastrulation. *Genes Dev* 17:295-309.

- Habas R, Kato Y, He X. 2001. Wnt/Frizzled activation of Rho regulates vertebrate gastrulation and requires a novel Formin homology protein Daam1. *Cell* 107:843-854.
- Hall T, Bush A, Fell J, Offiah A, Smith V, Abel R. 2009. Ciliopathy spectrum expanded? Jeune syndrome associated with foregut dysmotility and malrotation. *Pediatr Pulmonol* 44:198-201.
- Hamblet NS, Lijam N, Ruiz-Lozano P, Wang J, Yang Y, Luo Z, Mei L, Chien KR, Sussman DJ, Wynshaw-Boris A. 2002. Dishevelled 2 is essential for cardiac outflow tract development, somite segmentation and neural tube closure. *Development* 129:5827-5838.
- Handrigan GR, Haas A, Wassersug RJ. 2007. Bony-tailed tadpoles: the development of supernumerary caudal vertebrae in larval megophryids (Anura). *Evol Dev* 9:190-202.
- Handrigan GR, Wassersug RJ. 2007. The anuran Bauplan: a review of the adaptive, developmental, and genetic underpinnings of frog and tadpole morphology. *Biol Rev Camb Philos Soc* 82:1-25.
- Hardy KM, Garriock RJ, Yatskievych TA, D'Agostino SL, Antin PB, Krieg PA. 2008. Non-canonical Wnt signaling through Wnt5a/b and a novel Wnt11 gene, Wnt11b, regulates cell migration during avian gastrulation. *Dev Biol* 320:391-401.
- Harland R. 2008. Induction into the Hall of Fame: tracing the lineage of Spemann's organizer. *Development* 135:3321-3323.
- Hasegawa H, Zinsser S, Rhee Y, Vik-Mo EO, Davanger S, Hay JC. 2003. Mammalian ykt6 is a neuronal SNARE targeted to a specialized compartment by its profilin-like amino terminal domain. *Mol Biol Cell* 14:698-720.
- Hayes JM, Kim SK, Abitua PB, Park TJ, Herrington ER, Kitayama A, Grow MW, Ueno N, Wallingford JB. 2007. Identification of novel ciliogenesis factors using a new in vivo model for mucociliary epithelial development. *Dev Biol* 312:115-130.
- He X, Semenov M, Tamai K, Zeng X. 2004. LDL receptor-related proteins 5 and 6 in Wnt/beta-catenin signaling: arrows point the way. *Development* 131:1663-1677.
- Hildebrand JD. 2005. Shroom regulates epithelial cell shape via the apical positioning of an actomyosin network. *J Cell Sci* 118:5191-5203.
- Hoff K, Wassersug RJ. 2000. Tadpole locomotion: axial movement and tail functions in a largely vertebraeless vertebrate. *American Zoology* 40:62-76.
- Hopwood ND, Gurdon JB. 1990. Activation of muscle genes without myogenesis by ectopic expression of MyoD in frog embryo cells. *Nature* 347:197-200.
- Hopwood ND, Pluck A, Gurdon JB. 1989a. A *Xenopus* mRNA related to *Drosophila* twist is expressed in response to induction in the mesoderm and the neural crest. *Cell* 59:893-903.
- Hopwood ND, Pluck A, Gurdon JB. 1989b. MyoD expression in the forming somites is an early response to mesoderm induction in *Xenopus* embryos. *Embo J* 8:3409-3417.
- Hopwood ND, Pluck A, Gurdon JB. 1991. *Xenopus* Myf-5 marks early muscle cells and can activate muscle genes ectopically in early embryos. *Development* 111:551-560.

- Hotta K, Takahashi H, Ueno N, Gojobori T. 2003. A genome-wide survey of the genes for planar polarity signaling or convergent extension-related genes in *Ciona intestinalis* and phylogenetic comparisons of evolutionary conserved signaling components. *Gene* 317:165-185.
- Huangfu D, Anderson KV. 2005. Cilia and Hedgehog responsiveness in the mouse. *Proc Natl Acad Sci U S A* 102:11325-11330.
- Huangfu D, Liu A, Rakeman AS, Murcia NS, Niswander L, Anderson KV. 2003. Hedgehog signalling in the mouse requires intraflagellar transport proteins. *Nature* 426:83-87.
- Ikeya M, Lee SM, Johnson JE, McMahon AP, Takada S. 1997. Wnt signalling required for expansion of neural crest and CNS progenitors. *Nature* 389:966-970.
- Inaba K. 2003. Molecular architecture of the sperm flagella: molecules for motility and signaling. *Zoolog Sci* 20:1043-1056.
- Inglis PN, Boroevich KA, Leroux MR. 2006. Piecing together a ciliome. *Trends Genet* 22:491-500.
- Jang SB, Kim YG, Cho YS, Suh PG, Kim KH, Oh BH. 2002. Crystal structure of SEDL and its implications for a genetic disease spondyloepiphyseal dysplasia tarda. *J Biol Chem* 277:49863-49869.
- Jeanmougin F, Thompson JD, Gouy M, Higgins DG, Gibson TJ. 1998. Multiple sequence alignment with Clustal X. *Trends Biochem Sci* 23:403-405.
- Jekely G, Arendt D. 2006. Evolution of intraflagellar transport from coated vesicles and autogenous origin of the eukaryotic cilium. *Bioessays* 28:191-198.
- Jonassen JA, San Agustin J, Follit JA, Pazour GJ. 2008. Deletion of IFT20 in the mouse kidney causes misorientation of the mitotic spindle and cystic kidney disease. *J Cell Biol* 183:377-384.
- Karner C, Wharton KA, Jr., Carroll TJ. 2006. Planar cell polarity and vertebrate organogenesis. *Semin Cell Dev Biol* 17:194-203.
- Kato M. 2005. WNT/PCP signaling pathway and human cancer (review). *Oncol Rep* 14:1583-1588.
- Keller R. 2000. The origin and morphogenesis of amphibian somites. *Curr Top Dev Biol* 47:183-246.
- Keller R. 2002. Shaping the vertebrate body plan by polarized embryonic cell movements. *Science* 298:1950-1954.
- Keller R, Davidson L, Edlund A, Elul T, Ezin M, Shook D, Skoglund P. 2000. Mechanisms of convergence and extension by cell intercalation. *Philos Trans R Soc Lond B Biol Sci* 355:897-922.
- Keller R, Davidson LA, Shook DR. 2003. How we are shaped: the biomechanics of gastrulation. *Differentiation* 71:171-205.
- Keller RE, Danilchik M, Gimlich R, Shih J. 1985. The function and mechanism of convergent extension during gastrulation of *Xenopus laevis*. *J Embryol Exp Morphol* 89 Suppl:185-209.
- Kibar Z, Capra V, Gros P. 2007a. Toward understanding the genetic basis of neural tube defects. *Clin Genet* 71:295-310.
- Kibar Z, Torban E, McDearmid JR, Reynolds A, Berghout J, Mathieu M, Kirillova I, De Marco P, Merello E, Hayes JM, Wallingford JB, Drapeau P, Capra V, Gros P.

- 2007b. Mutations in VANGL1 associated with neural-tube defects. *N Engl J Med* 356:1432-1437.
- Kibar Z, Vogan KJ, Groulx N, Justice MJ, Underhill DA, Gros P. 2001. Ltap, a mammalian homolog of *Drosophila* Strabismus/Van Gogh, is altered in the mouse neural tube mutant Loop-tail. *Nat Genet* 28:251-255.
- Kim GH, Her JH, Han JK. 2008a. Ryk cooperates with Frizzled 7 to promote Wnt11-mediated endocytosis and is essential for *Xenopus laevis* convergent extension movements. *J Cell Biol* 182:1073-1082.
- Kim WK, Krumpelman C, Marcotte EM. 2008b. Inferring mouse gene functions from genomic-scale data using a combined functional network/classification strategy. *Genome Biol* 9 Suppl 1:S5.
- Kimelman D, Xu W. 2006. beta-catenin destruction complex: insights and questions from a structural perspective. *Oncogene* 25:7482-7491.
- Kimmel CA, Trammel C. 1981. A rapid procedure for routine double staining of cartilage and bone in fetal and adult animals. *Stain Technol* 56:271-273.
- Kinch LN, Grishin NV. 2006. Longin-like folds identified in CHiPS and DUF254 proteins: vesicle trafficking complexes conserved in eukaryotic evolution. *Protein Sci* 15:2669-2674.
- Kintner CR, Brockes JP. 1984. Monoclonal antibodies identify blastemal cells derived from dedifferentiating limb regeneration. *Nature* 308:67-69.
- Kishida S, Yamamoto H, Kikuchi A. 2004. Wnt-3a and Dvl induce neurite retraction by activating Rho-associated kinase. *Mol Cell Biol* 24:4487-4501.
- Kishimoto N, Cao Y, Park A, Sun Z. 2008. Cystic kidney gene seahorse regulates cilia-mediated processes and Wnt pathways. *Dev Cell* 14:954-961.
- Klingensmith J, Yang Y, Axelrod JD, Beier DR, Perrimon N, Sussman DJ. 1996. Conservation of dishevelled structure and function between flies and mice: isolation and characterization of Dvl2. *Mech Dev* 58:15-26.
- Kolb RJ, Nauli SM. 2008. Ciliary dysfunction in polycystic kidney disease: an emerging model with polarizing potential. *Front Biosci* 13:4451-4466.
- Kovacs JJ, Whalen EJ, Liu R, Xiao K, Kim J, Chen M, Wang J, Chen W, Lefkowitz RJ. 2008. Beta-arrestin-mediated localization of smoothened to the primary cilium. *Science* 320:1777-1781.
- Krasnow RE, Wong LL, Adler PN. 1995. Dishevelled is a component of the frizzled signaling pathway in *Drosophila*. *Development* 121:4095-4102.
- Kuhl M, Sheldahl LC, Malbon CC, Moon RT. 2000. Ca(2+)/calmodulin-dependent protein kinase II is stimulated by Wnt and Frizzled homologs and promotes ventral cell fates in *Xenopus*. *J Biol Chem* 275:12701-12711.
- Kusserow A, Pang K, Sturm C, Hroudá M, Lentfer J, Schmidt HA, Technau U, von Haeseler A, Hobmayer B, Martindale MQ, Holstein TW. 2005. Unexpected complexity of the Wnt gene family in a sea anemone. *Nature* 433:156-160.
- Kyttala M, Tallila J, Salonen R, Kopra O, Kohlschmidt N, Paavola-Sakki P, Peltonen L, Kestila M. 2006. MKS1, encoding a component of the flagellar apparatus basal body proteome, is mutated in Meckel syndrome. *Nat Genet* 38:155-157.
- LaBonne C, Bronner-Fraser M. 1998a. Induction and patterning of the neural crest, a stem cell-like precursor population. *J Neurobiol* 36:175-189.

- LaBonne C, Bronner-Fraser M. 1998b. Neural crest induction in *Xenopus*: evidence for a two-signal model. *Development* 125:2403-2414.
- LaBonne C, Bronner-Fraser M. 1999. Molecular mechanisms of neural crest formation. *Annu Rev Cell Dev Biol* 15:81-112.
- LaBonne C, Bronner-Fraser M. 2000. Snail-related transcriptional repressors are required in *Xenopus* for both the induction of the neural crest and its subsequent migration. *Dev Biol* 221:195-205.
- Lang MR, Lapierre LA, Frotscher M, Goldenring JR, Knapik EW. 2006. Secretory COPII coat component Sec23a is essential for craniofacial chondrocyte maturation. *Nat Genet* 38:1198-1203.
- Lassar AB, Munsterberg AE. 1996. The role of positive and negative signals in somite patterning. *Curr Opin Neurobiol* 6:57-63.
- Lee H, Adler PN. 2002. The function of the frizzled pathway in the *Drosophila* wing is dependent on inturnd and fuzzy. *Genetics* 160:1535-1547.
- Lee HS, Bong YS, Moore KB, Soria K, Moody SA, Daar IO. 2006. Dishevelled mediates ephrinB1 signalling in the eye field through the planar cell polarity pathway. *Nat Cell Biol* 8:55-63.
- Lee I, Lehner B, Crombie C, Wong W, Fraser AG, Marcotte EM. 2008a. A single gene network accurately predicts phenotypic effects of gene perturbation in *Caenorhabditis elegans*. *Nat Genet* 40:181-188.
- Lee I, Li Z, Marcotte EM. 2007a. An improved, bias-reduced probabilistic functional gene network of baker's yeast, *Saccharomyces cerevisiae*. *PLoS ONE* 2:e988.
- Lee JY, Harland RM. 2007. Actomyosin contractility and microtubules drive apical constriction in *Xenopus* bottle cells. *Dev Biol* 311:40-52.
- Lee PN, Kumburegama S, Marlow HQ, Martindale MQ, Wikramanayake AH. 2007b. Asymmetric developmental potential along the animal-vegetal axis in the anthozoan cnidarian, *Nematostella vectensis*, is mediated by Dishevelled. *Dev Biol* 310:169-186.
- Lee YN, Gao Y, Wang HY. 2008b. Differential mediation of the Wnt canonical pathway by mammalian Dishevelleds-1, -2, and -3. *Cell Signal* 20:443-452.
- Lei Q, Jeong Y, Misra K, Li S, Zelman AK, Epstein DJ, Matise MP. 2006. Wnt signaling inhibitors regulate the transcriptional response to morphogenetic Shh-Gli signaling in the neural tube. *Dev Cell* 11:325-337.
- Lijam N, Paylor R, McDonald MP, Crawley JN, Deng CX, Herrup K, Stevens KE, Maccaferri G, McBain CJ, Sussman DJ, Wynshaw-Boris A. 1997. Social interaction and sensorimotor gating abnormalities in mice lacking Dvl1. *Cell* 90:895-905.
- Lin F, Hiesberger T, Cordes K, Sinclair AM, Goldstein LS, Somlo S, Igarashi P. 2003. Kidney-specific inactivation of the KIF3A subunit of kinesin-II inhibits renal ciliogenesis and produces polycystic kidney disease. *Proc Natl Acad Sci U S A* 100:5286-5291.
- Linker C, Lesbros C, Gros J, Burrus LW, Rawls A, Marcelle C. 2005. beta-Catenin-dependent Wnt signalling controls the epithelial organisation of somites through the activation of paraxis. *Development* 132:3895-3905.

- Linker C, Lesbros C, Stark MR, Marcelle C. 2003. Intrinsic signals regulate the initial steps of myogenesis in vertebrates. *Development* 130:4797-4807.
- Liu A, Wang B, Niswander LA. 2005. Mouse intraflagellar transport proteins regulate both the activator and repressor functions of Gli transcription factors. *Development* 132:3103-3111.
- Lowe CJ. 2008. Molecular genetic insights into deuterostome evolution from the direct-developing hemichordate *Saccoglossus kowalevskii*. *Philos Trans R Soc Lond B Biol Sci* 363:1569-1578.
- Lowe CJ, Tagawa K, Humphreys T, Kirschner M, Gerhart J. 2004. Hemichordate embryos: procurement, culture, and basic methods. *Methods Cell Biol* 74:171-194.
- Lu J, Meng W, Poy F, Maiti S, Goode BL, Eck MJ. 2007. Structure of the FH2 Domain of Daam1: Implications for Formin Regulation of Actin Assembly. *J Mol Biol* 369:1258-1269.
- Luo ZG, Wang Q, Zhou JZ, Wang J, Luo Z, Liu M, He X, Wynshaw-Boris A, Xiong WC, Lu B, Mei L. 2002. Regulation of AChR clustering by Dishevelled interacting with MuSK and PAK1. *Neuron* 35:489-505.
- Luttrell LM, Lefkowitz RJ. 2002. The role of beta-arrestins in the termination and transduction of G-protein-coupled receptor signals. *J Cell Sci* 115:455-465.
- Malone AM, Anderson CT, Tummala P, Kwon RY, Johnston TR, Stearns T, Jacobs CR. 2007. Primary cilia mediate mechanosensing in bone cells by a calcium-independent mechanism. *Proc Natl Acad Sci U S A* 104:13325-13330.
- Mancias JD, Goldberg J. 2007. The transport signal on Sec22 for packaging into COPII-coated vesicles is a conformational epitope. *Mol Cell* 26:403-414.
- Mancilla A, Mayor R. 1996. Neural crest formation in *Xenopus laevis*: mechanisms of Xslug induction. *Dev Biol* 177:580-589.
- Mariani FV, Choi GB, Harland RM. 2001. The neural plate specifies somite size in the *Xenopus laevis* gastrula. *Dev Cell* 1:115-126.
- Martin BL, Kimelman D. 2009. Wnt signaling and the evolution of embryonic posterior development. *Curr Biol* 19:R215-219.
- Masckauchan TN, Agalliu D, Vorontchikhina M, Ahn A, Parmalee NL, Li CM, Khoo A, Tycko B, Brown AM, Kitajewski J. 2006. Wnt5a signaling induces proliferation and survival of endothelial cells in vitro and expression of MMP-1 and Tie-2. *Mol Biol Cell* 17:5163-5172.
- May SR, Ashique AM, Karlen M, Wang B, Shen Y, Zarbalis K, Reiter J, Ericson J, Peterson AS. 2005. Loss of the retrograde motor for IFT disrupts localization of Smo to cilia and prevents the expression of both activator and repressor functions of Gli. *Dev Biol* 287:378-389.
- McGuffin LJ, Bryson K, Jones DT. 2000. The PSIPRED protein structure prediction server. *Bioinformatics* 16:404-405.
- McGuffin LJ, Jones DT. 2003. Improvement of the GenTHREADER method for genomic fold recognition. *Bioinformatics* 19:874-881.
- McKendry R, Hsu SC, Harland RM, Grosschedl R. 1997. LEF-1/TCF proteins mediate wnt-inducible transcription from the *Xenopus* nodal-related 3 promoter. *Dev Biol* 192:420-431.

- McMahon AP, Moon RT. 1989. Ectopic expression of the proto-oncogene *int-1* in *Xenopus* embryos leads to duplication of the embryonic axis. *Cell* 58:1075-1084.
- Mikels AJ, Nusse R. 2006. Purified Wnt5a protein activates or inhibits beta-catenin-TCF signaling depending on receptor context. *PLoS Biol* 4:e115.
- Minier F, Carles D, Pelluard F, Alberti EM, Stern L, Saura R. 2005. [DiGeorge syndrome, a review of 52 patients]. *Arch Pediatr* 12:254-257.
- Mitchell B, Jacobs R, Li J, Chien S, Kintner C. 2007. A positive feedback mechanism governs the polarity and motion of motile cilia. *Nature* 447:97-101.
- Monsoro-Burq AH, Wang E, Harland R. 2005. *Msx1* and *Pax3* cooperate to mediate FGF8 and WNT signals during *Xenopus* neural crest induction. *Dev Cell* 8:167-178.
- Montcouquiol M, Jones JM, Sans N. 2008. Detection of planar polarity proteins in mammalian cochlea. *Methods Mol Biol* 468:207-219.
- Montcouquiol M, Rachel RA, Lanford PJ, Copeland NG, Jenkins NA, Kelley MW. 2003. Identification of *Vangl2* and *Scrb1* as planar polarity genes in mammals. *Nature* 423:173-177.
- Moody SA, Kline MJ. 1990. Segregation of fate during cleavage of frog (*Xenopus laevis*) blastomeres. *Anat Embryol (Berl)* 182:347-362.
- Moon RT, Bowerman B, Boutros M, Perrimon N. 2002. The promise and perils of Wnt signaling through beta-catenin. *Science* 296:1644-1646.
- Myers DC, Sepich DS, Solnica-Krezel L. 2002. Bmp activity gradient regulates convergent extension during zebrafish gastrulation. *Dev Biol* 243:81-98.
- Nagata S, Nakanishi M, Nanba R, Fujita N. 2003. Developmental expression of XEEL, a novel molecule of the *Xenopus* oocyte cortical granule lectin family. *Dev Genes Evol* 213:368-370.
- Nayak GD, Ratnayaka HS, Goodyear RJ, Richardson GP. 2007. Development of the hair bundle and mechanotransduction. *Int J Dev Biol* 51:597-608.
- Nieto MA, Bennett MF, Sargent MG, Wilkinson DG. 1992. Cloning and developmental expression of *Sna*, a murine homologue of the *Drosophila* snail gene. *Development* 116:227-237.
- Noordermeer J, Klingensmith J, Perrimon N, Nusse R. 1994. *dishevelled* and *armadillo* act in the wingless signalling pathway in *Drosophila*. *Nature* 367:80-83.
- Nurnberger J, Kribben A, Opazo Saez A, Heusch G, Philipp T, Phillips CL. 2004. The *Invs* gene encodes a microtubule-associated protein. *J Am Soc Nephrol* 15:1700-1710.
- Nusslein-Volhard C, Wieschaus E. 1980. Mutations affecting segment number and polarity in *Drosophila*. *Nature* 287:795-801.
- Oishi I, Kawakami Y, Raya A, Callol-Massot C, Izpisua Belmonte JC. 2006. Regulation of primary cilia formation and left-right patterning in zebrafish by a noncanonical Wnt signaling mediator, *duboraya*. *Nat Genet* 38:1316-1322.
- Oishi I, Suzuki H, Onishi N, Takada R, Kani S, Ohkawara B, Koshida I, Suzuki K, Yamada G, Schwabe GC, Mundlos S, Shibuya H, Takada S, Minami Y. 2003. The receptor tyrosine kinase *Ror2* is involved in non-canonical Wnt5a/JNK signalling pathway. *Genes Cells* 8:645-654.

- Olesen LE, Ford MG, Schmid EM, Vallis Y, Babu MM, Li PH, Mills IG, McMahon HT, Praefcke GJ. 2008. Solitary and repetitive binding motifs for the AP2 complex alpha-appendage in amphiphysin and other accessory proteins. *J Biol Chem* 283:5099-5109.
- Otto EA, Schermer B, Obara T, O'Toole JF, Hiller KS, Mueller AM, Ruf RG, Hoefele J, Beekmann F, Landau D, Foreman JW, Goodship JA, Strachan T, Kispert A, Wolf MT, Gagnadoux MF, Nivet H, Antignac C, Walz G, Drummond IA, Benzing T, Hildebrandt F. 2003. Mutations in INVS encoding inversin cause nephronophthisis type 2, linking renal cystic disease to the function of primary cilia and left-right axis determination. *Nat Genet* 34:413-420.
- Pan J. 2008. Cilia and ciliopathies: from Chlamydomonas and beyond. *Sci China C Life Sci* 51:479-486.
- Park TJ, Gray RS, Sato A, Habas R, Wallingford JB. 2005. Subcellular localization and signaling properties of dishevelled in developing vertebrate embryos. *Curr Biol* 15:1039-1044.
- Park TJ, Haigo SL, Wallingford JB. 2006. Ciliogenesis defects in embryos lacking inturned or fuzzy function are associated with failure of planar cell polarity and Hedgehog signaling. *Nat Genet* 38:303-311.
- Park TJ, Mitchell BJ, Abitua PB, Kintner C, Wallingford JB. 2008. Dishevelled controls apical docking and planar polarization of basal bodies in ciliated epithelial cells. *Nat Genet* 40:871-879.
- Park TJ, Mitchell, B., Abitua, P.B., Kintner, C., and Wallingford, J.B. 2008. Dishevelled controls apical docking and planar polarization of basal bodies in ciliated epithelial cells. *Nature Genetics* in press.
- Pedersen LB, Geimer S, Sloboda RD, Rosenbaum JL. 2003. The Microtubule plus end-tracking protein EB1 is localized to the flagellar tip and basal bodies in *Chlamydomonas reinhardtii*. *Curr Biol* 13:1969-1974.
- Pedersen LB, Rosenbaum JL. 2008. Intraflagellar transport (IFT) role in ciliary assembly, resorption and signalling. *Curr Top Dev Biol* 85:23-61.
- Pena-Castillo L, Tasan M, Myers CL, Lee H, Joshi T, Zhang C, Guan Y, Leone M, Pagnani A, Kim WK, Krumpelman C, Tian W, Obozinski G, Qi Y, Mostafavi S, Lin GN, Berriz GF, Gibbons FD, Lanckriet G, Qiu J, Grant C, Barutcuoglu Z, Hill DP, Warde-Farley D, Grouios C, Ray D, Blake JA, Deng M, Jordan MI, Noble WS, Morris Q, Klein-Seetharaman J, Bar-Joseph Z, Chen T, Sun F, Troyanskaya OG, Marcotte EM, Xu D, Hughes TR, Roth FP. 2008. A critical assessment of Mus musculus gene function prediction using integrated genomic evidence. *Genome Biol* 9 Suppl 1:S2.
- Phillips HM, Rhee HJ, Murdoch JN, Hildreth V, Peat JD, Anderson RH, Copp AJ, Chaudhry B, Henderson DJ. 2007. Disruption of planar cell polarity signaling results in congenital heart defects and cardiomyopathy attributable to early cardiomyocyte disorganization. *Circ Res* 101:137-145.
- Pizzuti A, Novelli G, Mari A, Ratti A, Colosimo A, Amati F, Penso D, Sangiuolo F, Calabrese G, Palka G, Silani V, Gennarelli M, Mingarelli R, Scarlato G, Scambler P, Dallapiccola B. 1996. Human homologue sequences to the Drosophila



- dishevelled segment-polarity gene are deleted in the DiGeorge syndrome. *Am J Hum Genet* 58:722-729.
- Poe S, Swofford DL. 1999. Taxon sampling revisited. *Nature* 398:299-300.
- Proux-Gillardeaux V, Raposo G, Irinopoulou T, Galli T. 2007. Expression of the Longin domain of TI-VAMP impairs lysosomal secretion and epithelial cell migration. *Biol Cell* 99:261-271.
- Pryor PR, Jackson L, Gray SR, Edeling MA, Thompson A, Sanderson CM, Evans PR, Owen DJ, Luzio JP. 2008. Molecular basis for the sorting of the SNARE VAMP7 into endocytic clathrin-coated vesicles by the ArfGAP Hrb. *Cell* 134:817-827.
- Putnam NH, Butts T, Ferrier DE, Furlong RF, Hellsten U, Kawashima T, Robinson-Rechavi M, Shoguchi E, Terry A, Yu JK, Benito-Gutierrez EL, Dubchak I, Garcia-Fernandez J, Gibson-Brown JJ, Grigoriev IV, Horton AC, de Jong PJ, Jurka J, Kapitonov VV, Kohara Y, Kuroki Y, Lindquist E, Lucas S, Osoegawa K, Pennacchio LA, Salamov AA, Satou Y, Sauka-Spengler T, Schmutz J, Shin IT, Toyoda A, Bronner-Fraser M, Fujiyama A, Holland LZ, Holland PW, Satoh N, Rokhsar DS. 2008. The amphioxus genome and the evolution of the chordate karyotype. *Nature* 453:1064-1071.
- Quinlan RJ, Tobin JL, Beales PL. 2008. Modeling ciliopathies: Primary cilia in development and disease. *Curr Top Dev Biol* 84:249-310.
- Rijsewijk F, Schuermann M, Wagenaar E, Parren P, Weigel D, Nusse R. 1987. The *Drosophila* homolog of the mouse mammary oncogene *int-1* is identical to the segment polarity gene *wingless*. *Cell* 50:649-657.
- Rogers JS, Swofford DL. 1999. Multiple local maxima for likelihoods of phylogenetic trees: a simulation study. *Mol Biol Evol* 16:1079-1085.
- Rosenbaum JL, Witman GB. 2002. Intraflagellar transport. *Nat Rev Mol Cell Biol* 3:813-825.
- Ross AJ, May-Simera H, Eichers ER, Kai M, Hill J, Jagger DJ, Leitch CC, Chapple JP, Munro PM, Fisher S, Tan PL, Phillips HM, Leroux MR, Henderson DJ, Murdoch JN, Copp AJ, Eliot MM, Lupski JR, Kemp DT, Dollfus H, Tada M, Katsanis N, Forge A, Beales PL. 2005. Disruption of Bardet-Biedl syndrome ciliary proteins perturbs planar cell polarity in vertebrates. *Nat Genet* 37:1135-1140.
- Rossi V, Banfield DK, Vacca M, Dietrich LE, Ungermann C, D'Esposito M, Galli T, Filippini F. 2004. Longins and their longin domains: regulated SNAREs and multifunctional SNARE regulators. *Trends Biochem Sci* 29:682-688.
- Rosso SB, Sussman D, Wynshaw-Boris A, Salinas PC. 2005. Wnt signaling through Dishevelled, Rac and JNK regulates dendritic development. *Nat Neurosci* 8:34-42.
- Rothbacher U, Laurent MN, Blitz IL, Watabe T, Marsh JL, Cho KW. 1995. Functional conservation of the Wnt signaling pathway revealed by ectopic expression of *Drosophila* dishevelled in *Xenopus*. *Dev Biol* 170:717-721.
- Rothbacher U, Laurent MN, Deardorff MA, Klein PS, Cho KW, Fraser SE. 2000. Dishevelled phosphorylation, subcellular localization and multimerization regulate its role in early embryogenesis. *Embo J* 19:1010-1022.
- Rual JF, Venkatesan K, Hao T, Hirozane-Kishikawa T, Dricot A, Li N, Berriz GF, Gibbons FD, Dreze M, Ayivi-Guedehoussou N, Klitgord N, Simon C, Boxem M,

- Milstein S, Rosenberg J, Goldberg DS, Zhang LV, Wong SL, Franklin G, Li S, Albala JS, Lim J, Fraughton C, Llamas E, Cevik S, Bex C, Lamesch P, Sikorski RS, Vandenhaute J, Zoghbi HY, Smolyar A, Bosak S, Sequerra R, Doucette-Stamm L, Cusick ME, Hill DE, Roth FP, Vidal M. 2005. Towards a proteome-scale map of the human protein-protein interaction network. *Nature* 437:1173-1178.
- Saint-Jeannet JP, He X, Varmus HE, Dawid IB. 1997. Regulation of dorsal fate in the neuraxis by Wnt-1 and Wnt-3a. *Proc Natl Acad Sci U S A* 94:13713-13718.
- Scaal M, Wiegreffe C. 2006. Somite compartments in anamniotes. *Anat Embryol (Berl)* 211 Suppl 1:9-19.
- Schmidt C, McGonnell IM, Allen S, Otto A, Patel K. 2007. Wnt6 controls amniote neural crest induction through the non-canonical signaling pathway. *Dev Dyn* 236:2502-2511.
- Scholey JM. 2003. Intraflagellar transport. *Annu Rev Cell Dev Biol* 19:423-443.
- Schwarz-Romond T, Fiedler M, Shibata N, Butler PJ, Kikuchi A, Higuchi Y, Bienz M. 2007. The DIX domain of Dishevelled confers Wnt signaling by dynamic polymerization. *Nat Struct Mol Biol* 14:484-492.
- Semenov MV, Tamai K, Brott BK, Kuhl M, Sokol S, He X. 2001. Head inducer Dickkopf-1 is a ligand for Wnt coreceptor LRP6. *Curr Biol* 11:951-961.
- Sheldahl LC, Park M, Malbon CC, Moon RT. 1999. Protein kinase C is differentially stimulated by Wnt and Frizzled homologs in a G-protein-dependent manner. *Curr Biol* 9:695-698.
- Sheldahl LC, Slusarski DC, Pandur P, Miller JR, Kuhl M, Moon RT. 2003. Dishevelled activates Ca<sup>2+</sup> flux, PKC, and CamKII in vertebrate embryos. *J Cell Biol* 161:769-777.
- Shimada Y, Yonemura S, Ohkura H, Strutt D, Uemura T. 2006. Polarized transport of Frizzled along the planar microtubule arrays in *Drosophila* wing epithelium. *Dev Cell* 10:209-222.
- Shindo A, Yamamoto TS, Ueno N. 2008. Coordination of cell polarity during *Xenopus* gastrulation. *PLoS ONE* 3:e1600.
- Sidow A. 1996. Gen(om)e duplications in the evolution of early vertebrates. *Curr Opin Genet Dev* 6:715-722.
- Sidow A, Bulotsky MS, Kerrebrock AW, Birren BW, Altshuler D, Jaenisch R, Johnson KR, Lander ES. 1999. A novel member of the F-box/WD40 gene family, encoding dactylin, is disrupted in the mouse dactylaplasia mutant. *Nat Genet* 23:104-107.
- Simons M, Gault WJ, Gotthardt D, Rohatgi R, Klein TJ, Shao Y, Lee HJ, Wu AL, Fang Y, Satlin LM, Dow JT, Chen J, Zheng J, Boutros M, Mlodzik M. 2009. Electrochemical cues regulate assembly of the Frizzled/Dishevelled complex at the plasma membrane during planar epithelial polarization. *Nat Cell Biol* 11:286-294.
- Simons M, Gloy J, Ganner A, Bullerkotte A, Bashkurov M, Kronig C, Schermer B, Benzing T, Cabello OA, Jenny A, Mlodzik M, Polok B, Driever W, Obara T, Walz G. 2005. Inversin, the gene product mutated in nephronophthisis type II,

- functions as a molecular switch between Wnt signaling pathways. *Nat Genet* 37:537-543.
- Simons M, Mlodzik M. 2008. Planar cell polarity signaling: from fly development to human disease. *Annu Rev Genet* 42:517-540.
- Sive HL, Grainger RM, Harland RM. 2000. Early Development of *Xenopus laevis*: A Laboratory Manual. Cold Spring Harbor, N.Y.: Cold Spring Harbor Press.
- Sive HL, R. M. Grainger, et al. 2000. Early Development of *Xenopus laevis*: A Laboratory Manual. Cold Spring Harbor, N.Y.: Cold Spring Harbor, N.Y., Cold Spring Harbor Press.
- Smalley MJ, Sara E, Paterson H, Naylor S, Cook D, Jayatilake H, Fryer LG, Hutchinson L, Fry MJ, Dale TC. 1999. Interaction of axin and Dvl-2 proteins regulates Dvl-2-stimulated TCF-dependent transcription. *Embo J* 18:2823-2835.
- Smith UM, Consugar M, Tee LJ, McKee BM, Maina EN, Whelan S, Morgan NV, Goranson E, Gissen P, Lillquist S, Aligianis IA, Ward CJ, Pasha S, Punyashtiti R, Malik Sharif S, Batman PA, Bennett CP, Woods CG, McKeown C, Bucourt M, Miller CA, Cox P, Algazali L, Trembath RC, Torres VE, Attie-Bitach T, Kelly DA, Maher ER, Gattone VH, 2nd, Harris PC, Johnson CA. 2006. The transmembrane protein meckelin (MKS3) is mutated in Meckel-Gruber syndrome and the wpk rat. *Nat Genet* 38:191-196.
- Snell G, Fekete E, Hummel K. 1948. The relation of mating, ovulation and the estrus smear in the house mouse to the time of day. *Anat Rec* 76:30-54.
- Sokol S, Christian JL, Moon RT, Melton DA. 1991. Injected Wnt RNA induces a complete body axis in *Xenopus* embryos. *Cell* 67:741-752.
- Sokol SY. 1996. Analysis of Dishevelled signalling pathways during *Xenopus* development. *Current Biology* 6:1456-1467.
- Sokol SYS, 2005 #101}, Klingensmith J, Perrimon N, Itoh K. 1995. Dorsalizing and neuralizing properties of Xdsh, a maternally expressed *Xenopus* homolog of dishevelled. *Development* 121:1637-1647.
- Solnica-Krezel L. 2005. Conserved patterns of cell movements during vertebrate gastrulation. *Curr Biol* 15:R213-228.
- Stark C, Breitkreutz BJ, Reguly T, Boucher L, Breitkreutz A, Tyers M. 2006. BioGRID: a general repository for interaction datasets. *Nucleic Acids Res* 34:D535-539.
- Steinman RM. 1968. An electron microscopic study of ciliogenesis in developing epidermis and trachea in the embryo of *Xenopus laevis*. *Am J Anat* 122:19-55.
- Steitz SA, Tsang M, Sussman DJ. 1996. Wnt-mediated relocalization of dishevelled proteins. *In Vitro Cell Dev Biol Anim* 32:441-445.
- Stubbs JL, Davidson L, Keller R, Kintner C. 2006. Radial intercalation of ciliated cells during *Xenopus* skin development. *Development* 133:2507-2515.
- Sun Z, Anderl F, Frohlich K, Zhao L, Hanke S, Brugger B, Wieland F, Bethune J. 2007. Multiple and stepwise interactions between coatamer and ADP-ribosylation factor-1 (Arf1)-GTP. *Traffic* 8:582-593.
- Sussman DJ, Klingensmith J, Salinas P, Adams PS, Nusse R, Perrimon N. 1994. Isolation and characterization of a mouse homolog of the *Drosophila* segment polarity gene dishevelled. *Dev Biol* 166:73-86.

- Sweetman D, Wagstaff L, Cooper O, Weijer C, Munsterberg A. 2008. The migration of paraxial and lateral plate mesoderm cells emerging from the late primitive streak is controlled by different Wnt signals. *BMC Dev Biol* 8:63.
- Tahinci E, Symes K. 2003. Distinct functions of Rho and Rac are required for convergent extension during *Xenopus* gastrulation. *Dev Biol* 259:318-335.
- Takahashi Y, Takagi A, Hiraoka S, Koseki H, Kanno J, Rawls A, Saga Y. 2007. Transcription factors *Mesp2* and *Paraxis* have critical roles in axial musculoskeletal formation. *Dev Dyn* 236:1484-1494.
- Takeda S, Yonekawa Y, Tanaka Y, Okada Y, Nonaka S, Hirokawa N. 1999. Left-right asymmetry and kinesin superfamily protein KIF3A: new insights in determination of laterality and mesoderm induction by *kif3A*<sup>-/-</sup> mice analysis. *J Cell Biol* 145:825-836.
- Takeuchi M, Nakabayashi J, Sakaguchi T, Yamamoto TS, Takahashi H, Takeda H, Ueno N. 2003. The prickle-related gene in vertebrates is essential for gastrulation cell movements. *Curr Biol* 13:674-679.
- Tamai K, Semenov M, Kato Y, Spokony R, Liu C, Katsuyama Y, Hess F, Saint-Jeannet JP, He X. 2000. LDL-receptor-related proteins in Wnt signal transduction. *Nature* 407:530-535.
- Tao Q, Yokota C, Puck H, Kofron M, Birsoy B, Yan D, Asashima M, Wylie CC, Lin X, Heasman J. 2005. Maternal *wnt11* activates the canonical wnt signaling pathway required for axis formation in *Xenopus* embryos. *Cell* 120:857-871.
- Theisen H, Purcell J, Bennett M, Kansagara D, Syed A, Marsh JL. 1994. *dishevelled* is required during wingless signaling to establish both cell polarity and cell identity. *Development* 120:347-360.
- Tissir F, Goffinet AM. 2006. Expression of planar cell polarity genes during development of the mouse CNS. *Eur J Neurosci* 23:597-607.
- Tobin JL, Di Franco M, Eichers E, May-Simera H, Garcia M, Yan J, Quinlan R, Justice MJ, Hennekam RC, Briscoe J, Tada M, Mayor R, Burns AJ, Lupski JR, Hammond P, Beales PL. 2008. Inhibition of neural crest migration underlies craniofacial dysmorphology and Hirschsprung's disease in Bardet-Biedl syndrome. *Proc Natl Acad Sci U S A* 105:6714-6719.
- Tochio H, Tsui MM, Banfield DK, Zhang M. 2001. An autoinhibitory mechanism for nonsyntaxin SNARE proteins revealed by the structure of Ykt6p. *Science* 293:698-702.
- Topczewski J, Sepich DS, Myers DC, Walker C, Amores A, Lele Z, Hammerschmidt M, Postlethwait J, Solnica-Krezel L. 2001. The zebrafish glypican *knypek* controls cell polarity during gastrulation movements of convergent extension. *Dev Cell* 1:251-264.
- Torres MA, Yang-Snyder JA, Purcell SM, DeMarais AA, McGrew LL, Moon RT. 1996. Activities of the Wnt-1 class of secreted signaling factors are antagonized by the Wnt-5A class and by a dominant negative cadherin in early *Xenopus* development. *J Cell Biol* 133:1123-1137.
- Townley AK, Feng Y, Schmidt K, Carter DA, Porter R, Verkade P, Stephens DJ. 2008. Efficient coupling of Sec23-Sec24 to Sec13-Sec31 drives COPII-dependent

- collagen secretion and is essential for normal craniofacial development. *J Cell Sci* 121:3025-3034.
- Tsang M, Lijam N, Yang Y, Beier DR, Wynshaw-Boris A, Sussman DJ. 1996. Isolation and characterization of mouse dishevelled-3. *Dev Dyn* 207:253-262.
- Vallin J, Thuret R, Giacomello E, Faraldo MM, Thiery JP, Broders F. 2001. Cloning and characterization of three *Xenopus* slug promoters reveal direct regulation by Lef/beta-catenin signaling. *J Biol Chem* 276:30350-30358.
- van Amerongen R, Berns A. 2006. Knockout mouse models to study Wnt signal transduction. *Trends Genet* 22:678-689.
- Wagner J, Schmidt C, Nikowits W, Jr., Christ B. 2000. Compartmentalization of the somite and myogenesis in chick embryos are influenced by wnt expression. *Dev Biol* 228:86-94.
- Walker MB, Trainor PA. 2006. Craniofacial malformations: intrinsic vs extrinsic neural crest cell defects in Treacher Collins and 22q11 deletion syndromes. *Clin Genet* 69:471-479.
- Wallingford JB. 2006. Planar cell polarity, ciliogenesis and neural tube defects. *Hum Mol Genet* 15 Spec No 2:R227-234.
- Wallingford JB, Habas R. 2005. The developmental biology of Dishevelled: an enigmatic protein governing cell fate and cell polarity. *Development* 132:4421-4436.
- Wallingford JB, Harland RM. 2002. Neural tube closure requires Dishevelled-dependent convergent extension of the midline. *Development* 129:5815-5825.
- Wallingford JB, Rowning BA, Vogeli KM, Rothbacher U, Fraser SE, Harland RM. 2000. Dishevelled controls cell polarity during *Xenopus* gastrulation. *Nature* 405:81-85.
- Walston T, Guo C, Proenca R, Wu M, Herman M, Hardin J, Hedgecock E. 2006. mig-5/Dsh controls cell fate determination and cell migration in *C. elegans*. *Dev Biol* 298:485-497.
- Wang J, Hamblet NS, Mark S, Dickinson ME, Brinkman BC, Segil N, Fraser SE, Chen P, Wallingford JB, Wynshaw-Boris A. 2006a. Dishevelled genes mediate a conserved mammalian PCP pathway to regulate convergent extension during neurulation. *Development* 133:1767-1778.
- Wang Y, Guo N, Nathans J. 2006b. The role of Frizzled3 and Frizzled6 in neural tube closure and in the planar polarity of inner-ear sensory hair cells. *J Neurosci* 26:2147-2156.
- Wedaman KP, Meyer DW, Rashid DJ, Cole DG, Scholey JM. 1996. Sequence and submolecular localization of the 115-kD accessory subunit of the heterotrimeric kinesin-II (KRP85/95) complex. *J Cell Biol* 132:371-380.
- Wehrli M, Dougan ST, Caldwell K, O'Keefe L, Schwartz S, Vaizel-Ohayon D, Schejter E, Tomlinson A, DiNardo S. 2000. arrow encodes an LDL-receptor-related protein essential for Wingless signalling. *Nature* 407:527-530.
- Weitzel HE, Illies MR, Byrum CA, Xu R, Wikramanayake AH, Ettensohn CA. 2004. Differential stability of beta-catenin along the animal-vegetal axis of the sea urchin embryo mediated by dishevelled. *Development* 131:2947-2956.
- Westfall TA, Brimeyer R, Twedt J, Gladon J, Olberding A, Furutani-Seiki M, Slusarski DC. 2003. Wnt-5/pipetail functions in vertebrate axis formation as a negative regulator of Wnt/beta-catenin activity. *J Cell Biol* 162:889-898.

- Wharton KA, Jr. 2003. Runnin' with the Dvl: proteins that associate with Dsh/Dvl and their significance to Wnt signal transduction. *Dev Biol* 253:1-17.
- Wilson J. 1965. Embryological considerations in teratology. In: Wilson J, editor. *Teratology: principles and techniques*. Chicago: University of Chicago Press. pp 251-277.
- Wilson PA, Oster G, Keller R. 1989. Cell rearrangement and segmentation in *Xenopus*: direct observation of cultured explants. *Development* 105:155-166.
- Witze ES, Litman ES, Argast GM, Moon RT, Ahn NG. 2008. Wnt5a control of cell polarity and directional movement by polarized redistribution of adhesion receptors. *Science* 320:365-369.
- Wolfe KH. 2001. Yesterday's polyploids and the mystery of diploidization. *Nat Rev Genet* 2:333-341.
- Wong HC, Mao J, Nguyen JT, Srinivas S, Zhang W, Liu B, Li L, Wu D, Zheng J. 2000. Structural basis of the recognition of the dishevelled DEP domain in the Wnt signaling pathway. *Nat Struct Biol* 7:1178-1184.
- Wong SY, Reiter JF. 2008. The primary cilium at the crossroads of mammalian hedgehog signaling. *Curr Top Dev Biol* 85:225-260.
- Yamaguchi TP, Takada S, Yoshikawa Y, Wu N, McMahon AP. 1999. T (Brachyury) is a direct target of Wnt3a during paraxial mesoderm specification. *Genes Dev* 13:3185-3190.
- Yamamoto H, Komekado H, Kikuchi A. 2006. Caveolin is necessary for Wnt-3a-dependent internalization of LRP6 and accumulation of beta-catenin. *Dev Cell* 11:213-223.
- Yamanaka H, Moriguchi T, Masuyama N, Kusakabe M, Hanafusa H, Takada R, Takada S, Nishida E. 2002. JNK functions in the non-canonical Wnt pathway to regulate convergent extension movements in vertebrates. *EMBO Rep* 3:69-75.
- Yan J, Huen D, Morely T, Johnson G, Gubb D, Roote J, Adler PN. 2008. The multiple-wing-hairs gene encodes a novel GBD-FH3 domain-containing protein that functions both prior to and after wing hair initiation. *Genetics* 180:219-228.
- Yang J, Li T. 2005. The ciliary rootlet interacts with kinesin light chains and may provide a scaffold for kinesin-1 vesicular cargos. *Exp Cell Res* 309:379-389.
- Youn BW, Keller RE, Malacinski GM. 1980. An atlas of notochord and somite morphogenesis in several anuran and urodelean amphibians. *J Embryol Exp Morphol* 59:223-247.
- Yu A, Rual JF, Tamai K, Harada Y, Vidal M, He X, Kirchhausen T. 2007. Association of Dishevelled with the clathrin AP-2 adaptor is required for Frizzled endocytosis and planar cell polarity signaling. *Dev Cell* 12:129-141.
- Zhao H, Rebbert ML, Dawid IB. 2007. Myoskeleton, a factor related to Myocardin, is expressed in somites and required for hypaxial muscle formation in *Xenopus*. *Int J Dev Biol* 51:315-320.

## **Vita**

Ryan Scott Gray attended Meridian High School, Meridian, Mississippi. In 1994 he entered the University of Mississippi in Oxford, Mississippi. It did not stick. After many years working construction, serving his country in the Mississippi Air National Guard, Ryan attended the University of Southern Mississippi, Hattiesburg, Mississippi in the fall of 2001. That was close. During the summer of 2001, Ryan worked for the United States Geological Survey in the backcountry of Alaska and along the Alagnak river basin learning to fly fish. He received his Bachelor of Science from the University of Southern Mississippi in December of 2002. After a wonderful semester living out of his truck in the great American west, he entered early rotations, May 2003 at the University of Texas at Austin.

Permanent Address: 4820 Arundel Road, Meridian, Mississippi 39305

This manuscript was typed by the author.